Optimisation of Neonatal Antimicrobial Therapy Using Pharmacokinetic-Pharmacodynamic Modelling

Eva Germovšek

A dissertation submitted in partial fulfillment

of the requirements for the degree of

Doctor of Philosophy

of

University College London.

Institute of Child Health

University College London

November 2015

I, Eva Germovšek, confirm that the work presented in this thesis is my own. Where information has been derived from other sources, I confirm that this has been indicated in the work.

Abstract

Bacterial infections, namely sepsis and meningitis, are among the major causes of morbidity and mortality during the neonatal period. In an era of increasing antimicrobial resistance, when few new types of antibiotics are being developed, antimicrobial therapy needs to be optimised to ensure that adequate doses are given. At the same time, since renal function is immature in neonates, the dosing regime needs to be designed to minimise toxicity.

The studies described here aimed to address the following questions: what is the appropriate way to scale drug clearance in the paediatric population; how can treatment be individualised and optimised to help improve the therapeutic drug monitoring of gentamicin; what meropenem dose should be recommended for neonates and infants with sepsis or meningitis; and finally how can a modelling approach be used to facilitate the definition of neonatal sepsis. The above questions were addressed using distinct strategies. An extensive comparison of published models for scaling clearance was performed. Population pharmacokinetic models using data from large gentamicin and meropenem studies in neonates were developed, and then either implemented in provisional software, or used to make dose recommendations, respectively. Also, in a preliminary study, item response theory models were applied to pharmacodynamic data from neonates with sepsis.

The use of allometric weight scaling with a postmenstrual age driven sig-

moidal maturation function was recommended as a standard approach for scaling clearance. The population pharmacokinetic model developed using gentamicin data showed that specifically timed trough levels are not needed for therapeutic drug monitoring. The results of the meropenem study imply that the current recommended dosing regimen for neonates is appropriate for susceptible bacteria. Finally, the proof-of-concept study suggested that metabolic acidosis provided the most information about the sepsis status of neonates.

Acknowledgements

There are many who I would like to thank for providing their support and for making my PhD experience a pleasant one.

Firstly, I would like to thank all the participating neonates and infants, as well as their parents and hospital staff, without whom I would not have been able to perform any of the analyses presented in this thesis.

I am very grateful to Joseph Standing for his supervision during my PhD, as well as his patience and guidance, and for introducing me to the academic world. I would also like to thank Nigel Klein for his support during the last three years.

To Sebastian Ueckert for giving advice and providing assistance with the item response theory models.

I have received funding from the NeoMero study, part of the European Union Seventh Framework Programme for research, technological development and demonstration, from Action Medical Research, and from the UCL IMPACT PhD studentship.

I would also like to thank: Charlotte Barker, Rollo Hoare, Hannah Jones, Felicity Fitzgerald, Julia Kenny, Liam Shaw, Deji Majekodunmi, Ronan Doyle, Sonia Melo Gomes, Vania de Toledo, and other students and staff at the Institute of Child Health, and members of the London Pharmacometrics Interest Group, for their kindness and support.

Also, to Judit Szalay, Andrea Csomor, Esther Odoom-Opoku, Veronika Šibelja, Alenka Gjuran, Petra Kovačič, and Nina Intihar for their friendship and for cheering me up when I needed it.

Finally, to my family for always being there for me.

Contents

List of Figures

List of Tables

Chapter 1

Introduction

1.1 Neonatal infections

Although a neonate is technically a newborn infant in the first four weeks of life, the term "neonate" will be for the purpose of this thesis occasionally used for infants older than one month. This is because sometimes infants older than one month also receive antimicrobial treatment on neonatal intensive care units.

Bacterial infections, including sepsis and meningitis, are among the main causes of morbidity and mortality during the neonatal period, both in the UK [1] and worldwide [2]. Although only a small proportion of newborns go on to develop sepsis (for example, Luck *et al* [3] found in their study that only 13 out of 413 screened neonates had probable or definite early-onset sepsis), it can result in death if untreated [4]. Antimicrobials can therefore have a life-saving effect, and are especially in the case of premature newborns used as empirical therapy that usually starts almost immediately after birth [5]. However, inappropriate use of antibiotics (such as over-prescribing) could have the opposite effect, resulting in prolonged treatment due to an infection with a resistant microorganism [4]. Rapid development of antimicrobial resistance could also contribute to the fact that developing new antibiotics is not a priority for pharmaceutical companies,

and consequently, it does not seem that any considerably new classes of antibiotic agents will be available soon [6], but there are some new types of β-lactamase inhibitors in the pipeline [7]. It is therefore vital that instead, the current antibiotic treatment is optimised. Optimising the treatment will also ensure that a neonate receives a high enough dose and help prevent the emergence of resistance.

Although most antimicrobials are not new drugs, it has been shown in a recent survey of neonatal intensive care units (NICU) in the UK that the variability in their prescribing and monitoring is large (in the gentamicin example there were 24 different dosing and monitoring regimens within 43 units) [8]. Another study found that 43 different combinations of empirical treatments for late-onset sepsis in neonates and infants were used in five European countries [9]. The variability in clinical practice is an indicator of the limited evidence base behind current standard of care, and shows the need for evidence-based guidelines that would standardise treatment. Furthermore, medicines used for treating neonates are often used "off-label" (outside their product license) [10], which is another reason for more research needed in this area.

1.2 Pharmacokinetic-pharmacodynamic modelling

In the past descriptive pharmacokinetic (PK) research in neonates and infants was limited [11] because to perform the traditional non-compartmental analysis (NCA) one usually requires a minimum of four (ideally more) blood samples to capture the main PK parameters. However, a model-based approach does not have this disadvantage. Both of these approaches are briefly described in the following Section 1.3.

Modelling is a technique where mathematical equations are used to simplify reality, and characterise the relationship between variables. Modelling can be

applied to describe and summarise data and to further understanding of biological processes that occur in the body (and which in some cases cannot be investigated with *in vivo* or *in vitro* experiments). After evaluation of the model, one can also use modelling for extrapolating beyond the study population, i.e. predicting the behaviour of the underlying biologic system through simulations from the data [12]. This so-called pharmacometric approach is especially important and valuable when conducting paediatric (particularly neonatal) studies, where recruitment can be challenging and data are often sparse [13].

More specifically, PK modelling mathematically characterises how different PK processes (i.e. absorption, distribution, metabolism, and elimination) of drugs change over time. Pharmacodynamic (PD) modelling, on the other hand, focuses more on the relationship between drug concentration at the site of action and the intensity of pharmacological response, which can either be the desired effect of a drug or a toxic effect (Figure 1.1). Pharmacokinetic-pharmacodynamic (PKPD) modelling is a combination of both, and thus tries to describe and quantify the relationship between the dose and/or drug concentration and the effect [14].

PKPD models can be empirical or mechanistic, the latter models using knowledge of biological processes and thus being more realistic from a physiological point of view [14, 15]. In addition to continuous data (e.g. drug concentration), PKPD models also allow one to model discrete data (e.g. bacterial eradication, progress of a disease, intensity of pain) [16, 17]. However, developing a PKPD model can in some cases prove difficult – for example, when dealing with neonates who have clinical signs of infection, since only a small percentage of them is actually culture positive [3, 18]. In this case, sepsis could be viewed as an underlying hidden or latent variable, and other PD markers (such as plasma concentrations of markers of infection, or increased/decreased white blood cell count) can be modelled using, for example, item response theory models [19, 20].

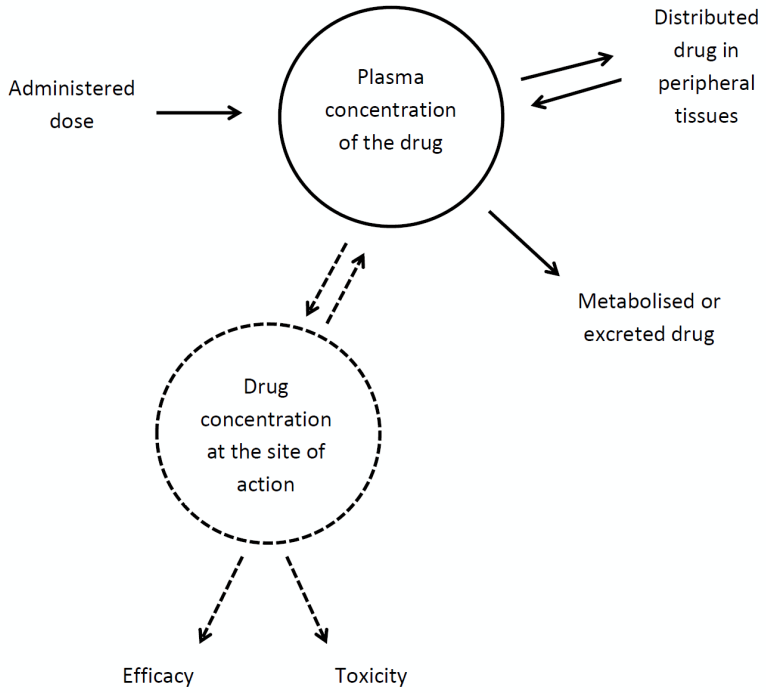

Figure 1.1: Schematic diagram showing pharmacokinetic (PK) - pharmacodynamic (PD) relationship. Solid lines represent the PK part and dashed lines the PD part of the pharmacological response of a drug.

1.3 Approaches for analysing data from multiple subjects

When analysing PK data the traditional method is the descriptive, or non-compartmental approach. NCA does not depend on a model, and involves taking multiple samples (across the entire PK profile of a drug (Figure 1.2)) from each subject to then calculate subject-specific PK parameters, such as, maximal drug concentration (C_{max}), time to C_{max} (t_{max}), and area under the concentration-time curve (AUC) [21]. This way, a summary of the concentration-time profile is obtained.

An alternative method for analysing PK data is a model-based (or, compartmental) method, where a complete PK profile for each subject is no longer needed as data from multiple subjects are pooled together and hence fewer samples per individual are required. Additionally, a model-based approach also allows

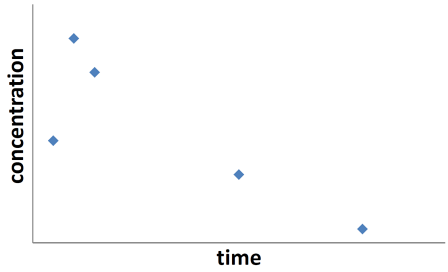

Figure 1.2: An example of concentration-time data.

for different covariates (such as age and weight) to be included, and their effects quantified [22, 23]; and so facilitates the investigation of the developmental differences between the paediatric and adult population [22]. Furthermore, model parameters can enable one to gain mechanistic insights [24], as, for example, clearance (CL) describes biological processes that represent drug elimination; this is especially obvious in renally eliminated drugs (such as gentamicin), where CL is often similar to the patient's glomerular filtration rate (GFR).

The best fit of a linear model can be found analytically, so where possible, statisticians advise transforming the data to create a linear relationship. However, drug concentration-time profiles are non-linear and apart from one exception (1-compartment intravenous bolus model) PK data cannot be transformed to be linear. Hence non-linear models are required when analysing PK data.

The paediatric population is not homogeneous, and drug disposition and the effects of the drugs differ among individuals [13]. It is therefore important to select an appropriate modelling approach that will not over-/under-estimate the variability and bias the PK parameter estimates.

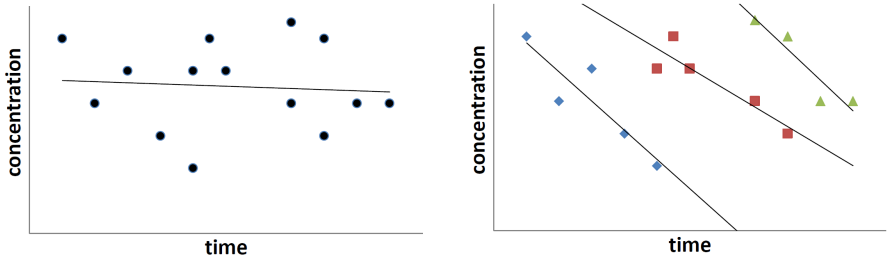

Figure 1.3: A schematic presentation of the effect of ignored between-subject variability on the overall trend line (left). Graph on the right shows how individual regression lines actually look like.

1.4 Statistical modelling

The simplest modelling techniques for statistical analysis of PK data from multiple subjects are the naïve data average and the naïve pooled data approaches. The data-average method involves calculating the average drug concentration at each sampling time for all individuals, which requires all individuals to have the same sampling regimen. This limits its usefulness for neonatal studies, where samples are taken opportunistically for other purposes (such as to check the blood gasses). Similarly, in the pooled-data method data from all subjects are pooled together and so considered as being from a single subject. In both approaches a single model is then fitted to the mean/pooled values, thus ignoring the fact that data points taken from the same individual may not be independent (i.e. correlated) and so ignoring the distinction between the between-subject and residual variability [24]. Where between-subject variability is large the model fit can be biased as highlighted by the example shown in Figure 1.3. Furthermore, in the data-average approach variability tends to be underestimated (since models are fitted to averaged data), and in the pooled-data approach (because between-subject variability is not allowed for), the residual variability tends to be overestimated.

Another method for analysing population data is the two-stage approach, where in the first stage a model is fitted to the data from each individual; and in the second step, the individual PK parameters from the first step are averaged to

obtain the estimates of the population PK parameters. This approach relies on each individual having rich data so that all model parameters can be identified. Ideally subjects should have the same number and timing of samples to enable the same model to be fitted to each individual. Whilst it is preferable to averaging and pooling approaches due to its ability to separate between-subject parameter-level and residual variability the standard two-stage approach has been shown to overestimate variability [24].

The drawbacks of these methods have led to a general consensus that the non-linear mixed-effects (NLME) modelling approach is the most appropriate for analysing population PK data. NLME models facilitate analysis of sparse and unbalanced data (meaning that the number of observations and/or sampling times can differ between individuals, allowing the use of opportunistic sampling) [22, 25]. This is particularly important when dealing with populations such as neonates, where rich sampling is not possible because of limitations on the total volume of blood that can be taken for testing purposes [26], or parents may not consent to repeated blood measurement for research. The significance of the NLME models for the neonatal population is also shown by the fact that one of the first uses of these models was for analysing phenobarbital PK data from neonates [27].

Whilst NLME methods are able to handle sparse data, rich data will always be more informative on individual PK parameters. Rich data can be defined as data originating from a study where there is more samples per subjects taken than there are parameters to estimate [28]. But in the case where all samples are crowded within one part of the dosing interval, even if the "criteria" for rich data is met, these samples may not be that informative. Therefore, sparse data, taken at optimal time points might provide a good balance between invasiveness (i.e. taking multiple samples) and informativeness.

Using the NLME approach, a model is fitted to all available data from all individuals simultaneously [24]. When modelling continuous data, a NLME model

can be summarised by Equation 1.1:

$$y_{ij} = f(t_{ij}, g\left(\theta, x_{ij}, \eta_i\right)) + h\left(t_{ij}, g(\theta, x_{ij}, \eta_i), \varepsilon_{ij}\right), \tag{1.1}$$

where an observation y_{ij} for an individual i at time t_{ij} is described by a prediction function f (which characterises the PK or PD relationship), and an error function h, which accounts for the differences between the observation and prediction. The function g describes subject-specific parameters as a function of: θ, which represents typical population values, x_{ij}, i.e. subject-specific covariates, and η_i, which are subject-specific random effects parameters [29, 30].

For binary data, a NLME model describes the probability of y_{ij} being 1, using a probability density function l (Equation 1.2) [31]:

$$P(y_{ij} = 1) = l(t_{ij}, g\left(\theta, x_{ij}, \eta_i\right)). \tag{1.2}$$

Variability in NLME models can be allocated to different sources, i.e. parameter-level between-subject variability (BSV, η) and within-subject variability (sometimes called inter-occasion variability), and observation-level variability or residual error (ε). Subject-specific covariates, such as, weight, age, markers of renal function, can explain some of the BSV. The residual variability can, for example, originate from the assay, or be a consequence of a measurement error, and represents the difference between the observation (usually plasma concentration of a drug) and the model predicted value.

Both η and ε are (after a transformation) assumed to follow a normal distribution with a mean of zero (assuring that the model predicted values go through the middle of the data), and a variance (ω^2 and σ^2, respectively), which is estimated [32]. Normality is assumed in modelling software, such as NONMEM (ICON Development Solutions Ellicott City, Maryland) [27], Monolix [33] and

ADAPT [34]. However, the assumption of normality (or some transformation of normal) is not mandatory and other computer programs (e.g. non-parametric adaptive grid and non-parametric Bayesian algorithm [35]) can be used to facilitate other distributions.

To obtain estimates of the PK and PD parameters that are most likely to occur in the data (i.e. such estimates that the observed data become most likely) the likelihood function (Equation 1.3) is maximised [36]. The likelihood function is a product of the marginal probability density functions of the individual observed values (or the individual likelihoods) over all (N) individuals (Equation 1.3):

$$\mathscr{L}(y,\Theta) = \prod_{i=1}^{N} \int_{-\infty}^{\infty} f(y_i,\eta_i) d\eta_i = \prod_{i=1}^{N} \mathscr{L}_i(y_i,\Theta), \tag{1.3}$$

where Θ represents a set of all estimated parameters, i.e. θ, Σ, Ω. However, it is computationally challenging to integrate over η, therefore approximations of the likelihood, such as first-order conditional estimation (FOCE) approximation, or Laplace approximation are used. Also, addition is a mathematically easier procedure than multiplication of likelihoods (especially if the likelihoods are very small), hence in most computer programs log likelihood is minimised instead (Equation 1.4).

$$log(\mathscr{L}(y,\Theta)) = \sum_{i=1}^{N} log(\mathscr{L}_i(y_i,\Theta)). \tag{1.4}$$

Two NLME models can be compared using the likelihood ratio test. The objective function value (OFV) is based on this test, and represents minus 2 log likelihood of the data. The difference between OFV (ΔOFV) for nested models is therefore χ^2-distributed with degrees of freedom equal to the number of parameters by which the models differ; for example, for a nested model with 1 parameter differing, or 1 extra degree of freedom, ΔOFV of >3.84 and >10.83, corresponds to a p-value of <0.05 and <0.001, respectively.

1.5 Evaluation of non-linear mixed-effect models

To asses whether a NLME model (i.e. a population PK model) has good descriptive and predictive properties, several (internal and external) methods can be used [37, 38].

Internal methods involve diagnostic goodness-of-fit (GOF) plots and statistics that are used to estimate the precision on final model parameters – e.g. standard errors (SE) and confidence intervals (CI) [12]. GOF plots are, for example, observations (DV) versus population (PRED) or individual (IPRED) predicted values. Also, to confirm the assumption of standardised residuals following a $\mathcal{N}(0,1)$ distribution, diagnostic plots, such as conditional weighted residuals (CWRES) versus time after dose or PRED, are examined for any potential trends. Another way of investigating the distribution of residuals is by plotting a histogram or a QQ-plot of the residuals [12, 37].

SEs are usually obtained from the covariance step in NONMEM. In the covariance step, the Fisher information matrix, i.e. the negative of the Hessian matrix (which is the second derivative of the log likelihood function) is computed. The covariance matrix is then the inverse of the Fisher information matrix, and SEs are the square roots of the diagonal elements in the covariance matrix. Uncertainty on model parameter estimates can also be obtained with a bootstrap, which is a technique where replicates (usually 1,000) of the original dataset are obtained by random sampling with replacement. A NLME model is then fitted to each of the replicated datasets, and the parameters are re-estimated. Then, a 95% non-parametric confidence interval of the final parameter estimates is obtained.

A model can also be evaluated by using Monte Carlo simulations, as for example, when performing a visual predictive check (VPC) [37, 39]. In a VPC a

large number (e.g. 1,000) of datasets is simulated using the estimates of the final parameters and the variability from the (final) NLME model. By performing a VPC one can inspect whether the NLME model is able to reproduce the distribution of the original dataset [40, 41], and it can help identify the presence of potential problems in the fixed or random effects model [42].

External techniques for NLME model evaluation involve testing a model that was developed using one dataset on another dataset and then comparing predictions from both. One can also divide the dataset used to develop the NLME model into two parts – i.e. a learning and an evaluation dataset; and then use the evaluation subset for external evaluation of the model. This can be repeated several times, as in the so-called cross-validation approach [37]. Then, metrics, such as prediction errors (PE), are calculated [37].

1.6 Developmental pharmacology

Changes in the human body due to growth and maturation are non-linear and especially obvious in the first year of life [43, 44]. A consequence of these changes are differences in the PK processes between neonates and adults.

1.6.1 Pharmacokinetic differences

Absorption of drugs is different in neonates compared to adults, especially due to higher gastric pH in neonates [45, 46]. But since drugs are absorbed from the gastrointestinal tract when given orally, and both gentamicin and meropenem (i.e. two drugs that are studied in this thesis) are administered intravenously, absorption will not be described in more detail.

Distribution of drugs in neonates is affected by higher membrane permeability, reduced total plasma proteins (and their binding affinity), and a higher (80-90% versus 55-60%) percentage of body water, compared to adults [44, 47].

Consequently, the fraction of protein bound drug is lower (therefore the fraction of free drug is increased), and the volumes of distribution of water soluble drugs (such as aminoglycoside and β-lactam antimicrobials; i.e. gentamicin and meropenem, respectively) are higher. Moreover, the penetration of small hydrophilic molecules (i.e. meropenem) into the central nervous system is increased in neonates, compared to adults, resulting in higher cerebrospinal fluid (CSF) concentrations [48].

Both gentamicin and meropenem are mainly renally excreted [49, 50], however, meropenem is also partly metabolised. Metabolism is a process in which a drug is transformed into a more hydrophilic form; and usually occurs in the liver, but can also take place in, for example, the kidneys [47]. There are two phases of hepatic metabolism. In the first phase drugs undergo oxidation (typically with cytochrome enzymes from the CYP P450 family), reduction, and hydroxylation. Most enzymes of the first phase of the hepatic metabolism are half-mature at birth, and reach adult activity at around 1 year of age [46]. Phase two involves chemical reactions, such as conjugation, glucoridation, sulphation, and acetylation. While enzymes involved in glucoridation achieve adult activity at approximately 3-4 years of age; sulphotransferase activity is already significant at birth [46, 51].

Most antimicrobial agents are excreted *via* the kidneys [47], by either glomerular filtration or tubular secretion. Maturation of renal function is a complicated process that starts *in utero* with nephrogenesis occurring between week 6 and 36 of gestation; hence it correlates better with postmenstrual age (PMA) than postnatal age (PNA) [52, 44]. PMA is a sum of gestational age (GA) and PNA, i.e. chronological age [53], and therefore encompasses both pre- and post-birth maturation, although it might not be able to completely describe the fast changes in the first day(s) after birth. At birth, newborn neonates exhibit approximately 35% of adult renal activity [22], but due to an increase in renal and intra-renal blood flow, the GFR and renal function improve rapidly. After that, renal function increases more gradually, until it reaches adult levels at the age of around

8-12 months [44, 52]. Similarly to GFR, tubular secretion is also immature at birth; reaching adult levels at the age of approximately one year [46]. The non-linear maturation of renal function makes scaling of clearance complicated, and different approaches have been utilised – as described in more detail in Chapter 2.

1.6.2 Pharmacodynamic differences

Only after accounting for the PK differences or PK maturation one can start focusing on the PD differences as well. Not many studies focus on measuring the PD in neonates, which may be because drug effect is more difficult to measure and evaluate in neonates [54]. It might also be contributed to the fact that the consensus on the appropriate endpoints is lacking, for example the endpoints one should look at when defining neonatal sepsis are not clearly defined [55].

PD differences between neonates and adults can be present as a result of different concentration of proteins (that the drug targets) and/or different function of receptors [22], which leads to a different response of the neonatal body to the drug given. An example of a PD difference is seen in the immature neonatal lung; it lacks smooth muscle, which reduces the effect of bronchodilatators [22, 56]. Another example is the central nervous system, more specifically, GABAergic inhibitory system, which is immature in neonates (especially premature neonates), compared to adults, which causes benzodiazepines to paradoxically worsen the seizures [57, 58]. A higher thymic output of T-cells in neonates [59], compared to adults, is also an example of a PD difference between neonates and adults.

Additionally, as neonates are not (usually) exposed to pathogens before they are born, their innate (and adaptive) immune response is still developing, therefore they are more vulnerable to infections with pathogens than adults [60, 61, 62]. Hence, higher PD targets for antimicrobial agents might be needed.

1.7 Pharmacokinetic-pharmacodynamic relationship of antimicrobial agents

Whilst PKPD relationship of drugs describes the link between exposure and effect, the antimicrobial PKPD has the advantage of having a surrogate measure of efficacy, namely the minimal inhibitory concentration (MIC). MIC is the lowest concentration of an antibiotic that averts the growth of bacteria (i.e. is needed for bacteriostasis). It is determined *in vitro*, which has some drawbacks, such as, the media that is used is artificial, and the duration of incubation (when visible growth of bacteria is determined) is usually 24 hours, whilst treatment might last for several days, or even weeks [63]. However, it is a simple, reproducible measure of antibacterial activity, and concentrations that are used to determine the MIC can be easily compared to free concentrations of a drug measured in plasma or, for example, CSF [63].

By using MIC alone, one does not get any information on the time course of the antimicrobial treatment, or on how to best increase the efficacy of an agent. Hence antibiotics have been divided into three groups, according to the PD measure that links their exposure to microbiological and clinical effects. Some antibiotics (such as gentamicin) exhibit concentration-dependent killing, meaning that they are most effective when their peak concentration (relative to the MIC of a pathogen) is maximised [17, 64, 65]. For time-dependent antibacterials (e.g. β-lactam meropenem) the time in the dosing interval when free drug concentration is above the MIC (%T>MIC) is best linked to their efficacy. Also, for some antimicrobial agents (e.g. fluoroquinolones), a related PKPD parameter – total drug exposure, i.e. AUC to MIC ratio, needs to be maximised [64].

Once the antimicrobial PD target has been determined, and the MIC breakpoints (or ideally, the MIC distribution of a pathogen in the environment where the drug is going to be used) are known, a dose that has the highest probability

of achieving this target can be selected (using, e.g. Monte Carlo simulations) [17]. The target might be increased for immunocompromised subjects (such as neonates) [64], however, clinical studies are needed to determine more specifically how high the PD target should be in this population.

Most antibiotics also exhibit a post-antibiotic effect (PAE), meaning that the bacterial growth continues to be suppressed even when their concentration is below MIC [66]. The PAE is longer when bacterial exposure to the antibiotics is longer, if maximal plasma concentration of a drug is higher, and if the MIC of a specific bacterium is lower [67, 49]. PAE for aminoglycosides usually lasts between 2 and 4 hours [49]; and for meropenem approximately 5 hours for *Escherichia coli* (*E. coli*) (with meropenem concentration 4-fold higher than the MIC) [68]. The proposed mechanism of the PAE is that it is a result of bacterial damage caused by the antibiotic [17].

1.8 Aims and Structure

The overall aim of the work described in this thesis was to optimise neonatal antimicrobial treatment by using non-linear mixed-effects modelling. More specifically, the aims were to determine which of the published clearance scaling methods provides the best results, so that this model could then be used in the following chapters. Population pharmacokinetic models for both gentamicin and meropenem were then developed and used to either individualise therapy, or to suggest an optimal dose, respectively. And since there is no agreement on the definition of sepsis in neonates, which makes the comparison of clinical sepsis trial results difficult, the aim was also to define which laboratory test (from a set of five predetermined tests) for defining sepsis is the most informative.

The structure of the following chapters 2-5 is similar throughout the whole thesis, and represents the main body of this work. Each chapter starts by in-

troducing the background and what is already known about the subject that is presented in the chapter, and then presents the methods needed to achieve the above-mentioned aims. The results are then presented and discussed, and a brief summary of the chapter is given. The work presented in the main chapters is as follows: comparison of clearance scaling approaches in the paediatric population, development of a population pharmacokinetic model to individualise therapy and so improve the current therapeutic drug monitoring of gentamicin, development of a model to describe the plasma and CSF pharmacokinetics of meropenem in neonates and infants with sepsis or meningitis (and make dosing recommendations), and development of an item response theory model using pharmacodynamic data from a neonatal study to facilitate the definition of sepsis.

Chapter 2

Comparison of methods for scaling clearance in neonates, infants and children

2.1 Introduction

As described in Section 1.6 children, especially neonates and infants, differ from adults. They are smaller, lighter, and have a different body composition to adults, namely a higher proportion of total body water. Also, the function of the eliminating organs, such as the kidneys, and the liver, is immature in neonates and infants, as indicated by the lower glomerular filtration rate (GFR) and lower expression of some hepatic enzymes [44]. These physiological differences are the main source of the differences in pharmacokinetic processes between adults and children, which results in altered PK parameters (such as drug clearance) in children [44]. Two approaches can be used to take these differences into account, and to scale adult PK to children: allometric scaling with varying allometric exponent or a mathematical function that describes the dynamics of the change in organ function, and physiologically-based pharmacokinetic (PBPK) models [69]. These approaches will briefly be discussed below.

Whole-body PBPK models use a system of equations, which is based on biological knowledge of physiological blood flows, anatomical organ structures, tissue and organ volumes [70]. The compartments in these models represent actual anatomical parts of the body. PBPK models are mostly useful in predicting first-in-man doses prior to human exposure, but have also been proposed for scaling PK predictions to special populations such as children [71, 72]. A major limitation of PBPK models for extrapolation is the requirement that the PBPK model must first describe the existing adult data well. Getting detailed information about many physiological processes and measurements can also be expensive and time consuming [73]. Moreover, for some compounds there is insufficient *in vitro* information to make accurate predictions, leading to poor predictive performance of the PBPK model. To address this some authors have looked at fitting PBPK models to data [74, 75] but as yet this approach has not been widely used in the paediatric research.

The alternative method (which is discussed in the remainder of this chapter) and a method more commonly used by paediatric pharmacologists for scaling PK from adults to the paediatric population is through fitting models to observed PK data and using demographic covariates to describe PK parameter ontogeny. The main focus is usually on CL since many pharmacological effects are driven by drug exposure (AUC), which is inversely proportional to CL. CL changes with size and age, so models accounting for these two processes are required.

To account for body size, it has been noted since the 1950s that body surface area (BSA) is a better predictor of optimal dosing than linear body weight [76]. More recently it has been proposed that the underlying biology of scaling of metabolic processes with body size (such as body weight raised to some power) can also provide explanation of changes in drug CL [77]. This so-called allometric

scaling approach is given by the following standard allometric equation:

$$y_i = a \cdot WT_i^b, \tag{2.1}$$

where y_i is the individual subjects body function of interest (that is being predicted), for example drug clearance, WT_i is the individuals body weight in kilograms, a is the allometric constant, which assumes the value of y when WT = 1 kg, and b is the allometric exponent [78]. Historically, several different values of the allometric exponent have been proposed. Almost 80 year ago Benedict [79] advocated that the basal metabolic rate scales best with body surface area, which approximates to WT raised to the power of 0.67. Around the same time Kleiber [80], having examined 13 different groups of mammals (ranging in weight from 150 grams to 679 kilograms), concluded that the allometric exponent should be 0.75. However, he also noticed that in order to see a difference in predictions relating to using the exponent of 0.67 versus 0.75, the difference between the lightest and the heaviest subjects studied needed to be at least 9-fold [81]. Nephrologists usually scale GFR per 1.73m^2 [82, 83] ($\sim$ weight raised to the power of 0.67), and a study of GFR maturation using data from 923 individuals with ages ranging from neonates to adults (31 years of age) by Rhodin *et al* provided an allometric exponent of 0.632 [52]. Concerning the maturation of hepatic elimination routes, both Noda *et al* [84] and Johnson *et al* [85] found that liver size (volume) scales approximately with body weight raised to the power of 0.78. Also, a recent meta-analysis of 484 PK studies by McLeay *et al* [86] examined the relationship between CL and weight and found that the median (estimated) allometric exponent in the studies was 0.65 (ranging from -1.2 to 2.2). This shows that allometric exponent is usually within the 0.63-0.78 range, and that there is no agreement on its exact value, but when the allometric exponent was fixed, the value of 0.75 was the most common when studying PK of children and/or neonates [86]. In practice, value of b <1 indicates that the process studied (e.g. CL maturation) increases with

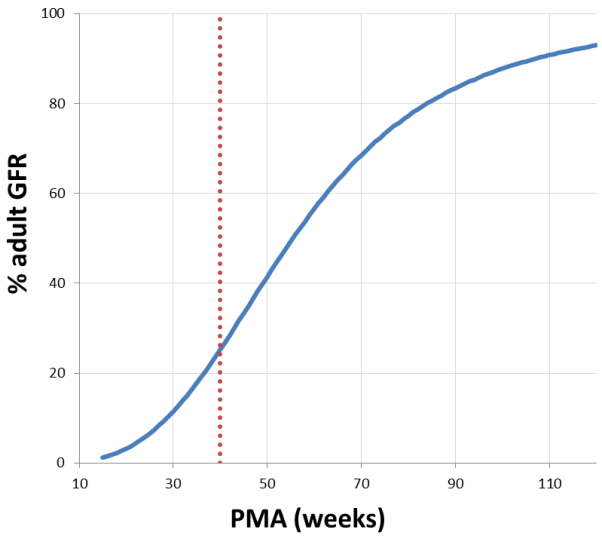

Figure 2.1: Maturation of renal function, specifically glomerular filtration rate (GFR). Red dotted line represents the postmenstrual age (PMA) of 37 weeks, which is when a full-term neonate is born. Adapted from [52].

body size at a slower rate than overall body weight.

Scaling of CL with allometric models alone is insufficient to capture the PK differences across the entire paediatric age range [72] because physiological immaturity in infants and neonates [51] means CL is lower than expected. One therefore also needs to account for maturation due to immaturity of organ function, especially in neonates, where body functions change rapidly [44]. As described in Section 1.6.1 maturation of renal function is a complicated and a non-linear process. Figure 2.1 illustrates this process.

Since every model is only a simplification of reality and it is known that "all models are wrong, some are useful" [87], many different approaches are utilised in order to account for both age and size related changes in CL (not considering the PBPK approach). These approaches can be divided into two groups: a) some models have an allometric exponent that varies with age or weight [73, 88], and b) some models use a single allometric exponent (which can be fixed or estimated) to explain the changes in CL with size, and an additional function accounting for the eliminating organ maturation. A widely used approach is to use a fixed

allometric exponent, and a sigmoid maturation function (Equation 2.2) [69, 89] – this method was recently suggested as a standard approach for scaling CL in the paediatric population in a study by Holford *et al* where it was evaluated on data from 46 different drugs [69].

$$maturationfunction = \frac{PMA^{Hill}}{PMA_{50}^{Hill} + PMA^{Hill}}, \tag{2.2}$$

where PMA is postmenstrual age in (usually) weeks, $Hill$ is a sigmoidicity coefficient and PMA_{50} is the PMA when maturation is half complete [52, 90].

2.2 Aim

Different modellers use different parameterisations for scaling drug clearance, and there is no agreement on how to best account for both maturation and size in paediatric PK studies [69, 73, 91]. The aim of this chapter of my thesis is to identify different approaches for scaling CL in neonates, infants and children used in the literature, and to compare them between each other, and against the suggested standard approach, which is allometric scaling with a single fixed allometric exponent combined with a sigmoid maturation function, by applying all models to the same dataset.

2.3 Methods

2.3.1 Search for published models for scaling clearance

The MEDLINE database was systematically searched through PubMed in January 2015 and again in March 2015 to identify models for scaling drug clearance using the allometric approach. Search key words included allometry, allometric, scaling, pharmacokinetic, and PK. Also, NMUsers discussion group (i.e. a forum for users of the NONMEM software) [92] was emailed in order to find models that could

have been missed by searching only through PubMed.

The search produced 14 distinct models for describing the change in CL between neonates and adults. Additionally, three simple allometric models (one model with a single estimated allometric exponent, and two with a fixed exponent of 0.75 or 0.67), and a model comprising allometric weight and a sigmoidal maturation function (with all parameters estimated and another model with all parameters fixed to the values of a previously published study of renal maturation [52]) were also compared.

2.3.2 Data collection

Electronic bibliographic database MEDLINE was searched through PubMed in December 2014 (and the search was updated in March 2015) to identify clinical PK studies where clearance of gentamicin was reported. Gentamicin was chosen as it is one of the drugs discussed in this thesis, and because it undergoes mainly renal elimination (the same as meropenem, the other drug that is discussed in this thesis). The filter "humans" was applied and the search strategy included key words gentamicin, pharmacokinetic, PK. Only reports where gentamicin was administered intravenously were chosen. Age of the subjects in the studies was not specified in the search as the goal was to find clearance values across the whole age range, from birth to adulthood. The reference lists of the publications that were identified were also manually searched.

Since it is known that during the first week of life due to changes in renal and intra-renal blood flow clearance changes very rapidly [51, 52], a study that only reported one mean value of the PK parameters for a group of subjects with a wide age range (from the first month of life, up to 16 years) was not included [93]. Also, as the kidney function decreases in adults and the elderly (Figure 2.2), publications that only included a single value of CL for subjects with their ages ranging from approximately 15 up to 80 or 90 years, were excluded [94, 95, 96].

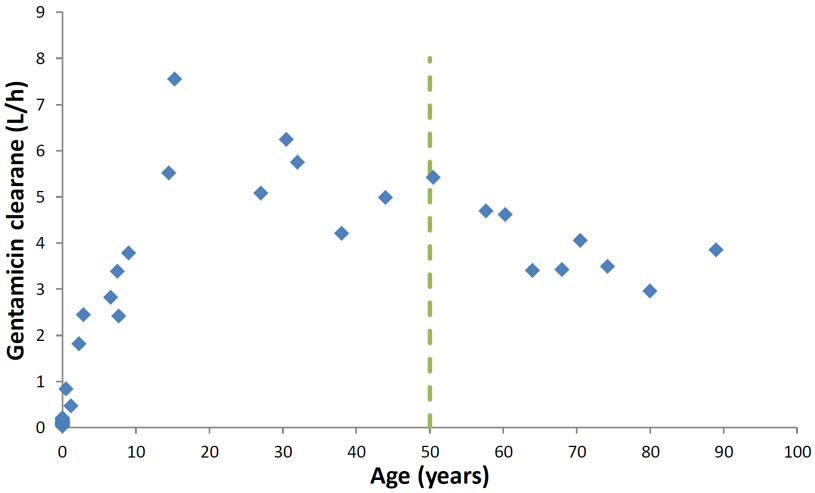

Figure 2.2: Gentamicin clearance plotted against age in years. Green dashed vertical line indicates age of 50 years. Data from Table 2.1 and the following references: [97, 98, 99, 100, 101, 102, 103].

Similarly, CL reports for only subjects with their ages >50 years were also not included (there were eight such CL values) [97, 98, 99, 100, 101, 102, 103].

There were 25 manuscripts in total that satisfied the search criteria, with 41 gentamicin clearance values reported. In addition to gentamicin CL, individuals' demographics (ages and weights) were also extracted from the publications. An overview of the dataset is shown in Table 2.1. If only a range of the subjects' weights or ages was given, the middle of the range was used. In neonatal studies, if only birth weight was reported, this was assumed as the current body weight. A gestational age (GA) of 40 weeks was assumed for children and adults that did not have GA reported. Some studies [101, 104, 105] did not report the weight of the subjects, thus their weight was calculated using a previously published weight-for-postmenstrual age formula [106].

Additionally, median gentamicin CL data predicted by a published PBPK model [71] were extracted from the plot, in order to allow for comparison of the PBPK model performance as well.

Table 2.1: Overview of the dataset used for model comparison

Reference	N	GA (weeks)	PNA range	PNA	PMA (weeks)	WT (kg)	CL (L/h)
Neonates			**(days or o.w.)**	**(days)**			
[107]	18	38	0 (few hours)	0	38	3.3	0.17
[108]	29	32	1-7	6	32.86	1.8	0.09
	5	33	12-24	15	35.14	1.95	0.2
[109]	113	33.5	1-46	23.5	36.86	2.2	0.1
[110]	7	39.3	<6h at inclusion	1	39.44	3.27	0.16
[111]	79	35.1	4.2 (3-7)	4.2	35.7	2.06	0.07
[112]	97	38.11	7.78 (2-30)	7.78	39.22	2.95	0.2
[113]	200	32.19	5.49 +/- 5.41	5.49	32.97	1.68	0.07
[114]	277	36	0 (0-27)	0	36	2.52	0.12
[115]	97	33.24	4.61 (1-26)	4.61	33.9	1.93	0.13
[116]	26	26.62	2	2	26.91	0.94	0.03
	5	26.8	3	3	27.23	0.9	0.03
	99	33.04	2	2	33.33	2.03	0.08
	43	32.65	3-4	3.5	33.15	2.13	0.09
	64	39.33	2	2	39.62	3.38	0.2
	30	39.2	3-4	3.5	39.7	3.14	0.16
[117]	19	29.6	1	1	29.74	1.288	0.06
	20	29.6	4	4	30.17	1.288	0.04
	18	33	1	1	33.14	1.827	0.11
	21	33	4	4	33.57	1.827	0.08
[118]	11	35	0.2-3	1.6	35.23	1.82	0.11
[119]	61	28.9	1 (0-45)	1	29.04	1.4	0.03
[105]	12	40	9 (5-16)	9	41.29	3.51*	0.2
[120]	139	32	0-10	5	32.71	1.92	0.07
Children			**(years or o.w.)**	**(years)**			
[121]	208	40	5.8 mo (1-24)	0.48	65.2	6.4	0.83
[104]	31	40	0.5-4	2.25	157	13.1*	1.81
		40	5-10	7.5	430	25.4*	3.38
		40	11-18	14.5	794	51.5*	5.51
[122]	13	40	2.9 (1-5)	2.9	190.8	14.9	2.44
	5	40	9.0 (6-12)	9	508	27	3.78
	7	40	15.3 (13-18)	15.3	835.6	53.5	7.54
[123]	52	40	6.6 +/- 4.1	6.6	383.2	24.1	2.82
		40	7.7 +/- 4.4	7.7	440.4	28.2	2.41
[124]	14	40	1.8 d (0.9-15.2)	0.005	40.3	3.3	0.11
	36	40	14 mo (5-50)	1.17	100.9	7.9	0.47
Adults			**(years)**	**(years)**			
[101]	469	40	21-40	30.5	1626	70.9*	6.24
	225	40	41-60	50.5	2666	72.2*	5.42
[125]	7	40	21-43	32	1704	77.5	5.75
[126]	10	40	22-32	27	1444	70.51	5.08
[127]	11	40	38 (18-55)	38	2016	73	4.21
[128]	11	40	44 +/- 14.1	44	2328	73.4	4.98

GA is gestational age, PNA is postnatal age, PMA is postmenstrual age, WT is weight, CL is clearance, o.w. is otherwise, d is days, mo is months; value +/- standard deviation, or () range; *WT was calculated using a formula from [106]

2.3.3 Comparison of different models for size and maturation

There were 14 models identified in the literature search, and additionally, another five models were compared (individual model equations are listed in Table 2.2). All parameters that were fixed and not estimated in the original study, were fixed during the model comparisons as well – except allometric exponents from the study by Wang *et al* [129], where the exponent was fixed to a different value according to the cut-off weight of 16.5 kg (1.68 and 0.614 for $\leq$ and >16.5 kg, respectively). The exponent was estimated in this case because it otherwise produced unrealistic final clearance estimates. Also, to facilitate comparison of the results, all models were normalised to 70 kg, a standard adult weight. There was no information on birth weight for children and adults, hence current body weight was used in model 10 instead [130].

The first group of models (that described the changes in CL from the neonatal/paediatric period throughout adulthood) included simple allometric models, with only allometric weight scaling and a single allometric exponent (Equation 2.3).

$$CL = \theta_1 \cdot \left(\frac{WT}{70}\right)^b, \tag{2.3}$$

where θ_1 is the predicted value of gentamicin clearance in L/h/70 kg and 70 kg is the standard weight for an adult. In model 1 (Table 2.2) the allometric exponent (b) was estimated, and in models 2 and 3 b was fixed to 0.75 and 0.67, respectively.

The second group of models comprised modelling approaches where the value of the allometric exponent varied as the demographics of the subjects changed. In some models a different value of the allometric exponent was assumed according to a cut-off age (model 4) [73] or weight (models 5 and 6) [73, 129]. A different approach was taken in model 7, where b changed exponentially with body weight

[131]. In models 8 and 9 the allometric exponent changed in a sigmoidal fashion with weight [88] or age [132].

The last group of compared models were models that had a single non-varying allometric exponent (either fixed or estimated) and a function, accounting for the maturation part of the differences between the adult and the paediatric clearance (Equation 2.4).

$$CL = \theta_1 \cdot \left(\frac{WT}{70}\right)^b \cdot maturation function. \tag{2.4}$$

Models 10, 11 and 12 had the age (either the postnatal or postmenstrual age) effect incorporated in the model in a linear way [130, 115, 89], and model 13 in an exponential manner [133]. The next set of models (models 14-16) were models with recently suggested approach for scaling clearance [69], that is, the maturation function was in this case a sigmoidal function, driven by the postmenstrual age. In model 14 all parameters were estimated, in model 15 the allometric exponent was fixed to 0.75 and the parameters of the maturation function were estimated [89], and in model 16 all parameters were fixed [52]. A similar approach was adapted in model 19 where the allometric exponent was fixed to 0.75, but the sigmoid maturation function was driven by the postnatal age, instead of PMA [134]. The remaining two models (models 17 and 18) are models where b was also fixed to 0.75; however, the maturation function was characterised either in an asymptotic exponential (model 17) [135], or an exponential manner, with special parameterisation for the magnitude and the rate constant of the maturation as well (model 18) [136].

The 19 described models (Table 2.2) were then fitted to the gentamicin clearance data extracted from the literature using NONMEM version 7.3 (ICON Development Solutions, Ellicott City, Maryland) [27]. An exponential residual error was assumed. Goodness-of-fit graphs were produced using the R program, version 3.1.0 [137], and R-package ggplot2 [138]. Numerical comparison of the models was

undertaken by comparing the Akaike information criterion (AIC) values (Equation 2.5), overall, and per age group. Age groups were defined as follows: neonates (0-28 days of life), infants (1 month-2 years), children (2-12 years), adolescents (12-18 years), adults (>18 years) [139]. AIC is a goodness-of-fit measure that penalises the value of the -2 log likelihood according to the p number of parameters used in the fitted model (Equation 2.5). The model with a lower value is therefore more parsimonious, and the preferred one.

$$AIC = -2 \cdot log\mathscr{L} + 2 \cdot p. \tag{2.5}$$

2.4 Results

All of the compared models are listed in Table 2.2, together with numerical results of the model comparisons. Goodness-of-fit of the model predictions to the literature gentamicin clearance data for each of the 19 models and also predictions from the PBPK model [71] are shown in Figure 2.3. In three models (models 7-9) the allometric exponent varied within a range of values – this change plotted against weight is shown in Figure 2.4. The AIC values per age group, relative to the AIC values for model 15, are presented in Table 2.3.

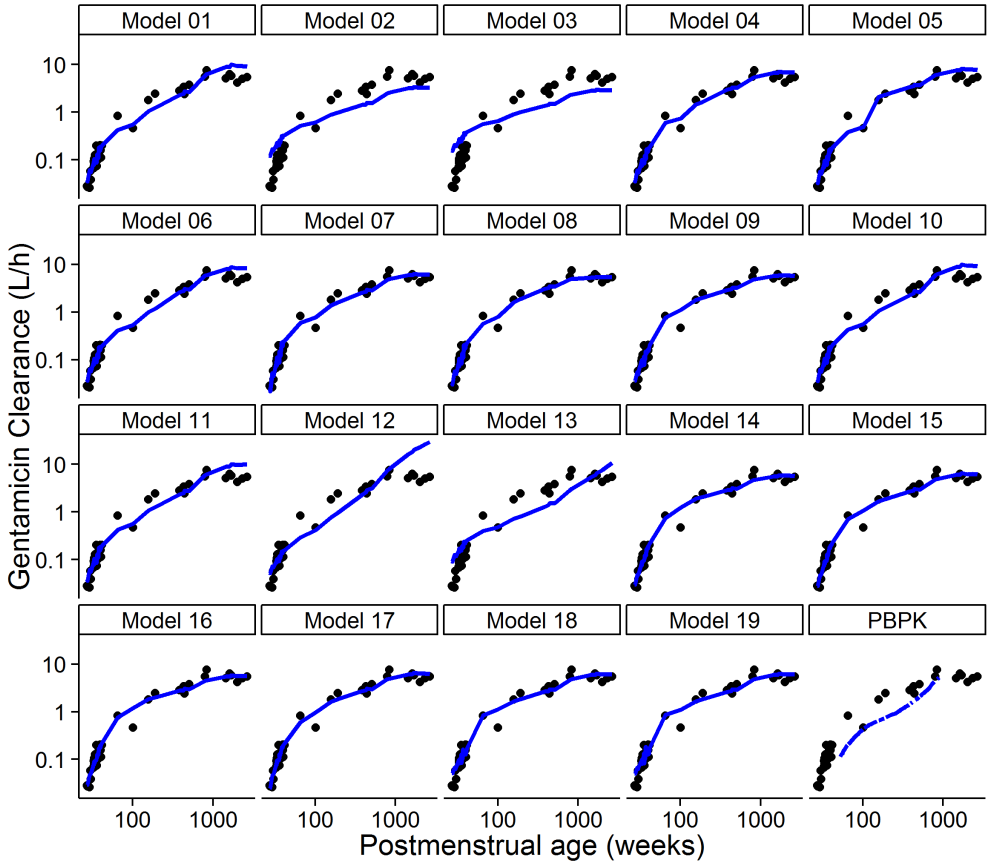

Figure 2.3: Plots showing goodness-of-fit of the compared models (described in Table 2.2) to the gentamicin dataset. Black dots are gentamicin clearance data from the literature (Table 2.1), and blue lines indicate model predictions. Postmenstrual age of 100 and 1000 weeks corresponds to approximately 1.15 and 18.4 years of postnatal (or chronological) age, respectively.

Table 2.2: Results of the model comparison

#	Ref	Equation	Studied population	AIC	θ_1	Allometric exponent	Other thetas
1		$CL = \theta_1 \cdot (\frac{WT}{70})^{\theta_2}$		-107	8.79	1.27	
2		$CL = \theta_1 \cdot (\frac{WT}{70})^{0.75}$		-34.3	3.15	0.75 fix	
3		$CL = \theta_1 \cdot (\frac{WT}{70})^{0.667}$		-18.4	2.81	0.667 fix	
4	[73]	$CL = \theta_1 \cdot (\frac{WT}{70})^{b}$, $b: 1.2 \leq 3mo, 1.0 > 3mo - 2y, 0.9 > 2 - 5y, 0.75 > 5y$	Neo-child	-131	6.62	1.2, 1.0, 0.9, 0.75 fix	
5	[73]	$CL = \theta_1 \cdot (\frac{WT}{70})^{b}, b: 1.25 \leq 9kg, 0.76 > 9kg$	Neo-child	-118	7.57	1.25, 0.76 fix	
6	[129]	$CL = \theta_1 \cdot (\frac{WT}{70})^{b}, b: \theta_2 \leq 16.5kg, \theta_3 > 16.5kg$	Neo-adu	-106	7.96	1.24, 1.04	
7	[131]	$CL = \theta_1 \cdot (\frac{WT}{70})^{b}, b = \theta_2 \cdot WT^{\theta_3}$	Neo-adu	-127	5.95	1.29-0.69	θ_2=1.27, θ_3=-0.147
8	[88]	$CL = \theta_1 \cdot (\frac{WT}{70})^{b}, b = \theta_3 - \frac{\theta_5 \cdot WT^{\theta_2}}{\theta_4^{\theta_2} + WT^{\theta_2}}$	Neo-adu	-127	5.31	1.19-0.21	θ_2=1.12, θ_3=1.23, θ_4=17.5, θ_5=1.27
9	[132]	$CL = \theta_1 \cdot (\frac{WT}{70})^{b}, b = \theta_3 - \frac{\theta_5 \cdot PNA^{\theta_2}}{\theta_4^{\theta_2} + PNA^{\theta_2}}$	Neo-child	-136	5.65	1.19-0.55	θ_2=0.66, θ_3=1.21, θ_4=0.36, θ_5=0.68
10	[130]	$CL = \theta_1 \cdot (\frac{WT}{70})^{\theta_2} \cdot (1 + \theta_3 \cdot PNA)$	Neo	-105	8.79	1.27	θ_3=$\sim$0
11	[115]	$CL = \theta_1 \cdot (\frac{WT}{70})^{\theta_2} + \theta_3 \cdot PNA$	Neo	-105	7.94	1.24	θ_3=0.0324
12	[89]	$CL = \theta_1 \cdot (\frac{WT}{70})^{0.75} \cdot (1 + \theta_2 \cdot (PMA - 40))$	Neo	-64.5	1.48	0.75 fix	θ_2=0.007
13	[133]	$CL = \theta_1 \cdot (\frac{WT}{70})^{0.75} \cdot e^{\theta_2 \cdot (PMA - 40)}$	Neo	-42.4	2.37	0.75 fix	θ_2=0.0006
14		$CL = \theta_1 \cdot (\frac{WT}{70})^{\theta_2} \cdot \frac{PMA^{\theta_3}}{\theta_4^{\theta_3} + PMA^{\theta_3}}$		-136	5.56	0.623	θ_3=3.21, θ_4=58
15	[89]	$CL = \theta_1 \cdot (\frac{WT}{70})^{0.75} \cdot \frac{PMA^{\theta_2}}{\theta_3^{\theta_2} + PMA^{\theta_2}}$	Neo	-136	5.99	0.75 fix	θ_2=3.25, θ_3=49.9
16	[52]	$CL = \theta_1 \cdot (\frac{WT}{70})^{0.632} \cdot \frac{PMA^{3.33}}{55.4^{3.33} + PMA^{3.33}}$	Neo-adu	-141	5.41	0.632 fix	
17	[135]	$CL = \theta_1 \cdot (\frac{WT}{70})^{0.75} \cdot (1 - \theta_2 \cdot e^{-(PMA - 40) \cdot \frac{ln2}{\theta_3}})$	Neo-adu	-138	6.07	0.75 fix	θ_2=0.68, θ_3=32.7
18	[136]	$CL = \theta_1 \cdot (\frac{WT}{70})^{0.75} \cdot (\theta_2 + (1 - \theta_2) \cdot (1 - e^{-PNA \cdot \theta_3}))$	Inf-child	-127	5.86	0.75 fix	θ_2=0.207,θ_3=3.59
19	[134]	$CL = \theta_1 \cdot (\frac{WT}{70})^{0.75} \cdot (\theta_4 + (1 - \theta_4) \cdot \frac{PNA^{\theta_2}}{\theta_3^{\theta_2} + PNA^{\theta_2}})$	Neo-child	-126	5.86	0.75 fix	θ_2=1.4, θ_3=0.132, θ_4=0.21

is the model number, Ref is reference, AIC is Akaike information criterion, θ_1 is gentamicin clearance (CL) in L/h/70 kg, WT is body weight in kilograms, mo is months, y is years, PMA is postmenstrual age, PNA is postnatal age, neo is neonates, inf is infants, child is children, adu is adults. All θs represent parameters that were estimated.

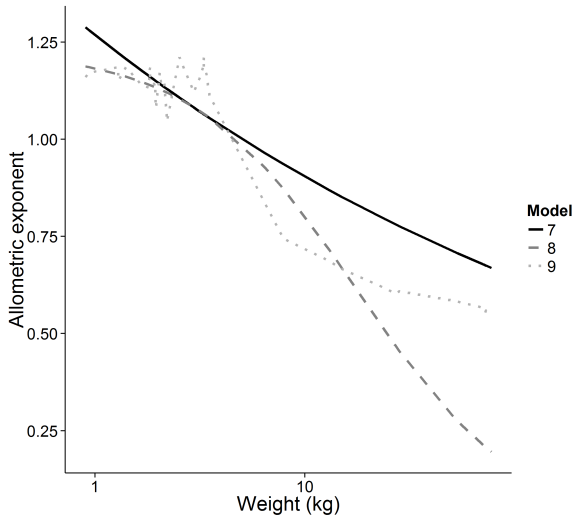

Figure 2.4: The relationship between the allometric exponent and weight for three models with varying allometric exponent. Model numbers correspond to models listed in Table 2.2. The allometric exponent in model 9 changes with age, which is the reason for the fluctuations.

Table 2.3: AIC values per age group for the compared models

Model	overall AIC	neonates	infants	children	adolescents	adults
1	29.5	6.8	-1.4	7.7	-3.4	11.8
2	102	76.4	-5.3	10.6	2	2.3
3	117.9	90.5	-4.9	9.7	2.8	3.8
4	5.2	2.9	-6.1	-1.8	-5.6	-0.3
5	18	3	0.5	-0.3	-5.7	4.5
6	30.6	9	1.1	11.3	-1.4	10.5
7	8.8	7.4	-3.7	0.9	-2.5	-1.3
8	9	12	3	4.8	3.6	1.5
9	0.6	2.6	4.5	3.1	4.5	1.9
10	31.5	8.8	0.6	9.7	-1.4	13.8
11	31.4	8.3	0.8	9	-1.4	14.7
12	71.8	20	2.8	12.8	-1	29.2
13	93.9	57.5	-3.1	19.7	1.4	10.4
14	0.7	1.4	3.1	1.3	3.1	-0.1
15	**0**	**0**	**0**	**0**	**0**	**0**
16	-4.9	-4.5	-3.1	-4.6	-2.1	-6.6
17	-1.2	-1.5	0.3	-0.1	-0.2	0.3
18	8.9	7.9	0.1	0.7	0.1	0.1
19	10.1	9.2	2	2.7	2.1	2.1

Model numbers correspond to the models described in Table 2.2. AIC is Akaike information criterion. All AIC values are relative to AIC values for model 15 (in bold), negative values indicate a better fit than model 15.

2.5 Discussion

Different approaches for scaling CL in the paediatric population were identified and compared on the same dataset, using gentamicin as an example drug. This approach differed than that taken by most authors trying to answer the question of which model to use, who have tended to compare a limited range of models [140] on data from multiple drugs. This important question has been addressed by systematically searching for published models, and then comparing all of them on the same dataset, thereby providing an objective comparison of model fits.

No model consistently out-performed the fixed allometric weight and sigmoidal maturation model across all age groups (see Table 2.3), but for gentamicin (a renally cleared drug) a fixed exponent of 0.63 performed better than 0.75. This result should perhaps not be a surprise, given that gentamicin is mainly cleared by glomerular filtration, and 0.63 was the exponent estimated from a study of glomerular filtration rates across a wide age spectrum [52].

Visual examination of the diagnostic plots (Figure 2.3) showed that using only allometric scaling (without accounting for maturation) with a single fixed allometric exponent of either 0.75 or 0.67 ($\sim$BSA) overpredicted the neonatal gentamicin CL, and underpredicted the adult CL. This is in agreement with Mahmood [141], who also found that using this approach results in overprediction of CL in neonates. Moreover, fixing the allometric exponent resulted in a lower estimate of a typical value of CL, compared to when the allometric exponent was estimated (models 2 and 3 versus model 1, respectively; see Table 2.2). When a non-varying allometric exponent was estimated the predictions proved better than when it was fixed; however, CL in adults was overpredicted in this case (this was probably because the allometric exponent was estimated to be 1.3, which agrees more with what was previously found for neonates [73]). The reason for the estimated value of the allometric exponent to be closer to the value for neonates

might be that more than half of the data points (i.e. 25 out of 41) came from neonates, and only 6 from adults (>18 years of age). Allometric scaling with a single value of the allometric exponent could possibly be used for drugs with their CL mature at birth; however, this is almost never true. Or, this approach could be used if the age group studied is older than the age when the maturation of the eliminating organ is completed.

Models with body weight- or age-dependent allometric exponent, where the exponent changed according to a cut-off value of a demographic (models 4-6) or with a function (models 7-9) provided a good fit to gentamicin CL data; except when models 5 and 6 were used there was some overprediction of adult CL (Figure 2.3). These two models had higher AIC values (overall and per age group) compared to other models from this group (Table 2.3).

When size and age effect were taken into account separately – with allometric equation and a maturation function – and a linear or exponential maturation function was used (models 10-13) this provided a worse overall fit (Table 2.3) and under- and overprediction of CL data from children and adults, respectively (Figure 2.3). Whilst these models did not manage to describe gentamicin CL in adults, they could still be used when describing CL changes in a population with a small age range, for example, neonates [115, 142, 143].

The remaining models (models 14-19) managed to describe the CL data (Figure 2.3), which was seen from the low AIC values for these models (Table 2.3). Model 16 (namely the model where the parameters were fixed to values from a renal maturation study [52]) gave consistently the lowest AIC values, in each age group (Table 2.3). Despite the ability of these models to describe gentamicin CL, PMA (i.e. the sum of gestational age and PNA) should be used instead of PNA, since renal maturation begins *in utero* [44].

For exploratory purposes, median gentamicin CL prediction from a published

PBPK model [71] was overlaid on the CL data extracted from the literature (Table 2.1). The PBPK model underpredicted paediatric CL data, which was also what was observed by Johnson *et al* [71]. The neonatal and adult CL data could not be compared as only data from individuals of 3 months up to 16 years of age could be extracted from the graph [71].

All of the compared models except models with only allometric scaling, where the allometric exponent had a single non-changing value, and models where maturation was taken into account in a linear or exponential way, provided a good fit to the data (Figure 2.3). Many models had similar AIC values, but none had consistently better AIC value (across age groups) than the suggested approach, namely a combination of allometric weight scaling and a sigmoidal maturation function (Table 2.3); therefore this type of model can be proposed as a standard approach for describing the changes in CL due to age and weight. The only model that had lower AIC values (overall and per age groups) was a variation of this model, i.e. the parameters were fixed to values shown to provide the best fit when describing the maturation of GFR [52].

There are several advantages of using a combination of the allometric scaling with a sigmoid maturation function approach. For example, parameters are easy to interpret – PMA_{50} indicates the PMA when maturation of the eliminating organ is half complete (the sigmoidal function approaches the value of 1 with increasing age, meaning that for older children/adults it is no longer important), and thus helps to gain more knowledge about the underlying biology. The Hill parameter, responsible for the steepness of the maturation slope, is flexible enough to be able to describe both rapid and slow organ maturation. Furthermore, this model was already evaluated for 46 drugs by Holford *et al* [69].

Using a model where the allometric exponent varies with age or weight (models 4-9; Figure 2.4) is perhaps less intuitive; for example in model 7 (see Table 2.2) the allometric exponent (i.e. exponent on weight) is estimated by having another

exponent on weight. Moreover, in models 4-6 the threshold when the allometric exponent changes is arbitrary.

Although some advocate that the allometric exponent should be estimated [73], this is not always possible, especially when analysing data from a population with a small age/weight range (and is important particularly when developing a model that one wants to use to extrapolate to other populations). When the exponent on weight was estimated (model 14, it was estimated to be 0.623) it provided a very similar fit to when it was fixed (model 15). Whether the exponent was fixed to 0.75 (model 2) or 0.67 (model 3) provided similar results (Table 2.3); which confirmed what was previously found [69] – that the difference between the value of allometric exponent of 0.75 or 0.67 is not clinically important when extrapolating within humans. Also, as described in Section 2.1, the variability in the value of the allometric exponent is such that any value within 0.63 to 0.78 seems appropriate. Thus, it would be more parsimonious to fix (rather than estimate) the value of the allometric exponent, especially when analysing data from a population with small age/weight ranges.

Since gentamicin is not metabolised and is mainly excreted *via* glomerular filtration [144]; similarly to meropenem, approximately 75% of which is eliminated unchanged *via* the kidneys [50, 145], the allometric exponent and the parameters of the maturation function could be fixed to values from a study of renal maturation that involved over 1,000 observations, from neonates to adults [52]. The model where the allometric exponent was fixed to 0.632, and Hill and PMA_{50} values were fixed to 3.33 and 55.4, respectively (model 16), had consistently lower AIC values than model 15, where the allometric exponent was fixed to 0.75 and the parameters of the maturation function were estimated (Table 2.3).

2.6 Summary

Nineteen different models to describe the change in CL between the neonatal period and adulthood were compared on a dataset, containing CL values from the same drug (gentamicin). The models (apart from a few exceptions) predicted gentamicin CL data similarly; however, no model performed better than a model with allometric weight scaling (with a single fixed allometric exponent) and a PMA driven sigmoidal maturation function. For gentamicin (a renally cleared drug) a value of the allometric exponent of 0.63 (taken from a study of GFR maturation) provided lower AIC values than 0.75. Hence, this approach can be suggested as a standard approach for scaling CL of renally cleared drugs in the paediatric population. Having one standard model would facilitate comparison of similar compounds, make meta-analysis easier, and help one to learn more about CL maturation. Future work should involve testing whether this approach (with 0.75 fixed allometric exponent) can also be used for drugs with hepatic or mixed clearance.

Chapter 3

Pharmacokinetic model for treatment individualisation

3.1 Introduction

Gentamicin was discovered in the 1960s [146] and its PK have been studied more extensively since the 1970s, in adults [147], as well as in neonates [148]. However, whilst it is definitely not a new drug, there are still problems with its dosing and monitoring, especially in neonates, as reported in the UK National Patient Safety Agency alert [149] and a recent study by Valitalo *et al*, where simulations were used to define dosing guidelines [150]. To try to improve gentamicin monitoring (and therefore contribute towards safer use) in the neonatal population the neoGent study was designed and undertaken, and the results from it are presented in this chapter.

3.1.1 Gentamicin pharmacodynamics

Gentamicin is an aminoglycoside antibiotic, and like other antimicrobials from this group is produced by Gram-positive bacteria from the order Actimycetales (more specifically, gentamicin is produced by *Micromonospora purpurea*) [151]. Chem-

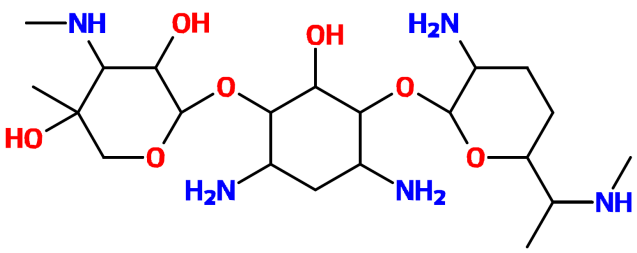

Figure 3.1: Chemical structure of gentamicin.

ically it is a cyclitol ring, linked through a glycosidic bond to two 6-membered sugars, with five amino groups attached to this structure [151] (Figure 3.1).

3.1.1.1 Gentamicin mode of action

Due to its chemical structure gentamicin exhibits high water solubility and has a basic character [151], which means it cannot easily cross cell membranes [152]. Having a polycationic charge, gentamicin firstly binds to the anions on the outer cell membrane, which increases the permeability of the membrane. Then, to pass through the membrane into the cytosol, an electron transport system is required, and since the source of the electrons is cell's respiratory cycle, gentamicin is not effective against anaerobic pathogens [144]. Once in the cytosol, gentamicin irreversibly binds to the 16S rRNA receptor on the 30S subunit of the bacterial ribosome and interrupts synthesis of proteins that are involved in the production of the bacterial membrane. This causes the bacterial membrane to sustain increasing damage, therefore more gentamicin is able to penetrate the cell, which finally leads to bacterial cell death [144, 153, 154].

Gentamicin is effective and primarily used against Gram-negative aerobic bacteria (e.g. *Acinetobacter*, *Pseudomonas*, *Enterobacter* species, *Escherichia coli* (*E. coli*)) and staphylococci [155, 154, 156]. It exhibits a synergistic effect when administered with drugs that increase its permeability to the bacterial cell – for example, penicillins or vancomycin, a combination that is commonly used in neonatal intensive care units (NICU) [154, 144, 157]. Because of its effectiveness

against *E. coli*, one of the main pathogens of early-onset neonatal sepsis, especially in pre-term newborns [1, 158, 159], gentamicin is one of the most frequently administered antimicrobials in NICU [160, 161]. However, gentamicin use is limited by its narrow therapeutic index and risk of toxicity, specifically nephro- and ototoxicity [157].

3.1.1.2 Gentamicin toxicity

Due to similar structures of human mitochondrial ribosomes and bacterial ribosomes, gentamicin (especially in higher concentrations) not only affects prokaryotic cell proteins but also the synthesis of human proteins [153]. This leads to toxic effects, specifically tubular cytotoxicity and toxicity of the eighth cranial nerve (causing ototoxicity) [157]. Gentamicin toxicity is related to total drug exposure (AUC) [162], and not to peak concentrations (C_{max}) as its effectiveness.

Tubular necrosis is said to occur in 10-30% of adults, when gentamicin treatment lasts longer than 7 days [152, 163, 164]. Studies in neonates are lacking, however, the incidence of nephrotoxicity appears to be lower in neonates [165]. Nephrotoxicity is caused by the accumulation of gentamicin within the epithelial cells of proximal tubules (15% of the administered dose is reabsorbed in the tubuli [166]), where it induces apoptosis of the cell mitochondria. This causes a decrease in the total number of the proximal tubule cells, activation of local renin-angiotensin system, local vasoconstriction, tubular obstruction, which reduces renal blood flow and consequently causes the glomerual filtration rate (GFR) to decrease [163, 152]. GFR is additionally lowered since gentamicin (in addition to tubuli) also affects glomeruli [152]. Uptake of the aminoglycoside into the tubular epithelium is a saturable process, meaning that higher doses (and therefore higher peak concentrations) do not directly lead to higher nephrotoxicity. Conversely, it is more common with elevated trough concentrations (i.e. increased total drug exposure) [49, 153], because renal damage causes reduced renal clearance and

therefore increased trough concentrations. Nephrotoxicity is reversible [49], but excretion of aminoglycosides from proximal tubules is not a fast process [166] – renal function is said to return to normal within 3 to 6 weeks [49].

The second most common adverse effect of gentamicin is ototoxicity. It can occur independently of nephrotoxicity and is usually not reversible, since sensory hair cells are permanently destroyed [49, 167]. More studies are needed to ascertain the incidence of ototoxicity in neonates, however, it seems to occur less frequently and only transiently in this population, compared to adults [165, 168]. It has been suggested that genetic mutations in mitochondrial DNA (e.g. A1555G mutation) could be the most common reason for the occurrence of ototoxicity [169, 170, 171, 172]. This mutation makes mitochondrial rRNA appear similar to prokariontic rRNA, making it a target for gentamicin [169]. Even though all human cells would be affected by this mutation, it is thought to be only important in tissues with a lot of mithochondria, such as sensory cells of the ear [169]. An American study by Ealy *et al* found that the prevalence of mitochondrial mutation is approximately 1.8% in population of subjects who were once in NICU [173]. A noisy environment in the neonatal units could also increase the susceptibility to aminoglycoside induced ototoxicity [170].

3.1.2 Therapeutic drug monitoring of gentamicin

Gentamicin is an antibiotic with a narrow therapeutic window, i.e. the difference between its effective and toxic dose is small [174, 175]. Therapeutic drug monitoring (TDM) is therefore advised when administering it to ensure adequate peak concentrations (that is, maximise its efficacy) and trough concentrations – to minimise the risk for nephro- or ototoxicity [153, 174]. TDM uses measured circulating drug concentrations to define or regulate the dosing regimen, and is particularly important for subpopulations at higher risk of gentamicin toxic effects, such as neonates, who have immature kidney function and consequently higher gentamicin

AUC [162, 95, 174]. Additionally, neonates have a large between-subject variability in their PK parameters, therefore dose individualisation is also required in this population [49].

There are three main approaches for model-based/guided dose individualisation: single-level methods or nomograms, AUC methods and Bayesian methods.

a) Using a nomogram or a concentration dosing table is the simplest and an inexpensive method. It involves taking one blood sample in the elimination phase and then comparing it to a nomogram [49, 176, 162]. A study by Dersch-Mills *et al*, who validated a nomogram on data from 104 and 38 neonates in their first week of life and with ages >7 days, respectively, showed that nomograms can be a useful tool for individualising the dose interval [177, 178]. However, because nomograms only involve a sample from the elimination phase, C_{max} could be underestimated and clinical effects not reached in case of an increased volume of distribution [162], which is common during sepsis [100]. Nomograms are also difficult to design for neonatal data, as it is not possible to incorporate covariates that would affect the clearance, such as PNA, PMA, and markers of renal function.

b) AUC methods involve taking two or more samples, and then estimating the AUC using a simplified 1-compartment PK model [49, 176, 162, 179]; or using a full AUC method (without an underlying model assumption) which requires ≥4 samples per subject. This method may not be the most suitable for neonates, as rich sampling is rarely possible in this population due to their limited blood volume. Using a 1-compartment model is also not appropriate as gentamicin mostly shows multi-compartment kinetics [180].

c) Bayesian methods use prior knowledge from a population PK model and involve taking one or two samples [49, 176, 162, 181]. Particularly the drawbacks of nomograms and 1-compartment methods make the Bayesian

method the most appropriate for neonates.

TDM is typically used to define the optimal dosing interval, and/or an optimal dose. Historically, gentamicin was administered several times a day, but, now the preferred dosing regimen is once-daily or an extended-interval dosing regimen [66, 49, 153]. This has several advantages over the multiple-daily dosing, for example, higher peak and lower trough concentrations, meaning higher efficacy and lower toxicity [182, 183, 184, 67]. Higher C_{max} means that the post-antibiotic effect is prolonged and the risk of bacteria developing adaptive resistance is minimised, as more of them get initially killed [182, 185]. What is especially important for the neonatal population is that an extended-interval dosing regimen ensures lower toxicity even when renal function is impaired [182] and allows for less frequent TDM [177], lowering the burden on neonates.

Dosing in neonates is usually based on their body weight and/or age [153], and the British National Formulary for Children (BNFC) recommends a dose of 5 mg/kg for neonates with PNA <7 days and >7 days with a dosing interval of 36 and 24 hours, respectively [186]. According to the European Committee on Antimicrobial Susceptibility Testing (EUCAST) the most common MIC for *E. coli* when treated with gentamicin is between 0.25 and 1 mg/L [187]; and the resistance and susceptibility breakpoints for Enterobacteriaceae are 4 and 2 mg/L, respectively [188]. Considering this and the fact that C_{max}/MIC ratio for gentamicin should be approximately 8-12 [65, 64], it can be concluded that gentamicin target peak level in neonates should be >16 mg/L for MIC of 2 mg/L (i.e. sensitivity breakpoint for Enterobacteriaceae [188]). However, this is a worst-case scenario, the majority of e.g. *E. coli* has MIC below that value. Recommended trough levels (to prevent the onset of toxicity) for gentamicin in neonates are <2 mg/L or <1 mg/L, according to BNFC [186] and the National Institute for Health and Care Excellence (NICE) [189] guidelines.

3.1.3 Gentamicin pharmacokinetics

Gentamicin is not absorbed from the gastrointestinal tract [183, 66], hence has to be administered intravenously. Because of its hydrophilic nature gentamicin distributes mainly into the extracellular water [66, 49], with <10% of the drug in the systemic circulation bound to plasma proteins [49, 190]. Due to a higher proportion of total body water and other specific developmental differences, described in Section 1.6.1 neonates exhibit higher volume of distribution (V) of gentamicin compared to older children and adults [49, 179, 47]. Establishing reference values for V in neonates proved difficult as there was no agreement on PK parameters reporting. For example, V was reported for groups of neonates with different demographic characteristics (e.g. sometimes neonates were grouped by their current body weight, birth weight, GA or PMA), or medical conditions were not the same [191, 192, 193, 107]. Still, according to some studies, premature neonates (GA<37 weeks) in the first week of life had gentamicin V of 0.34-0.77 L/kg [177, 157, 194], and mature neonates (GA≥37 weeks) 0.4-0.5 L/kg [177, 109, 195].

Gentamicin is not metabolised in the liver, and is almost entirely eliminated by the kidneys as an active compound [152, 144]; approximately 90% of administered dose is cleared by glomerular filtration [153]. Gentamicin clearance (CL) is thus highly dependent on renal function, specifically GFR. The kidneys of neonates are immature, thus their renal function is reduced, and they have lower CL and longer half-lives, compared to adults [157]. Because renal maturation starts *in utero*, gentamicin CL is better correlated with PMA than PNA [153, 119, 114, 44, 46]. CL of gentamicin was in some studies 0.03-0.05 L/h/kg for preterm [157, 194, 114, 109, 195], and 0.05-0.07 L/h/kg for term newborns [153, 194, 109].

3.1.4 Previously published population pharmacokinetic models

Deriving a Bayesian prior for TDM requires a non-linear mixed-effect PK model, and gentamicin has been widely studied in neonates previously. Therefore, to find previously published such studies, electronic databases, PubMed and EMBASE (through Ovid), were searched in April 2013 (the search was updated in September 2014). There were 12 such studies [196, 197, 109, 198, 199, 115, 114, 113, 119, 124, 200, 111], and a summary of the final model equations from publications is given in Table 3.1.

Table 3.1 shows that published population PK models for gentamicin in neonates are very heterogeneous. Moreover, the majority of them found that the final model is a 1-compartment model, even though gentamicin usually exhibits multi-compartment kinetics [201, 180]. The reason for most studies finding a single compartment kinetics was probably that in general the models were developed using a sparse dataset (with mean number of samples of approximately two per subject). Additionally, serum creatinine has not been found a covariate often (although it is a marker of GFR, and therefore a proxy for gentamicin CL), and the changes in SCr have not been properly accounted for before.

3.1.5 Creatinine

Creatinine, a nitrogenous end product of creatine metabolism in the muscle, is the most commonly used marker of kidney function, more specifically GFR.

3.1.5.1 Creatinine as a marker of glomerular filtration rate

There are three processes that control the elimination of a substance through the kidneys; these are: glomerular filtration, tubular reabsorption and tubular secretion. Glomerular filtration is the easiest to define, therefore it is used to

Table 3.1: A summary of published neonatal gentamicin population pharmacokinetic models

Ref	N	Samples per subject	Cmt	Final model equations
[196]	143*	3.4	1	$CL = \theta \cdot WT + \theta \cdot PNA + \theta \cdot SCr$ $V = \theta \cdot WT$
[197]#	84	NR	1	$CL = \theta \cdot WT + \theta \cdot PNA - \theta \cdot GA$ $V = \theta \cdot WT$
[109]	113	2.4	1	$CL = \theta \cdot WT \cdot \theta_{PMA \leq 34} \cdot \theta_{Apgar<7}$ $V = \theta$
[198]#	NR	NR	1	$CL = \theta \cdot \left(\frac{WT}{2.4}\right)^{1.36}$ $V = \theta \cdot WT$
[199]	469	2.3	1	$CL = \theta \cdot \left(\frac{WT}{2.6}\right)^{0.78} \cdot \left(\frac{GA}{1.21}\right)^{1.21} \cdot \left(\frac{SCr}{96}\right)^{-0.35}$ $V = \theta \cdot \left(\frac{WT}{2.6}\right)^{0.78}$
[111]	79	1.7	1	$CL = \theta \cdot BWT \cdot GA \cdot genderfactor$ $V = \theta \cdot BWT$
[115]	97	2	1	$CL = \theta \cdot WT^{\theta} + \theta \cdot PNA$ $V = \theta \cdot WT^{\theta}$
[114]	277	2.1	1	$CL = \theta + \theta \cdot (GA - 20) + \theta \cdot Apgar_5$ $V = \theta + \theta \cdot sepsis$
[113]	200	2.1	2	$CL = (\theta \cdot WT + \theta \cdot CL_{CR}) \cdot WT + \theta \cdot PNA$ $V_C = \theta \cdot WT$ $Q = \theta$ $V_P = \theta \cdot WT$
[119]	61	14.9	3	$CL = \theta \cdot WT^{0.75} \cdot (1 + \theta \cdot (GA - 28.9)) \cdot (1 + PNA^{\theta})$ $V = \theta \cdot WT \cdot (1 + \theta \cdot (GA - 28.9))$
[124]	50*	4.7	2	$CL = \theta \cdot \left(\frac{WT}{70}\right)^{0.75} \cdot \left(\frac{PNA}{162}\right)^{\theta}$
[200]	1449	2.1	2	$CL = \theta \cdot \left(\frac{WT}{2170}\right)^{0.75} \cdot \left(1 + \theta \cdot \frac{GA-34}{34}\right) \cdot$ $\cdot \left(1 + \theta \cdot \frac{PNA-1}{1}\right) \cdot (1 + \theta_{dopamine})$ $V_C = \theta \cdot \frac{WT}{2170} \cdot \left(1 + \theta \cdot \frac{GA-34}{34}\right)$

Ref is a reference, N is the number of subjects in the study (* denotes that the study included neonates and also infants and children), NR is not reported, # indicates that only an abstract was available, Cmt is the number of compartments in the final model, CL is gentamicin clearance, V is gentamicin volume of distribution, WT is body weight, BWT is birth weight, GA is gestational age, PNA is postnatal age, PMA is postmenstrual age, SCr is serum creatinine, CL_{CR} is creatinine clearance, $Apgar_5$ is Apgar score at 5 minutes.

assess the overall kidney function. The rate of glomerular filtration (GFR) can be either measured or estimated/calculated [202, 203, 204].

Measuring GFR actually means knowing the urinary and plasma concentration of a substance, and the urine flow rate, and then calculating the CL of this substance, which approximates GFR [202, 203]. There are several markers that can be used for measuring GFR, for example, exogenous markers (e.g. inulin, iothalamate, iodothalamate, chromium ethylendiamine tetraacetic acid (Cr-EDTA), iohexol), which are not suitable for routine clinical use due to expensive and lengthy procedures needed to define their concentration [205, 202, 203, 206]. Another option is to use an endogenous marker (such as creatinine, urea, urate, cystatin C, β-microglobulin, α-microglobulin, retinol binding protein [202, 203]), which also eliminates the possibility of an allergic reaction [207]. An ideal endogenous marker for measuring GFR is produced at a stable rate, has a constant plasma concentration, is not protein bound, and is excreted only by GFR [202, 207].

Creatinine is an adequate marker since it is produced at a fairly constant rate, is unbound to proteins, and its concentration can be defined using a rapid, simple, and cheap technique [208]. But, being a small molecule, it is (in addition to glomerular filtration) also eliminated by tubular secretion, which can overestimate GFR by 10-40% (compared to inulin clearance), when renal function is low (GFR <10 mL/min), as creatinine then mostly undergoes tubular secretion [209]. Furthermore, serum creatinine concentration (SCr) can vary, depending on the method that was used to determine it [210], with SCr values determined by enzymatic methods approximately 10-30% lower than when using the Jaffe method [205, 211] (Figure 3.2).

Additionally, due to a non-linear, parabolic relationship between SCr and GFR, normal SCr values do not necessarily indicate normal renal function (Figure 3.3) [212]. Recently, cystatine C has been suggested as a preferred marker of GFR

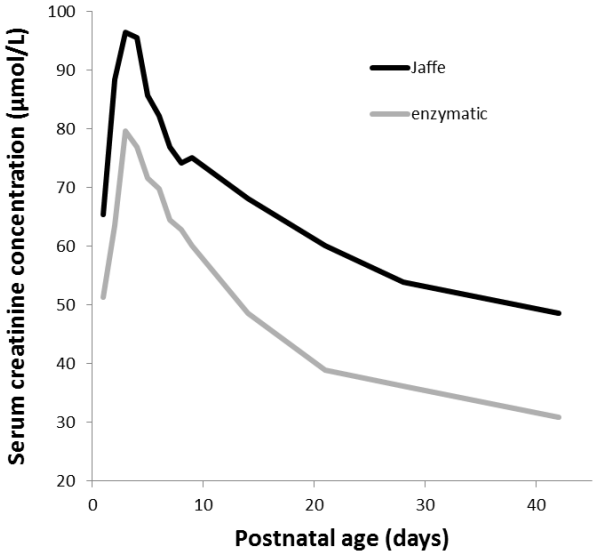

Figure 3.2: Graph of serum creatinine concentration in μmol/L determined using the Jaffe (black line) or enzymatic method (grey line) versus postnatal age in days. Data from a study on preterm newborns [211].

over creatinine as it more sensitive, eliminated only by glomerular filtration, and its plasma concentration is independent of muscle mass, sex, or body composition [213, 214]. Also, unlike SCr, it does not cross the placenta [215]. However, its plasma concentration could be affected by high levels of C-reactive protein [216], it cannot be used to measure GFR as it is completely metabolised in renal tubules [209], and methods for measuring its concentration are more expensive [208, 217], compared to SCr. So, despite its drawbacks, creatinine is still widely used in clinical settings.

Measuring GFR can prove difficult, as collecting a 24-hour urine sample is impractical, time-consuming, and not always possible. An alternative option is to estimate the GFR. However, most GFR estimating equations were developed using data from adults and are intended for that population, for example, the Cockroft-Gault equation [213, 218], the Modification of Diet in Renal Disease (MDRD) equation [219, 213, 220], and the Chronic Kidney Disease Epidemiology Collaboration (CKD-EPI) equation [220]. There is only one equation designed for

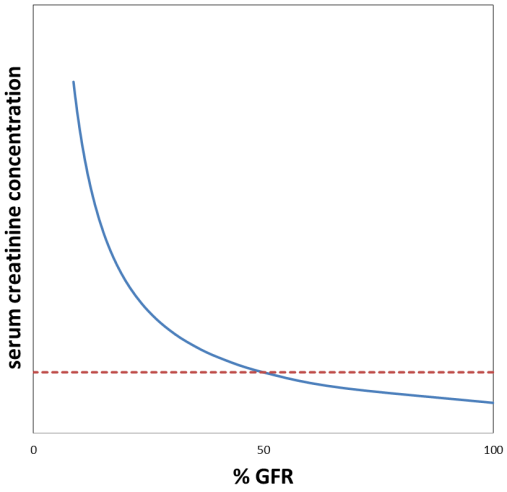

Figure 3.3: Graph of serum creatinine concentration versus percentage of glomerular filtration rate (GFR) from total. The dashed line represents the upper limit of normal serum creatinine concentration. Adapted from [212].

the paediatric population, the Schwartz equation [209, 213]:

$$eGFR(mL/min/1.73m^2) = \frac{k \cdot height(cm)}{SCr(mg/dL)}, \tag{3.1}$$

where ***eGFR*** is estimated GFR, and k is the proportionality constant that describes the relationship between body size and renal elimination of creatinine. However, there are several disadvantages to using this formula in neonates. The proportionality constant is different for preterm and term neonates [213, 221], but, it assumes the same value for infants from birth up to 1 year of age, which is when renal function changes dramatically. Additionally, the equation is not appropriate for GFR <50 mL/min/1.73m^2 [209], which is common in neonates [216, 222]. Moreover, the neonatal renal function is changing rapidly [223], hence making a correct estimation of GFR difficult [210].

3.1.5.2 Reference values of serum creatinine

Serum creatinine concentration is inversely related to GFR, meaning that higher values of SCr indicate lower GFR, and thus renal function. Values of SCr are lower in females [224], as they have less muscle mass, compared to men. After

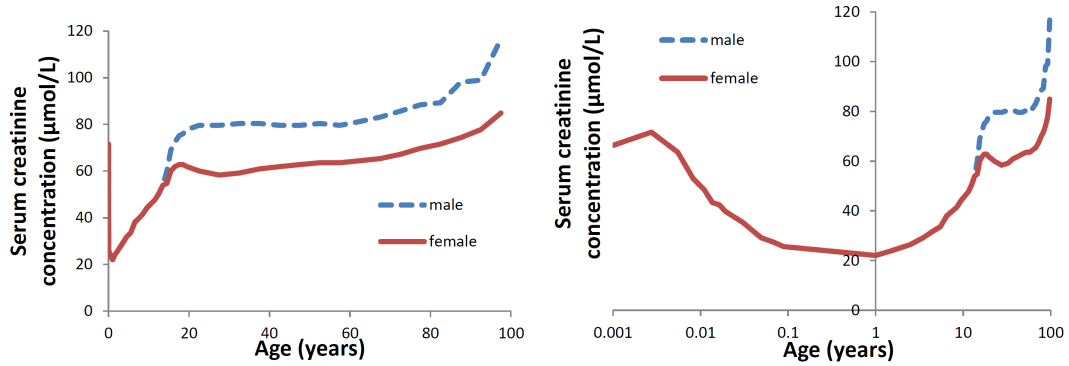

Figure 3.4: Serum creatinine concentration versus age for males (blue dashed line) and females (red solid line). The x-axis in the plot on the right is logarithmic. Serum creatinine concentrations were determined by an enzymatic method. Data include levels from preterm and term newborns and are from [224].

reaching adulthood, renal function starts slowly deteriorating, which is seen as an increase in SCr (Figure 3.4) [224].

At birth SCr is around 73-80 μmol/L [224, 214] or 55-60 μmol/L [225, 223, 226], determined by the Jaffe or enzymatic method, respectively. The initial level appears to be independent of GA, and reflects maternal SCr (Figure 3.5) [202, 224, 223, 226]. However, Finney *et al* found in their study that even the first level differs between term and preterm newborns [225]. A possible reason for their conclusion could be that they measured SCr in preterm newborns on day 1 of life and in term newborns on day 2. This makes the comparison between both groups difficult, as SCr changes rapidly within the first days of life.

Some studies [211, 224, 223, 226] found a rise in SCr 1-2 days after birth. This rise appears to be bigger in less mature newborns [228, 223, 226], and might occur as a result of terminated maternal clearance, some early creatinine production (in neonate's muscles), and low neonatal GFR [211, 214]. Since nephrogenesis is only complete by approximately 34 weeks of PMA, newborns that are born with GA<34 weeks have lower GFR and consequently higher SCr [223]. Additionally, tubular reabsorption or passive tubular diffusion (showing as a back leak) of creatinine might be bigger in more premature newborns, as the tubules are not yet fully mature [211, 225, 228, 229]. This could be confirmed by studies of only

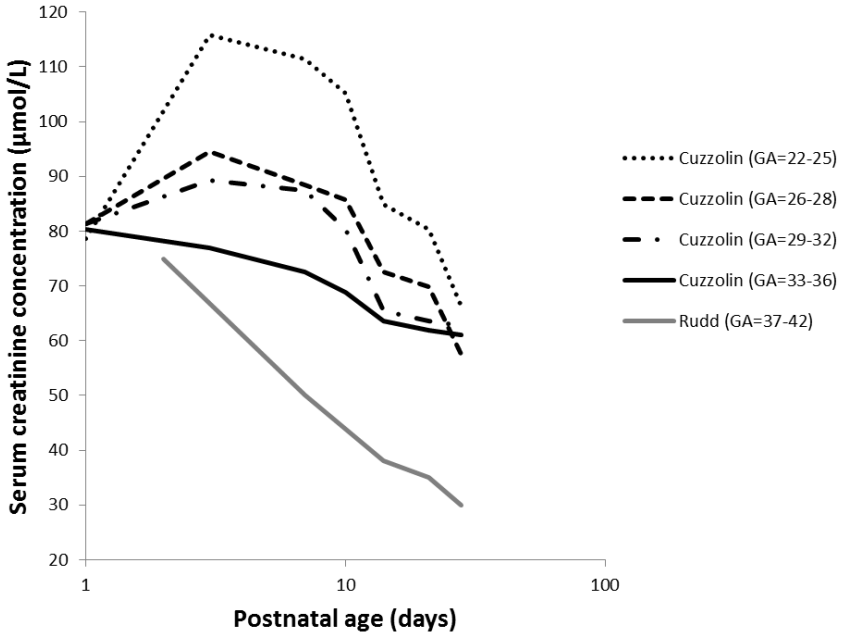

Figure 3.5: Graph of serum creatinine concentration in μmol/L versus postnatal age in days on a logarithmic scale. Data include levels from preterm (black lines) and term (grey line) newborns and are from [226] and [227], respectively. The gestational age (GA) in the brackets is in weeks. Creatinine concentration was determined by the Jaffe assay.

full-term neonates by Boer *et al* [214] and Manzar *et al* [230], who did not find a statistically significant rise in SCr on the second day of life.

From birth, throughout the first month of life, neonatal SCr steeply falls to approximately 35 μmol/L [231, 232] or 20-25 μmol/L [224, 214, 233], determined by the Jaffe or enzymatic method, respectively; reaching the nadir (Figure 3.4). This fall has been shown by Miall *et al* [223] and Kim *et al* [234] to occur later in neonates born more prematurely or with lower birth weight. The steep decrease in SCr is probably due to a significant increase in neonate's renal function [228], caused by the increase in renal and intra-renal blood flows [52]. Then, from the first month of life until approximately 2 years SCr remains almost constant [224], which is most likely a result of increased production (because of higher muscle mass [214]) and increased elimination (as kidney function continues to improve [230]) of creatinine. After the plateau, SCr starts to gradually rise again (the muscle mass continues to increase, but not renal function), reaching adult levels

at approximately age of 20 years [224, 214].

3.2 Aim

The aim of the study described in this chapter was to develop and prospectively evaluate a new population pharmacokinetic model for gentamicin in neonates, which would be perhaps more mechanistic, meaning that it would include biological prior information by accounting for changes in serum creatinine. This model was then used for building a Bayesian computer tool, called neoGent, which enables using gentamicin concentrations collected opportunistically for other purposes (such as blood gasses) to predict the time when the concentration is expected to fall below a pre-specified threshold of 1 mg/L or 2 mg/L, as suggested by the NICE and BNFC guidelines. Doing so, it should help improve gentamicin monitoring in neonates, and could make TDM more convenient for babies, their parents and the clinicians who care for them.

3.3 Methods

3.3.1 Study population

There were two separate datasets used in this study: a model building dataset (i.e. learning) and an evaluation dataset.

To obtain data for model development, electronic bibliographic databases (PubMed/MEDLINE and Embase through Ovid) were searched in April 2013 with no time limitations. The search strategy included the following keywords: (neonates OR neonate OR neonatal OR newborn OR newborns) AND (gentamicin) AND (pharmacokinetic OR PK OR pharmacokinetics). Additionally, the reference lists in relevant papers were manually searched. The inclusion criteria comprised of: a study in neonates, an observational study and not a review,

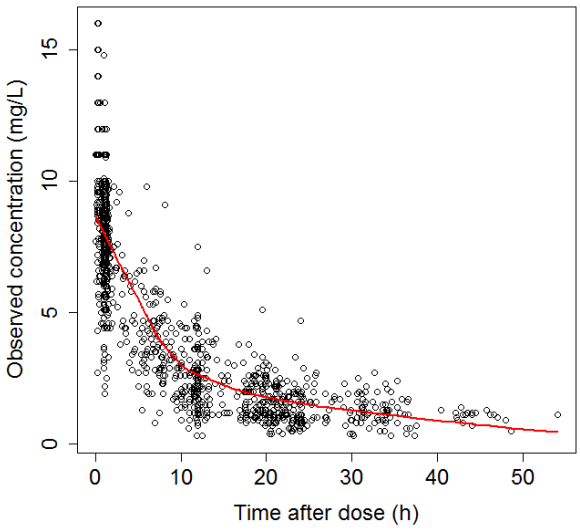

Figure 3.6: Observed gentamicin concentrations (from the model building dataset) versus time in hours after the gentamicin dose has been given. Red line is a lowess smooth line.

intravenous administration of gentamicin, gentamicin concentrations had to be prospectively collected, covariates (weight, GA, PNA, SCr measurements) had to be reported, and the manuscript being in English. The search and screening process is presented in more detail in Appendix A.

Authors of the publications that met the inclusion criteria (n=8) were then invited to share their data [179, 109, 119, 124, 117, 235, 236, 237]. However, despite some email correspondence with a few authors, only data from a study by Nielsen *et al* [119] and data that were freely available online from Thomson *et al* [109] were obtained. Data from both studies were then pooled and included 1163 gentamicin serum concentrations from 174 neonates with their GA ranging from 23.3-42.1 weeks, and PNA 0-65 days. Figure 3.6 shows the PK profile of the dataset used for model development.

Data for the evaluation of the developed PK model and consequently the Bayesian software were collected as a prospective observational cohort study that ran from July 2012 to November 2013 and was performed in five UK hospitals: St George's Healthcare NHS Trust, Liverpool Women's NHS Foundation Trust,

Table 3.2: Summary of analytical methods

	LOD (mg/L)	Precision		
		within-run (%CV)	total (%CV)	measured at
Coventry	0.24	5.2	6.7	1.6 mg/L
Liverpool	0.3	1	2.9	3.4 mg/L
Oxford	0.17	5.59	6.27	1.52 mg/L
Portsmouth	0.13	3.8	5.3	2.1 mg/L
St George's	0.4	5	6.4	2.3 mg/L

LOD is limit of detection, CV is coefficient of variation; for each participating hospital in the neoGent study.

Oxford University Hospitals, Portsmouth Hospitals NHS Trust and Coventry & Warwickshire University Hospitals NHS Trust. For a neonate to be included in the study, the following criteria had to be met: <90 days PNA, expected to survive the study period (as judged by the clinical team), >36 hours gentamicin therapy anticipated, and not currently receiving extracorporeal membrane oxygenation, peritoneal dialysis or hemofiltration. The study was approved by the London Central Ethics committee (reference 12/LO/0455) and a written consent was obtained from parents. Each subject had at least two gentamicin concentrations taken: a routine pre-dose sample, and additional study sample that was taken opportunistically when the neonate required blood level for other reasons. In addition to gentamicin dosing and sampling information, infant's weight, age and SCr were also recorded.

Gentamicin serum concentrations from the model building dataset were analysed using an enzyme immunoassay (EMIT, Syva) [109] and/or fluorescence polarization immunoassay (TDx, Abbot) [109, 119]. Similarly, to determine gentamicin concentrations from the evaluation dataset immunoassay techniques were used (for details see Table 3.2). SCr was determined by the Jaffe method in the model building dataset, and by both the Jaffe and enzymatic method (data from 137 neonates and 26 neonates, respectively) in the evaluation dataset.

3.3.2 Non-linear mixed-effects model building

The non-linear mixed-effects analysis was performed by pooling and simultaneously modelling the concentration-time data from only the model building dataset, i.e. previously published studies [119, 109], using NONMEM version VII (ICON Development Solutions, Ellicott City, Maryland) [27]. The first order conditional estimation method with interaction (FOCE-I) was used.

To define the basic structural model, 1-, 2-, and 3-compartment models were fitted to the data. The between-subject variability (BSV) and inter-occasion variability (IOV) were assumed to follow a log-normal distribution and were tested on all parameters. Occasion was defined as a single dosing interval, with at least one observation following a dose. Regarding the residual variability, an additive, a proportional, and a combination of both models (Equation 3.2) were tested.

$$y_{ij} = f(t_{ij};\Theta_i) + f(t_{ij};\Theta_i) \cdot \varepsilon_{ij,proportional} + \varepsilon_{ij,additive}, \tag{3.2}$$

where y_{ij} is observed gentamicin concentration for an individual i at time t_{ij}, f is gentamicin structural model, Θ_i is a vector of individual parameters, and ε_{ij} is either a proportional or and additive error term.

All PK parameters were *a priori* scaled by weight, standardised to 70 kg using allometric scaling. Allometric exponents were fixed to 0.632 for central CL, 0.75 for inter-compartmental CL, and 1 for volumes of distribution. Different exponents were used for central and inter-compartmental CL as these values were shown best for describing renal CL maturation [52], and tissue blood flows. A PMA driven maturation function (with fixed parameters [52]) was also used to scale CL – i.e. the approach described and suggested in Chapter 2 was applied.

Serum creatinine is an important indicator of GFR and thus gentamicin CL, and gentamicin CL changes rapidly within first days of life (PNA), therefore these

two covariates were tested on CL (this decision was also based on the posthoc estimates of etas versus covariates plots). The covariates were included in the model and considered to significantly improve the fit if the difference in the objective function value (ΔOFV) after their inclusion was >3.84 (p <0.05). Also, to avoid SCr and PNA (time-varying covariates) being interpreted in a step-like fashion, linear extrapolations between observations were made (using a special parameterisation within NONMEM; see Appendix B).

As described in Section 3.1.5 the dynamics of SCr are complicated in newborns as shortly after birth neonatal SCr levels still reflect maternal SCr. Hence, to account for maternal creatinine (and also for endogenous creatinine, and the change in renal function with PMA) literature was systematically searched in April 2013 to find a typical value of serum creatinine (TSCr) for a specific PMA. The search produced 25 publications that satisfied the inclusion criteria, i.e. a study of creatinine in neonates. But, there was considerable variability in SCr sampling techniques and times, as well as the reporting of SCr values. Also, in some cases GA or the exact study day was not reported, the first day of life was was not specified (day 0 or day 1), the sample size was very small (e.g. n<10), the sampling was sparse (e.g. one sample in the first 7 days), or SCr results were given in a graph/bar chart only. The variability between studies made pooling data impossible, therefore two prospective studies (with SCr determined by the Jaffe method, the same as in the model building dataset) were selected. Data from Cuzzolin *et al* [226] were used to determine TSCr for preterm neonates, and data from Rudd *et al* [227] for term neonates (there was no prospective study with good SCr sampling/reporting that included both preterm and term neonates). Equation 3.3 describes a linear decline in TSCr with increasing PMA (Figure 3.7).

$$TSCr = -2.8488 \cdot PMA + 166.48, \tag{3.3}$$

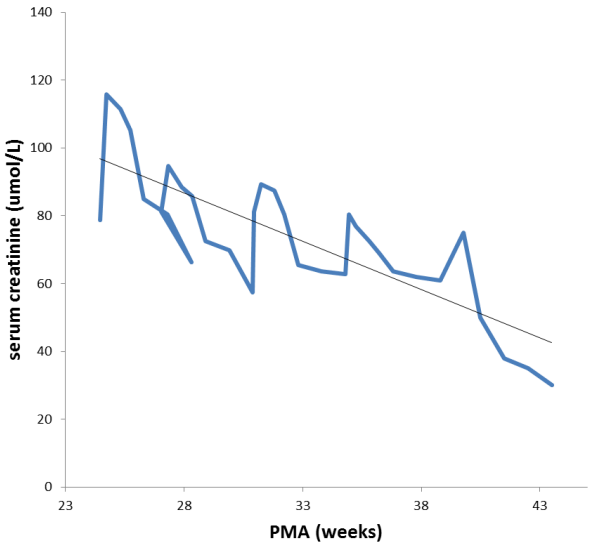

Figure 3.7: Serum creatinine concentration in μmol/L determined using the Jaffe assay from [226, 227] plotted against postmenstrual age in weeks.

where $TSCr$ is typical serum creatinine concentration in μmol/L for a specific postmenstrual age (in weeks).

Measured serum creatinine from the dataset was standardised by TSCr and departures from it were estimated according to Equation 3.4.

$$\left(\frac{measured\ SCr}{typical\ SCr}\right)^{\theta}. \tag{3.4}$$

A function described in Equation 3.5 was used to test PNA and its effects on the rapid changes in gentamicin clearance in the first days of life (first day of life was defined as day 1).

$$postnatal\ age\ function = \frac{PNA}{PNA_{50} + PNA}, \tag{3.5}$$

where PNA_{50} is PNA when clearance is half mature.

After the inclusion of all covariates, the structural model was re-evaluated

and the covariates re-tested. This was done as a backward elimination, meaning that the covariate only stayed included in the model if after it was removed, the OFV increased by >10.83 units, which corresponds to a p-value of 0.001.

3.3.3 Model evaluation

3.3.3.1 Internal model evaluation

Basic goodness-of-fit plots (as described in Section 1.5) were produced and visually examined for any misspecification in the model. The diagnostic plots included observations versus population and individual predictions, CWRES versus time after dose and versus population predictions, and were produced using statistical software R version 2.15.1 [137].

Precision on the final PK parameters was assessed by checking standard errors from NONMEM covariance step and by performing a non-parametric bootstrap analysis (n=1000) using Perl-speaks-NONMEM (PsN) [238].

A visual predictive check was produced (using PsN) by simulating 1,000 datasets from the final model. From the simulated data points, a non-parametric 95% confidence interval was calculated for the 2.5^{th}, 50^{th}, and 97.5^{th} percentiles. Simulated and original gentamicin levels were then plotted against time after dose. R package Xpose4 [239] was used to graphically present the results of VPC.

3.3.3.2 External model evaluation

The evaluation dataset (i.e. the prospectively collected data from the neoGent study) was used to externally evaluate the predictive performance of the population PK model. Basic GOF plots and a VPC were produced as described above with no additional fitting of the model to the evaluation data.

Then, only the information from opportunistically collected study samples

was taken, and the final model was used as a Bayesian prior to predict trough levels. The predicted trough levels were then compared with measured (routinely collected) trough levels by calculating the prediction errors (PE) (Equation 3.6) [37].

$$PE = observed - predicted. \tag{3.6}$$

Additionally, predictions that were below/above currently recommended [186, 189] thresholds for gentamicin trough levels of 1 or 2 mg/L and agreed with measured trough concentrations were counted. This was also done for a subset of paired samples (i.e. both study and routine samples taken in the same dosing interval) with a study sample $\geq$1, $\geq$2, and $\geq$3 mg/L, and only unpaired samples (i.e. study and routine samples not collected within the same dosing interval). In some dosing intervals more than one routine sample was collected, so technically these were not pairs, but will sometimes still be referred to as "pairs" (the same as before, in these situations only the information from the study (i.e. earlier) samples was used, and routinely taken trough concentrations were predicted). Paired samples were tested as this is how the neoGent software will be used – using the data from an opportunistically taken sample to predict the later sample, in the same dosing interval. Unpaired samples were tested for exploratory reasons, to test how good the predictive power is if a sample from a different dosing interval is used.

3.3.3.3 Cross validation

The most interesting comparison was when study sample was $\geq$3 mg/L, as in this case the concentration used to predict the trough level was not already below/very close to the pre-specified trough threshold. However, only 18 "pairs" of such characteristics were available in the evaluation dataset; therefore, pairs with the earlier sample $\geq$3 mg/L from both the model building and the evaluation datasets were pooled. The pooled dataset (n=260 "pairs") was then randomly split into

five subsets, and each time 20% of the pairs were randomly removed and the model was re-estimated. The models with re-estimated parameters were then used as a prior to predict trough concentrations in previously excluded pairs. Then, the predicted concentrations were compared to measured concentrations as described in Section 3.3.3.2.

Although the focus of this study was on safety, rather than on efficacy, the ability of the model to predict peak gentamicin concentration (from one randomly-selected non-peak sample) was also tested for exploratory purposes. Peak concentration was defined as a concentration with time after dose $\leq$1.5 hours, and there were 213 peak – non-peak pairs. Cross validation was performed the same way as described above.

For both trough and peak levels, mean PE (MPE) and root mean square errors (RMSE), i.e. measures of bias and precision, respectively, were calculated according to Equations 3.7 [240].

$$\begin{aligned} MPE &= \frac{1}{N}\sum_{i=1}^{N} PE_i, \\ RMSE &= \sqrt{\frac{1}{N}\sum_{i=1}^{N} PE_i{}^2} \end{aligned} \tag{3.7}$$

3.3.4 Comparison with published models

The developed model was compared with other previously published population PK models for gentamicin in neonates (described in Section 3.1.4), to check whether a more mechanistic model could produce better results. Some covariates from these models were not available in the evaluation dataset, for example, Apgar score [109] and information on co-medication with dopamine [200], so these covariates were not included. The information about the sepsis status [114] was also missing, but as all neonates were treated for suspected sepsis, this was as-

sumed to be 1. A model by Garcia *et al* [113] was not included in the comparison as one of the important covariates (creatinine clearance) was unavailable. For models where only an abstract was available ([197, 198]), and the magnitude but not the structure of the error model was given, an exponential and a proportional model was chosen to describe the inter-individual and the residual variability, respectively. The models were then used to predict the trough concentrations from the evaluation dataset as described above (Section 3.3.3.2).

3.3.5 neoGent software

The model that was externally evaluated was used to develop the so-called neoGent software, which was implemented in R and NONMEM, and could be used in the clinic as is. The neoGent program works by reading patient's data into R, then NONMEM is run, using the model as a Bayesian prior, and a prediction of the trough (together with a graphical presentation of when gentamicin serum concentration falls below 2 mg/L) is given.

3.4 Results

3.4.1 Study population

The model building dataset was described in Section 3.3.1. A total of 194 neonates and infants were enrolled in the neoGent study, but 31 were excluded, therefore data from 163 neonates were used in the evaluation dataset. Reasons for exclusion included inaccurately reported sampling times, or insufficient number of samples taken. Also, if a study level (the level used to predict the trough level) was already below the limit of quantification, this level was also excluded (there were 12 such levels). The final evaluation dataset included a total of 483 gentamicin serum measurements, out of which 229 were opportunistic study levels and 254 were routinely taken trough concentrations. Median (range) time after dose for these

Table 3.3: Summary of demographics and dosing/sampling from both the model building and the evaluation datasets

	Model-building dataset	Evaluation dataset
number of subjects	174	163
weight (kg)*	1.94 (0.53-5.05)	2.03 (0.48-5.05)
gestational age (weeks)*	30.0 (23.3-42.1)	34.3 (23.9-42.3)
postnatal age (days)*	6 (1-66)	6 (1-78)
postmenstrual age (weeks)*	32.4 (23.3-43.8)	34.9 (24.0-43.3)
females (%)	76 (43.7%)	68 (41.7%)
gentamicin samples per patient#	6.7	3.0
gentamicin concentration (mg/L)*	3.4 (0.3-16.0)	1.0 (0.1-13.2)
time after the dose (h)*	8.5 (0.08-54.1)	23.5 (0.08-79.7)
occasion*	3 (1-22)	2 (1-7)

Weight is weight at treatment initiation, the rest (expect gestational age) are values at time of gentamicin serum concentration measurements/dosing; an occasion was defined as a dose with subsequent gentamicin samples taken; day of birth was defined as day 1; * median (range); # mean.

levels was 13.3 (0.08-53.3) h for study concentrations, and 31.1 (8.0-79.7) h for routine levels. A summary of demographic characteristics of subjects from both datasets is given in Table 3.3; and Figure 3.8 shows the concentration-time profile of the evaluation dataset.

3.4.2 Non-linear mixed-effects model building

Initially, a 2-compartment model was chosen as a basic structural model as there was no further improvement in the OFV when a 3-compartment model was tested. However, once the fixed allometric and renal function parameters, the covariates, and IOV, were added in the model, a 3-compartment model provided a better fit to the data (ΔOFV=64). The residual error was best described with a combination of a proportional and an additive error, and the BSV was described with an exponential model. Postnatal age and typical SCr proved significant (ΔOFV=88.1 and ΔOFV=60.1, respectively), therefore they were included in the final model.

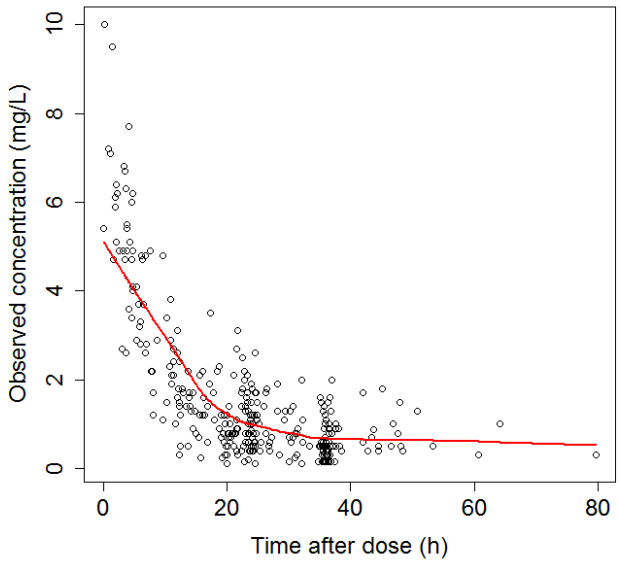

Figure 3.8: Observed gentamicin concentration plotted against time after gentamicin dose in hours, data from the evaluation dataset. Red line is a lowess smooth line.

They remained significant even with a 3-compartment model, when tested with a p-value retention cut-off of 0.001. Equations 3.8 summarise the final population PK model for gentamicin in neonates.

$$
\begin{aligned}
CL &= \theta_{CL} \cdot \left(\frac{WT}{70}\right)^{0.632} \cdot \left(\frac{PMA^{3.33}}{55.4^{3.33} + PMA^{3.33}}\right) \cdot \left(\frac{PNA}{PNA_{50} + PNA}\right) \cdot \left(\frac{SCr}{TSCr}\right)^{\theta_{SCr}} \cdot e^{(\eta_{CL} + \kappa_{CL})}, \\
V &= \theta_V \cdot \left(\frac{WT}{70}\right) \cdot e^{\eta_V}, \\
Q &= \theta_Q \cdot \left(\frac{WT}{70}\right)^{0.75} \cdot e^{\eta_Q},
\end{aligned}
\tag{3.8}
$$

where CL is gentamicin clearance, V is gentamicin volume of distribution, Q is inter-compartmental CL, WT is body weight in kilograms, PMA is postmenstrual age in weeks, PNA is postnatal age in days, η is BSV, and κ is IOV.

When time-varying covariates (SCr and PNA) were parameterised so that there were linear extrapolations between observations, this provided only a slight improvement in the fit (ΔOFV=3.1); however, this parameterisation is more biologically plausible, hence it was chosen for the final model. NONMEM control file for the final model (in a format that is ready to be implemented in the neoGent

Table 3.4: Final parameter estimates from NONMEM output file and from the bootstrap analysis

	Parameters from the final model				Bootstrap analysis		
	mean	SE	%CV	η-shrinkage	median	2.5%ile	97.5%ile
CL (L/h/70kg)	6.71	0.3	-	-	6.69	6.12	7.28
θ on creatinine	-0.17	0.05	-	-	-0.17	-0.29	-0.07
PNA_{50} (days)	1.77	0.55	-	-	1.77	1.3	2.33
V (L/70kg)	27.5	0.96	-	-	27.4	26.2	28.7
Q (L/h/70kg)	0.3	0.11	-	-	0.3	0.2	0.39
V2 (L/70kg)	157	133	-	-	160	81.8	316
Q2 (L/h/70kg)	2.2	0.37	-	-	2.23	1.79	2.72
V3 (L/70kg)	21.2	2	-	-	21.4	19.1	23.8
IOV	0.024	0.015	15.5	-	0.023	0.01	0.041
BSV on CL	0.066	0.022	25.6	13.6	0.064	0.038	0.107
BSV on V	0.009	0.004	9.6	54.7	0.009	0.001	0.017
BSV on V2	0.022	0.342	14.7	92.6	0.000002	0.000002	0.847
BSV on Q2	0.019	0.153	13.8	83.5	0.006	0.000002	0.174
BSV on V3	0.021	0.026	14.5	75.8	0.018	0.000002	0.095
ε_{prop}	0.024	0.004	15.5	-	0.024	0.017	0.032
ε_{add}	0.01	0.019	-	-	0.005	0.000001	0.018

BSV is between-subject variability, IOV is inter-occasion variability; CL is clearance, V is volume of distribution, Q is inter-compartmental CL, ε is residual error for proportional or additive model, SE is standard error obtained with NONMEM 7.2 covariance step, CV is coefficient of variation.

software) is presented in Appendix B.

The OFV dropped from 1889.6 to 530.7 (ΔOFV=1358.9), between the basic and the final model, respectively. Including covariates in the model reduced the BSV on CL and V, which were 70.8% and 61.1%, respectively, using the basic model, and 25.6% and 9.6%, respectively, when the final model was used. The final PK parameter estimates with the uncertainty are presented in Table 3.4. η-shrinkage was calculated according to the Equation 3.9 [241].

$$\eta_{shrinkage} = 1 - \frac{SD(\eta_{EBE})}{\omega}, \tag{3.9}$$

where η_{EBE} and ω are the estimated random effects and standard deviation of the random effects, respectively.

3.4.3 Model evaluation

3.4.3.1 Internal model evaluation

Figures 3.9 and 3.10 show basic goodness-of-fit plots. There is no obvious bias seen in the observations versus predictions plots (Figure 3.9), the points are distributed uniformly around the line of unity. Residual plots (Figure 3.10) look homogeneous, there is no systematic trend seen; the points are distributed around the line of zero residuals, and at least approximately 95% of the points lie within -2 and 2 interval. A VPC of the final model is shown in Figure 3.11.

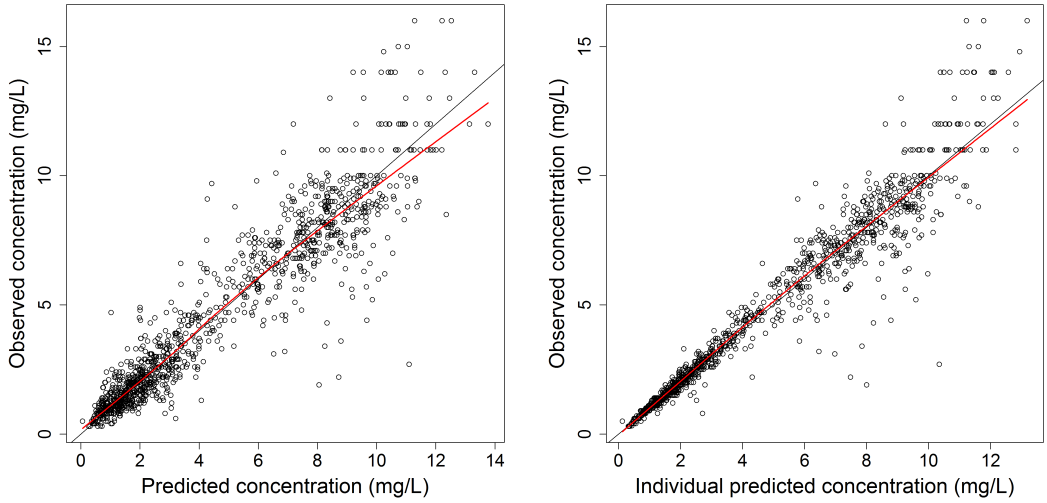

Figure 3.9: Observed gentamicin concentrations plotted against population (left) and individual (right) predicted concentrations. Red line is a lowess smooth line and black line is the line of unity.

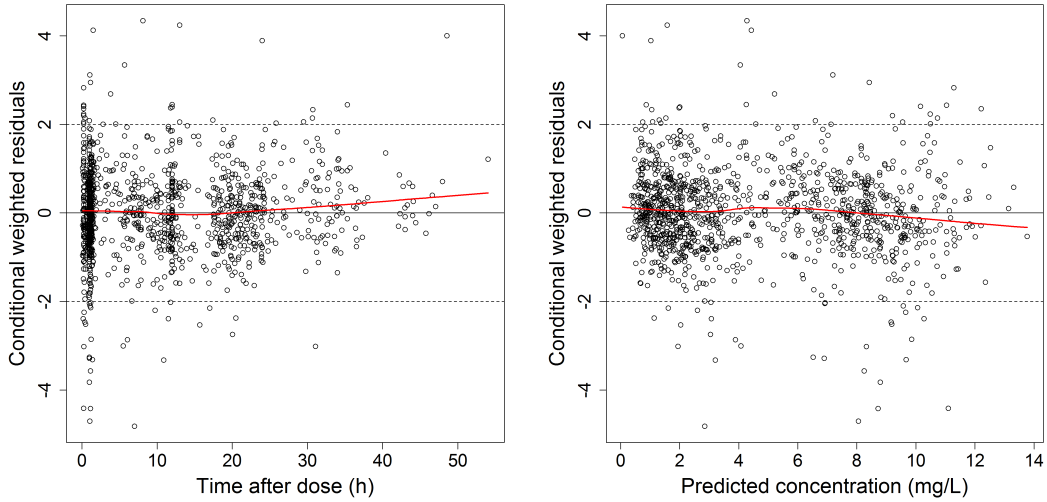

Figure 3.10: Conditional weighted residuals versus time after dose (left) and versus population predictions (right). Red line is a lowess smooth line.

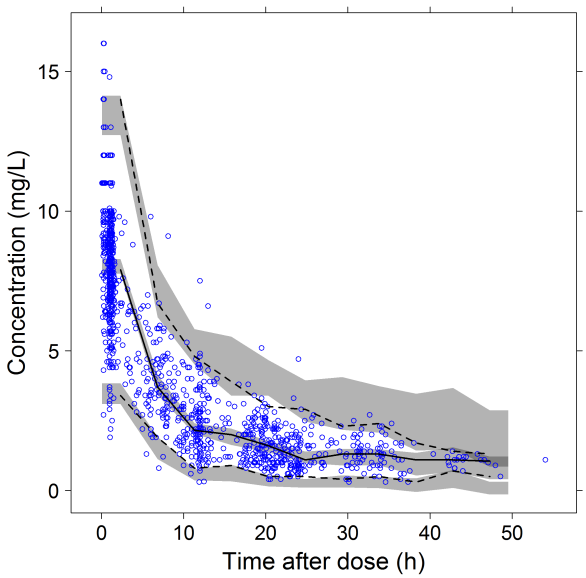

Figure 3.11: Visual predictive check (n=1000) of gentamicin concentration versus time after dose; points are observations, black lines are the 2.5^{th}, 50^{th} and 97.5^{th} percentiles of the observed data, and the shaded area is a non-parametric 95% confidence interval for the corresponding predicted concentrations.

3.4.3.2 External model evaluation

Basic GOF plots that were produced using the external evaluation dataset without parameter re-evaluation are shown in Figure 3.12. There is some overprediction by the model seen in the high concentration end (also observed in the residuals plot (Figure 3.13)), but, individual predictions (especially for the low concentrations, i.e. trough levels) appear to agree with the observations well. Figure 3.14 shows a VPC performed using the evaluation dataset.

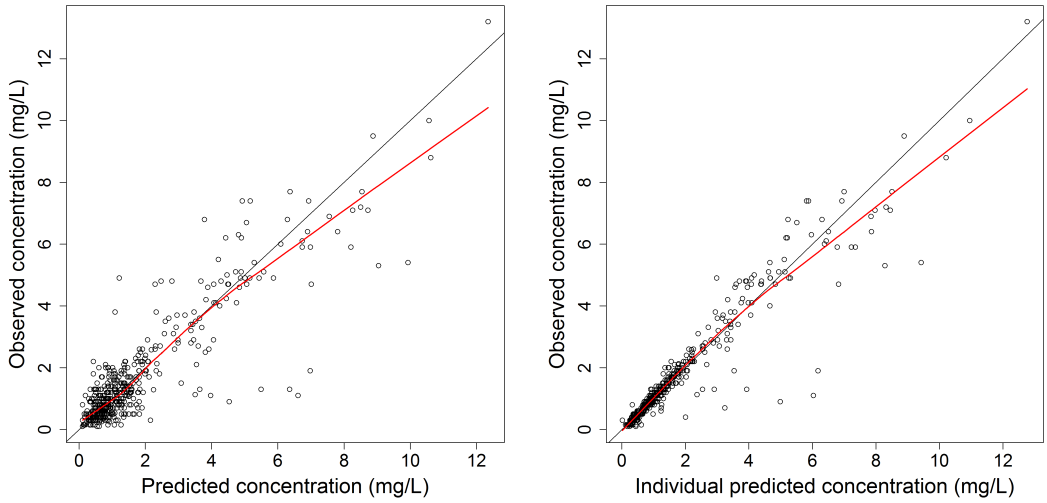

Figure 3.12: Observed gentamicin concentrations (from the external evaluation dataset) plotted against population (left) and individual (right) predicted concentrations. Predictions were performed without parameter re-evaluation. Red line is a lowess smooth line and black line is the line of unity.

Results of the comparison of observed and trough concentrations for five different subsets of data from the evaluation dataset and pooled results from the cross validation (for thresholds of 1 and 2 mg/L) are presented in Table 3.5. Figure 3.15 shows the distribution of prediction errors in the same datasets. In the dataset that contained both paired and unpaired samples, the median (95% confidence interval (CI)) PE was -0.002 (-0.87, 0.85) mg/L.

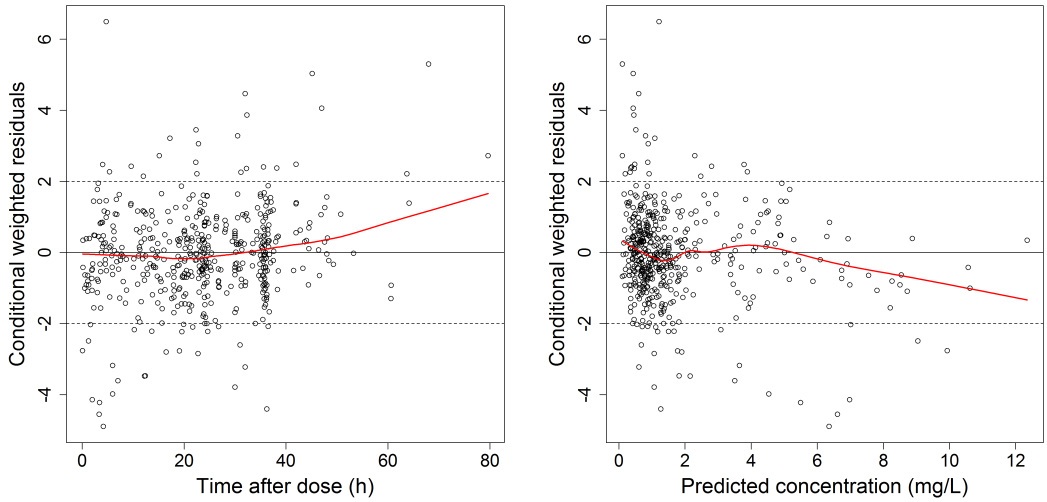

Figure 3.13: Conditional weighted residuals versus time after dose (left) and versus population predictions (right). Red line is a lowess smooth line.

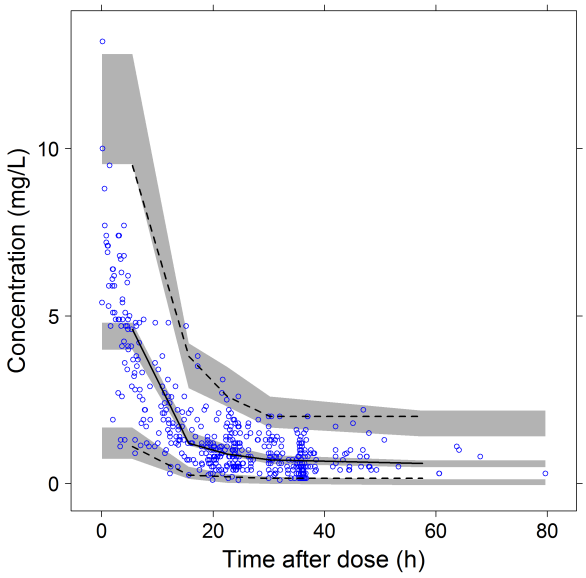

Figure 3.14: Visual predictive check (n=1000) of gentamicin concentration versus time after dose performed using an external evaluation dataset; points are observations, black lines are the 2.5^{th}, 50^{th} and 97.5^{th} percentiles of the observed data, and the shaded area is a non-parametric 95% confidence interval for the corresponding predicted concentrations.

Table 3.5: Summary of the external evaluation

	Limit = 1 mg/L			Limit = 2 mg/L		
dataset	n correct (%)	OP	UP	n correct (%)	OP	UP
paired and unpaired	215/254 (84.6)	17	22	246/254 (96.9)	6	2
paired: study≥1mg/L	51/57 (89.5)	3	3	57/57 (100)	0	0
paired: study≥2mg/L	30/33 (90.9)	2	1	33/33 (100)	0	0
paired: study≥3mg/L	18/20 (90.0)	0	2	20/20 (100)	0	0
unpaired	136/161 (84.5)	12	13	158/161 (98.1)	2	1
XV, paired: study≥3mg/L	428/456 (93.9)	13	15	421/456 (92.3)	20	15

OP is overprediction, UP is underprediction, correct means that predicted trough concentration corresponds to observed concentration (i.e. is above/below the limit), XV is cross validation.

Table 3.6: Cross-validation results

	PE (mg/L)			RMSE (mg/L)
	median	mean	95% CI	
trough	-0.06	-0.09	(-1.55, 1.04)	0.68
peak	0.14	0.01	(-3.56, 2.25)	1.46

PE is prediction error and RMSE is root mean square error.

3.4.3.3 Cross validation

The median PE from the cross validation was -0.06 (-1.55, 1.04) mg/L (Table 3.6), for trough sample prediction. Individual plots of paired samples (from the evaluation dataset) where study sample was ≥3 mg/L are presented in Appendix C. When cross validation was performed to test the ability of the model to predict peak gentamicin concentrations, the median PE (95% CI) was 0.14 (-3.56, 2.25) mg/L, mean PE was 0.01 mg/L, and RMSE was 1.46 mg/L (Table 3.6).

3.4.4 Comparison with published models

Figure 3.16 shows prediction errors for this model and previously published neonatal gentamicin PK models.

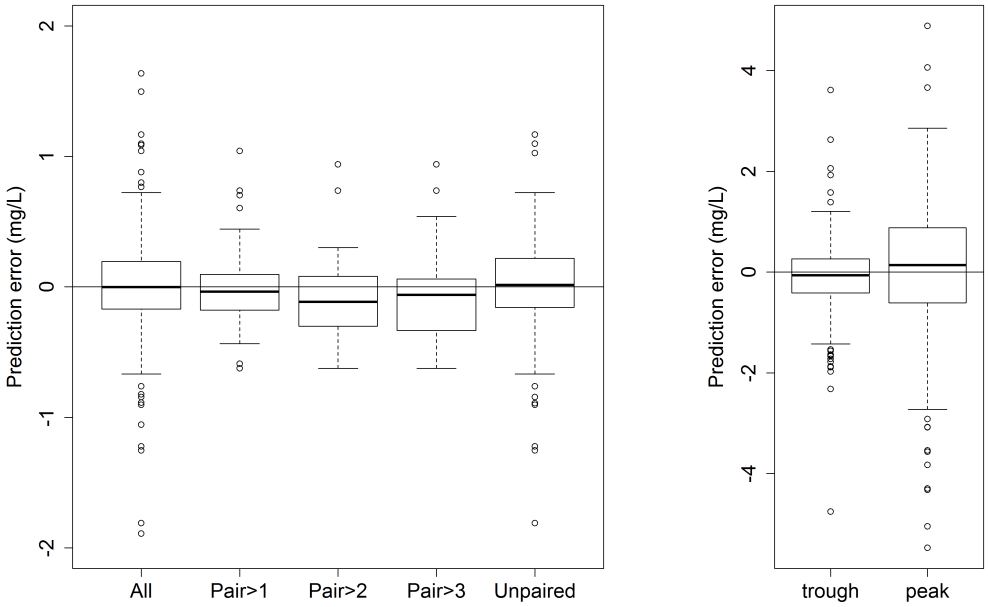

Figure 3.15: Prediction errors for different subsets (listed in Table 3.5) of the evaluation dataset (left) and for cross-validation results for both trough and peak prediction (right). Note that left and right plot are on a different scale.

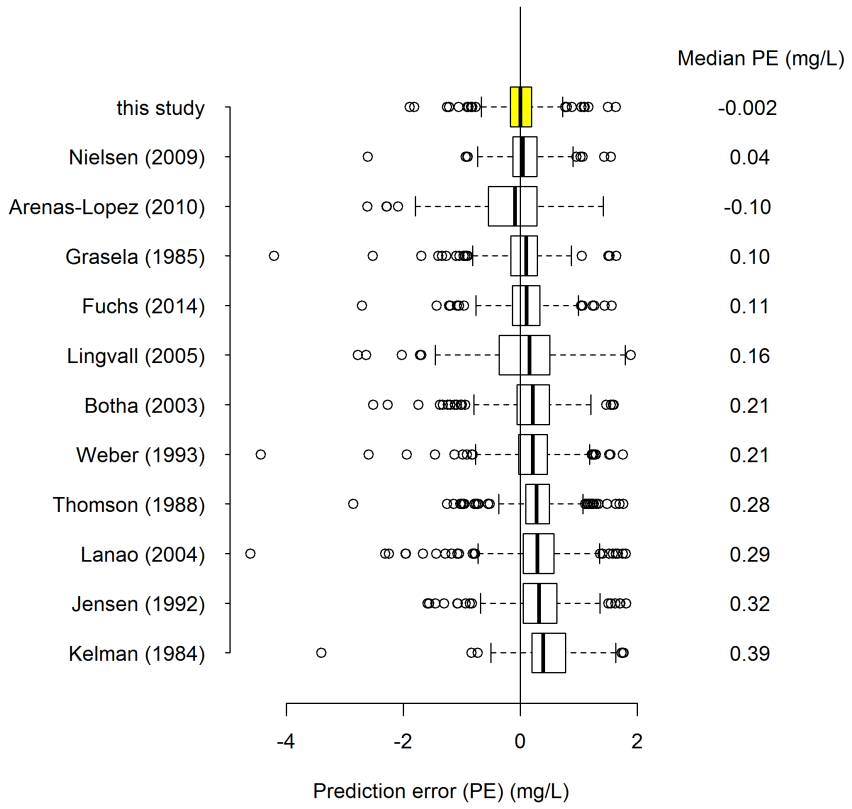

Figure 3.16: Comparison of the model from this study/chapter (shaded box) with other previously published neonatal gentamicin PK models.

3.4.5 neoGent software

The provisional software neoGent was developed as described in Section 3.3.5. The R code for neoGent is given in Appendix D, and an example output of it is presented in Appendix E.

3.5 Discussion

A new gentamicin population PK model for neonates and infants was developed using literature data and evaluated with prospectively collected data. The evaluation of the model showed that the model is able to give unbiased predictions (median prediction error was -0.002 mg/L) of the trough concentrations, using information from levels collected opportunistically for other clinical purposes; and comparison with previously published models showed that the predictions are less biased compared to other models (Figure 3.16). The reason for this might be that this model was more mechanistic, namely, it included biological information about serum creatinine.

Although only two datasets [109, 119] were obtained by contacting authors identified in the literature search, the pooled data was of sufficiently high quality (approximately 7 samples per subject) to allow developing a model that was shown to describe both model-building and evaluation data well (Figures 3.11 and 3.14, respectively).

The values of allometric exponents and maturation function parameters were fixed to values from a study that focused specifically on how glomerular filtration (and consequently kidney function) matures [52], a process that is important for renally eliminated gentamicin. This approach was shown in Chapter 2 to be able to describe the change in gentamicin CL with age and weight well; and also since the PMA range in the model-building dataset was insufficient (23.3-43.8 weeks, Table 3.3) to estimate these parameters (for example, PMA_{50} is usually

approximately 50 weeks (Table 2.2)). Also, this type of scaling enables using the model for extrapolations to other populations (such as neonates or infants with different weights and ages).

However, using only a PMA based maturation function is not sufficient for describing the rapid changes that occur in the neonatal renal function in the first days (and even hours) of life, regardless of the GA. An additional function was therefore used to capture the short-termed changes in CL with PNA directly after birth. By fixing the parameters of a well-established relationship between PMA and renal function, PNA_{50} was possible to estimate, showing that the CL does change rapidly at the beginning of life (the estimate was 42.5 hours). Gentamicin CL was at 36% of a typical adult's value on the first day of life.

Typical serum creatinine that was used in the model originated from SCr concentrations that were determined using the Jaffe method. This method was selected since SCr in the model-building dataset was also determined using this assay. But, in the evaluation dataset, SCr was determined with both the Jaffe and enzymatic methods and they were shown to affect SCr concentrations [211] as described in Section 3.1.5 of this thesis. However, since the model fit to the data and its predictive power was good (and also, only 16% of subjects from the evaluation dataset had SCr determined with an enzymatic method), no correction factor to account for this was included. As SCr data from neonates with PMA up to 44 weeks (e.g. a term neonate of 4 weeks of age) was used to define typical SCr, this is also the range of PMA for which the model can be used. The value of the power exponent on the creatinine function was estimated as -0.17, indicating that if measured SCr was 70 μmol/L and TSCr 60 μmol/L, clearance would be reduced by 2.6%.

The final estimates for gentamicin CL and volume of distribution (V) were 6.71 L/h/70 kg and 27.5 L/70kg, respectively (Table 3.4). The values of the PK parameters for a typical neonate from the model-building dataset (with the fol-

lowing demographics: weight 1.83 kg, PMA 32.8 weeks, PNA 10.3 days, MSCr 75.7 μmol/L, TSCr 73.0 μmol/L) were 0.086 L/h and 0.719 L (and 0.126 L/h and 0.880 L for a neonate from the evaluation dataset) for CL and V, respectively. These values are in agreement with estimates for CL from other neonatal PK studies of gentamicin [196, 197, 115, 124, 200, 111]. The neonates from the model-building dataset were more premature, compared to the evaluation dataset (median GA of 30 versus 34 weeks, respectively), which is probably the reason for slightly lower CL in that population. In some cases the estimated values of PK parameters from this study and previously published studies initially appeared to differ, which was mostly due to different demographic features of the neonates in those studies, as the values became similar, when the same demographics were used. For example, reported CL from a study by Nielsen *et al* [119] was 0.026 L/h, but when the median demographic values from this study were used (in their model), CL was 0.090 L/h, similar to the estimate from this study. Another example is an estimate of V, which was found to be 0.252 L by Garcia *et al* [113], but when weight from this study was used, the V was 0.968 L.

Aminoglycoside antibiotics often follow a multiphasic elimination, and Schentag *et al* [242] and Laskin *et al* [180] found evidence of deep tissue accumulation of gentamicin. The rich data in the model-building dataset supported a 3-compartment model with a deep compartment possibly representing the characteristics that could indicate uptake into the renal cortex and slow excretion [166]. This is shown by the final parameter estimates for the inter-compartmental clearance (Q) and the peripheral volume of distribution (V2), which were small (0.3 L/h/70kg) and large (157 L/70kg), respectively. Also, the terminal half-life for a typical subject from the evaluation dataset (weight 2.24 kg, PMA 35.0 weeks, PNA 12.2 days, MSCr 47.7 μmol/L, TSCr 66.7 μmol/L) was 182.2 hours. However, the estimates of Q and V2 are rather imprecise (relative standard errors were 35.5% and 84.8%, respectively).

The η-shrinkage was large on most of the PK parameters of the final model, except CL (Table 3.4). Large shrinkage indicates that there is not enough information in the data to make a reliable individual estimation. Still, the shrinkage on clearance is relatively small (13.6%), which is important for making predictions of the trough gentamicin concentrations.

The small median PE (-0.002 mg/L) suggests that the model implemented in neoGent can predict gentamicin trough concentrations well, but there were some outliers that were not captured (range: -1.89-1.64 mg/L). When subsets of study-routine paired samples were used, the median PEs were negative, meaning that the model is overpredicting rather than underpredicting, which is preferable from a safety perspective.

The results of the cross validations for trough gentamicin concentrations (MPE=-0.09 mg/L) demonstrated that the model will give unbiased predictions when used as clinically intended (Table 3.6). This means that an opportunistic sample can define when gentamicin serum concentration will drop below a certain threshold and hence specific blood sampling times for trough samples are not required for TDM using this model. As this study was not designed to test the impact of a specific sample time, this was not tested. However, the samples were taken from a range of times (0.1-53.3 h), as they would be in routine hospital tests.

Whilst comparison of this model with previously published models (Figure 3.16) showed that the prediction errors were the smallest when the model described in this chapter was applied to the evaluation dataset, three models did not include all of the covariates reported, which could affect their predictive performance. The information on these covariates (i.e. Apgar score [109, 114], and co-medication with dopamine [200]) was not available in the evaluation dataset, thus these covariates were not included.

For exploratory purposes the ability of the model to predict peak gentamicin concentrations was also tested and showed that the model can give unbiased (MPE=0.01 mg/L) but imprecise (95% confidence interval: -3.56, 2.25 mg/L; RMSE=1.46 mg/L) predictions of the peak concentrations (Table 3.6). However, this was only tested using a cross validation, and an external validation is needed before any conclusions can be made. Also, although peak levels are related to efficacy, monitoring peak concentrations might be of less importance in neonates, due to their low CL. Giving a higher dose to achieve higher peak concentration would possibly lead to higher trough levels, and thus to toxicity in this population. More research is needed to identify the optimal balance between efficacy targets and toxicity in infants, particularly in light of increasing pathogen MICs [243].

3.6 Summary

A new population pharmacokinetic model for gentamicin in neonates was developed using published literature data and evaluated with prospective data from an observational study. The evaluation showed that the model is able to predict trough gentamicin concentration from a sample taken for other clinical purposes than TDM. Thus, by using this model, the need for specifically timed trough gentamicin levels could be reduced, and the safety concerns about gentamicin monitoring in neonates (raised by the NPSA) improved. The model was implemented in a provisional software tool, neoGent, and could already be used in the clinic. However, it does not yet have a user-friendly interface, and also further clinical evaluation is needed before it can be used in routine neonatal clinical practice.

Chapter 4

Pharmacokinetic-pharmacodynamic modelling for population-level dose recommendation

4.1 Introduction

As previously mentioned (in Section 1.1), untreated sepsis and bacterial meningitis are amongst the most common causes of morbidity and mortality in neonates and infants [2, 244, 245]. Antimicrobial treatment can reduce mortality, but, due to several challenges in rapid diagnosis of bacterial infections, empirical therapy is used [5], meaning that even suspected sepsis or meningitis are treated. Additionally, antimicrobial resistance to standard agents in increasing, therefore meropenem (which can penetrate into the cerebrospinal fluid (CSF)) is being used as a first-line therapy in countries, where this is already a problem. But even when used as a second-line therapy, it is used off-label in neonates and infants younger than three months [246], since data are limited in this population. In order to address this, work was carried out as part of the NeoMero studies and is described

in more detail in this chapter.

4.1.1 Meropenem pharmacodynamics

Meropenem is a β-lactam antibiotic from the carbapenem family and as all β-lactams exhibits bactericidal activity by interrupting bacterial cell wall synthesis. It does so by binding to specific proteins in the bacterial cell wall (namely penicillin binding proteins), which prevents peptidoglycan strands to crosslink, and inhibits bacterial cell wall formation [247, 248].

Meropenem is a concentration-independent or time-dependent antimicrobial agent, meaning that the percentage of a dosing interval that unbound plasma (or, for example, CSF) concentration is above the MIC of a pathogen (%T>MIC) is most closely related to the clinical outcome [17]. For meropenem to exhibit bactericidal effect (i.e. killing 99.99% of a bacterial population), %T>MIC has to be approximately 40%, and around 20% for bacteriostasis (i.e. averting bacterial growth) [17, 249, 250]. However, for treating severe bacterial infections, or if patients are immunocompromised, 70%T>MIC might be needed for a bactericidal effect [64].

Meropenem is bactericidal against Gram-negative and Gram-positive, aerobic and anaerobic microorganisms [251]. For example, meropenem is effective against some of the most common pathogens that cause late-onset sepsis (LOS, usually defined as sepsis that starts 48 to 72 hours after birth [244]), such as, *E. coli*, *Klebsiella* spp, *Enterobacter* spp, *Pseudomonas* spp [244, 188]. The maximal susceptibility breakpoint for these organisms for meropenem is $\leq$2 mg/L, and resistance breakpoint >8 mg/L, according to EUCAST [188]. Additionally, meropenem also exhibits antimicrobial activity against common organisms that cause bacterial meningitis, for example, Group B streptococcus (*Streptococcus agalactiae*), *E. coli*, *Listeria monocytogenes*, *Haemophilus influenzae*, *Streptococcus pneumoniae*, *Neisseria meningitidis* [245, 188, 252]. The highest suscepti-

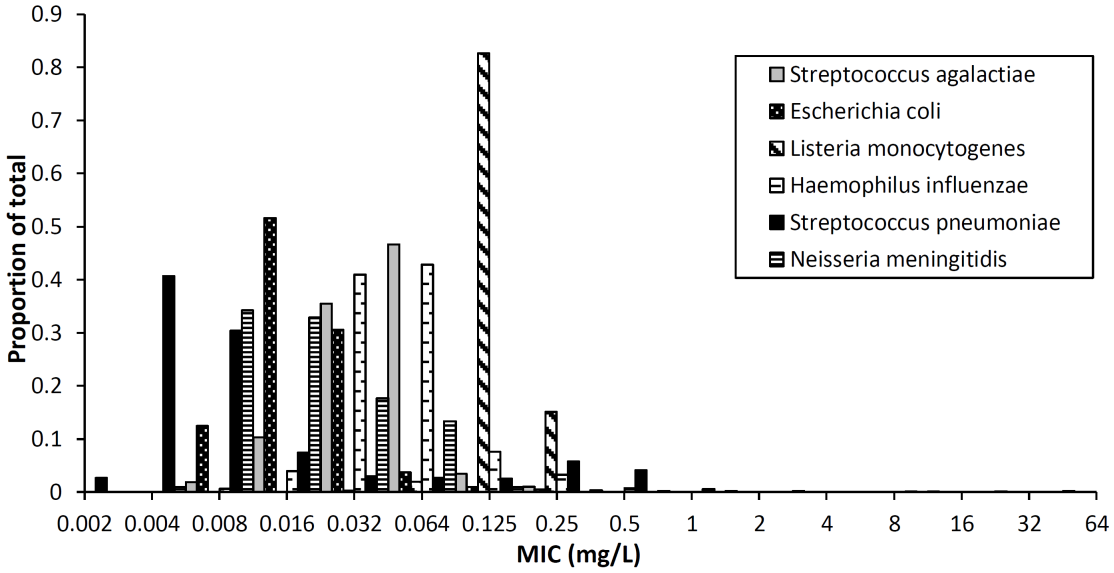

Figure 4.1: Data from the European Committee on Antimicrobial Susceptibility Testing (EUCAST). Data for *Streptococcus agalactiae* came from 8 data sources (1146 observations) [253], for *Escherichia coli* from 69 sources (8011 observations) [254], for *Listeria monocytogenes* from 4 sources (317 observations) [255], for *Haemophilus influenzae* came from 4 sources (6541 observations) [256], for *Streptococcus pneumoniae* from 5 sources (675 observations) [257], and for *Neisseria meningitidis* from 2 data sources (301 observations) [258].

bility breakpoint for these pathogens is $\leq$0.25 mg/L, and resistance breakpoint $>$1 mg/L, as reported in the EUCAST clinical breakpoint tables (for breakpoints that only relate to meningitis isolates) [188]. The available distributions of MICs (for meropenem) for bacteria causing meningitis are presented in Figure 4.1.

Studies in animals have shown that meropenem does not damage renal tubules, and causes only minor histopathological changes in the kidneys [259]. Furthermore, studies of meropenem in humans did not report an increase in markers of renal function (serum creatinine or urea) [247], thus it appears that meropenem has low potential for nephrotoxicity.

4.1.2 Meropenem pharmacokinetics

Meropenem has to be administered parenterally (e.g. in neonates and infants it is often given as an intravenous infusion) as it is not absorbed through the gastrointestinal tract when given orally [50, 145]. Once administered it penetrates

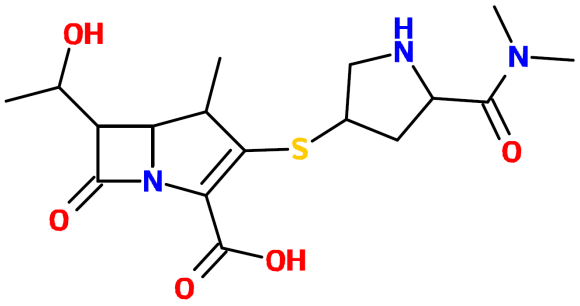

Figure 4.2: Chemical structure of meropenem.

into several body fluids (e.g. CSF) and tissues (such as, muscle, heart); and distributes mainly into the extracellular water and plasma (since it is a polar, hydrophilic drug) [249, 260] (Figure 4.2). Meropenem is only 2% protein bound [145, 261], and its volume of distribution (V) in neonates is around 0.3-0.7 L/kg [262, 263, 264, 265, 266], with more premature infants usually having a higher V.

Compared to other carbapenem antibiotics, meropenem is hydrolysed by renal dehydropeptidase-I in a much smaller extent, due to a methyl substitution on the carbapenem ring, and therefore does not need to be co-administered with an inhibitor of this enzyme (e.g. cilastatin). Approximately 25% of the administered dose of meropenem is metabolised – either renally, or extrarenally, producing one metabolite without antimicrobial activity [50, 145].

Renal elimination represents the main route of elimination for meropenem, and approximately 75% of administered dose is excreted unchanged *via* glomerular filtration and also partly by tubular secretion [50, 247]. Meropenem clearance in neonates is in the region of 0.1-0.2 L/h/kg [262, 263, 264, 265, 266]; neonates with lower gestational age and postnatal age have lower clearance.

4.1.3 Cerebrospinal fluid

Cerebrospinal fluid is mainly ultrafiltrate of the plasma that perfuses the choroid plexus, and partly a by-product of the metabolism in the central nervous system (CNS) [267]. The function of the CSF is to support the neurons (e.g. by providing

nutrients, transporting hormones), to protect the brain from mechanical damage, to minimise the pressure to the neurons in the lower sections of the brain (by decreasing the weight of the brain), and to remove waste products [267, 268]. The volume of the CSF is around 150 mL [268, 267].

For an antibiotic agent to effectively treat infections in the CNS, such as bacterial meningitis, its concentration in the CNS (i.e. infection site) has to be sufficient. Usually CSF concentration is taken as a proxy for CNS availability of a drug, as it is the easiest to measure [269]. A drug can reach the CSF by choroid plexus; but the majority of the drug reaches the CSF indirectly by passing the blood-brain barrier (BBB) [269]. However, under normal healthy conditions the permeability of BBB for drugs is very limited, and depends on their molecular size and the degree of lipid solubility, meaning that small, simple, lipid molecules pass through the BBB more easily, but the uptake of meropenem is low [270, 271]. During inflammation the pH in the CSF changes due to acidosis, which facilitates the penetration of meropenem into the CSF [270, 272, 48].

Markers of bacterial meningitis include CSF total protein concentration, CSF lactate concentration (which are both increased during infection [273, 252, 274]), and CSF glucose concentration (which is lower when the meninges are inflamed [273, 274]).

4.1.4 Previously published population pharmacokinetic models

Pharmacokinetics of meropenem in plasma have been previously described in neonates and infants [264, 265, 266, 263, 262]. However, meropenem CSF concentrations have only been measured in a study by Smith *et al* [265], where they collected nine samples from six patients and used the CSF concentrations to determine the uptake of meropenem into the CSF. This study is further discussed

in Section 4.5.

4.2 Aim

This study aimed firstly to characterise the pharmacokinetics of meropenem in plasma and cerebrospinal fluid in neonates and infants younger than three months, who were receiving intravenous meropenem for treatment of clinical or confirmed late-onset sepsis or bacterial meningitis. Secondly, the objective was to establish the optimal dose and the length of infusion for meropenem in infants $\leq$90 days of age by using Monte Carlo simulations and the population pharmacokinetic model.

4.3 Methods

4.3.1 Study population

Data for the population PK analysis were collected in two European trials (conducted in eight European countries), NeoMero-1 and NeoMero-2. NeoMero-1 was an open-label phase III randomised controlled trial (where infants were randomly allocated 1:1 to either meropenem or standard of treatment arm), and NeoMero-2 was an open-label phase I-II observational study. The NeoMero-1 and -2 trials run from September 2012, or February 2013, respectively, until December 2014. Ethical approval was obtained for both studies for each participating country.

An infant was included in the NeoMero-1 trial if the following criteria were met: postnatal age of $\leq$90 days and $\geq$72 hours at the beginning of the sepsis onset, confirmed (by a positive bacterial culture) sepsis with an abnormal clinical or laboratory measurement; or clinical sepsis, meaning that the bacterial culture was negative. In the case of a negative bacterial culture, clinical and laboratory criteria for sepsis consistent with Goldstein *et al* [275] or the European Medicines Agency (EMA) [276] had to be met, according to the postmenstrual age of the

infant. Also, an infant could not have been administered systemic antimicrobials for >24 hours prior to the randomisation [26].

The inclusion criteria for NeoMero-2 trial were: postnatal age ≤90 days, clinical signs indicating bacterial meningitis, or pleocytosis (i.e. increased number of CSF lymphocytes), or a positive Gram stain of the CSF. An infant was excluded if the CSF device was present, or if meningitis was proven to be non-bacterial.

Also, an informed written consent form had to be obtained (from the parents or legal guardians) for an infant to be enrolled in either NeoMero-1 or NeoMero-2 trial, and the infant could not have renal failure, severe congenital malformations (if the expected survival time was less than three months), a causative pathogen that was suspected or known of being resistant to meropenem, or a known intolerance or contraindications to meropenem.

Infants in the NeoMero-1 trial received 20 mg/kg of meropenem every 8 hours (if their GA was ≥32 weeks, or if their GA was <32 and PNA >2 weeks) or every 12 hours (if the infant's GA was <32 weeks and PNA <2 weeks). The doses were doubled in the NeoMero-2 trial, meaning the infants received 40 mg/kg of meropenem; and the dosing intervals were the same as in the NeoMero-1 trial.

Meropenem plasma samples were planned to be collected at steady state. Some patients had only one plasma sample taken (usually a pre-dose sample), and some infants had three samples taken (if the dosing interval was 8 hours, the samples were planned to be taken before the dose, at the stop of infusion (i.e. at approximately 30 minutes after the infusion start), and between 5 and 6 hours after the dose; and when meropenem was administered 12-hourly, the last sample would ideally be collected approximately 7-9 hours after the infusion start). Optimal design was used to define sampling times for infants, who had more than one sample collected from. A meropenem CSF sample was planned to be collected on the same day as plasma sample from all infants undergoing a

lumbar puncture.

Meropenem concentration in both plasma and the CSF was determined using ultra-high performance liquid chromatography coupled to tandem mass spectrometry (UHPLC-MS/MS). Plasma samples were prepared using protein precipitation (with methanol) and cerebrospinal fluid samples using filtration through 0.22 μm syringe filters. Ertapenem was used as an internal standard. Limit of detection was 10 ng/mL and 2 ng/mL for plasma and CSF meropenem assays, respectively. The between-day variability was 4.1-5% for plasma, and 3-5% for CSF assay, over the whole calibration range.

4.3.2 Non-linear mixed-effects model building

All available meropenem concentration-time data were simultaneously modelled using NONMEM 7.3 (ICON Development Solutions, Ellicott City, Maryland). Typical population values for the parameters of the structural model with between-subject variability, and also the residual error estimates were obtained by using FOCE method with interaction.

4.3.2.1 Plasma pharmacokinetic model

Firstly, the model was developed only for meropenem plasma concentrations; and then the CSF concentrations were added in. To define the structural model which best describes the plasma meropenem data, 1-, 2- and 3-compartment models were tested. A log-normal distribution was assumed for BSV, and a proportional and a combination of proportional and additive models were tried for residual variability.

Weight and postmenstrual age were included *a priori* by using allometric weight scaling and a maturation function with fixed parameters to the values from a renal maturation study [52]; as described in Chapter 3, Section 3.3.2.

Tested covariates involved covariates for which there was a biological rationale, and/or a trend seen in the empirical Bayes estimates versus covariates plots; these were: serum creatinine concentration and postnatal age. Equation 3.4 (described in Chapter 3) was used to standardise measured SCr according to the typical SCr, and deviations from it were estimated. The influence of PNA on meropenem clearance was examined by incorporating PNA in the model as a non-linear logistic function as described in Chapter 3, and also in a linear way. A covariate was included in the model if ΔOFV between two nested models after the inclusion was >6.63 (p <0.01), and if there was an improvement seen in the diagnostic plots. After all covariates with a significant effect were included, the structural model was re-tested.

4.3.2.2 Plasma and CSF pharmacokinetic model

Once the population PK model for plasma meropenem concentration-time data was developed, a separate peripheral compartment relating to the CSF compartment was added into the model. Two different published models, represented by Equations 4.1 [277, 278] and 4.2 [279, 280] (shown for an example when the plasma kinetics follow a 1-compartment model), were tested to describe the CSF pharmacokinetics of meropenem.

$$\begin{aligned} \frac{dC_{PL}}{dt} &= -C_{PL} \cdot \frac{CL}{V_C} - C_{PL} \cdot \frac{Q_{CSF}}{V_C} \cdot f_{CSF} \cdot f_u + C_{CSF} \cdot \frac{Q_{CSF}}{V_{CSF}}, \\ \frac{dC_{CSF}}{dt} &= C_{PL} \cdot \frac{Q_{CSF}}{V_C} \cdot f_{CSF} \cdot f_u - C_{CSF} \cdot \frac{Q_{CSF}}{V_{CSF}}, \end{aligned} \tag{4.1}$$

where C_{PL} is meropenem plasma concentration, C_{CSF} is meropenem CSF concentration, CL is clearance, V_C is volume of distribution of the central compartment, f_{CSF} represents the uptake into the CSF, f_u is the unbound fraction of meropenem (which was fixed to 0.98 [145, 261]), and Q_{CSF} is inter-compartmental CL between plasma and CSF compartments. Volume of the CSF compartment (V_{CSF}) was fixed to 0.15 L/70kg [267].

The second model tested is summarised by Equations 4.2, where k_{CSF} is distribution rate constant between plasma and CSF compartments.

$$\begin{aligned} \frac{dC_{PL}}{dt} &= -C_{PL} \cdot \frac{CL}{V_C}, \\ \frac{dC_{CSF}}{dt} &= k_{CSF} \cdot (C_{PL} \cdot f_{CSF} - C_{CSF}). \end{aligned} \tag{4.2}$$

As rarely more than one CSF sample was collected per patient, BSV was not estimated on inter-compartmental CL between the central and the CSF compartment. Additive, proportional, and a combination of both residual error models were tested for the CSF compartment (separately from the plasma compartment). Once the best of the two models for describing the CSF PK was determined, the influence of covariates was examined. A trend was observed in CSF concentration versus markers of CNS inflammation plots, and also because it is known that the concentration of these markers correlates with the BBB permeability, the relationship between CSF proteins, CSF lactate, CSF glucose concentration, or white blood cell count (WCC) and the fraction of meropenem plasma concentration that reaches CSF was investigated. One protein concentration (102 g/L) was excluded due to being physiologically implausible. The median value of a CSF marker of infection was assumed if no measurements were available for an individual.

4.3.2.3 Model evaluation

The final model was internally evaluated by inspecting the precision of the model parameter estimates using standard errors obtained during the NONMEM covariance step, and the 95% non-parametric confidence interval obtained from a bootstrap analysis with 1000 replicates. Additionally, diagnostic plots, as described in Chapter 1, Section 1.5 were examined, and a prediction-corrected VPC (pcVPC) (n=1000) was performed using PsN. During a pcVPC predictions and observations (Y_{ij}) within each bin are standardised, or, corrected for the differences originating from variations in the independent variables according to the

Equation 4.3 [40].

$$pcY_{ij} = Y_{ij} \cdot \frac{\widetilde{PRED}_{bin}}{PRED_{ij}}, \tag{4.3}$$

where pcY_{ij} is prediction-corrected Y_{ij} for an ith individual at the jth time point, $PRED_{ij}$ is typical population prediction, and $\widetilde{PRED}_{bin}$ is median $PRED_{ij}$ for each bin of independent variables [40].

4.3.3 Probability of target attainment

A dataset for the simulations was prepared using the same ranges and standard deviations of PNA and GA as in the original dataset; PNA was randomly sampled from a log-normal distribution, and a uniform distribution was used for GA. Weight was calculated using a published equation [106] and the PMA (PMA was obtained from GA and PNA).

Monte Carlo simulations of 1,000 simulated patients for each of the following MIC values: 0.25, 0.5, 1, 2, 4, 8, 16, 32 mg/L, was performed using parameter estimates from the final model. Dosing intervals were the same as in the original dataset (i.e. every 8 hours, unless GA <32 weeks and PNA <2 weeks, then every 12 hours). Simulated infants were allocated to a group according to their GA and PNA:

1. GA <32 weeks, PNA <2 weeks,
2. GA <32 weeks, PNA ≥2 weeks,
3. GA ≥32 weeks, PNA <2 weeks,
4. GA ≥32 weeks, PNA ≥2 weeks.

Different doses and lengths of infusions were tested for PD targets of 40%T>MIC and 70%T>MIC [64]; for all four age groups. The unbound meropenem fraction was fixed to 0.98 [145].

Table 4.1: Summary of demographic and sampling characteristics

	all data	NeoMero-1	NeoMero-2
n**	167	123	49
weight (kg)*	2.12 (0.48-6.32)	1.68 (0.48-5.01)	2.96 (0.60-6.32)
gestational age (weeks)*	33.3 (22.6-41.9)	31.9 (22.6-41.3)	37.1 (23.4-41.9)
postnatal age (days)*	17 (1-105)	17 (3-85)	16 (1-105)
postmenstrual age (weeks)*	37.4 (23.7-51.3)	36.0 (23.7-51.3)	38.8 (24.9-51.1)
females (%)	78 (46.7%)	59 (48.4%)	19 (42.2%)
plasma samples per patient#	2.4	2.1	3.0
CSF samples per patient#	0.47	0.26	0.94
plasma concentration (mg/L)*	7.94 (0.01-147.7)	5.27 (0.01-147.7)	12.4 (0.1-139.0)
CSF concentration (mg/L)*	1.58 (0.04-35.4)	1.23 (0.04-7.34)	1.90 (0.05-35.4)
plasma time after the dose (h)*	5.66 (0-12.4)	5.93 (0-12.4)	5.19 (0-12.2)
CSF time after the dose (h)*	5.27 (0-12.0)	5.99 (0-12.0)	5.03 (0-11.5)
creatinine (μmol/L)*	32.0 (3.54-197.4)	34.5 (3.54-197.4)	27.0 (6.0-133)
C-reactive protein (mg/L)*	23.0 (0.3-280)	23.2 (0.3-242)	22.4 (0.4-280)
procalcitonin (ng/mL)*	2.7 (0.1-377.2)	2.8 (0.1-128.6)	1.8 (0.1-377.2)

CSF is cerebrospinal fluid, *is median (range), #is mean, **five infants switched from NeoMero-1 to NeoMero-2, which is why the numbers do not add up. First day of life is day 0.

4.4 Results

4.4.1 Study population

A total of 167 infants with PK samples were enrolled in the NeoMero studies, with median (range) gestational age of 33.3 (22.6-41.9) weeks, and postnatal age of 17 (1-105) days. Two plasma and two CSF concentrations of meropenem could not be determined (because either the sample tube was empty, or the sample was whole blood and not plasma, which was what the assay was developed for), and 11 meropenem plasma peak concentrations were below 10 mg/L, so these 15 samples were excluded. There were therefore 401 plasma samples and 78 CSF samples available for non-linear mixed-effects analysis, with 7 and 1 duplicated (i.e. taken at the same time) plasma and CSF concentrations, respectively. A summary of the patients demographic and sampling characteristics is presented in Table 4.1.

Raw plots of meropenem concentration-time profile for both plasma and CSF is presented in Figure 4.3, and the relationship between CSF meropenem concen-

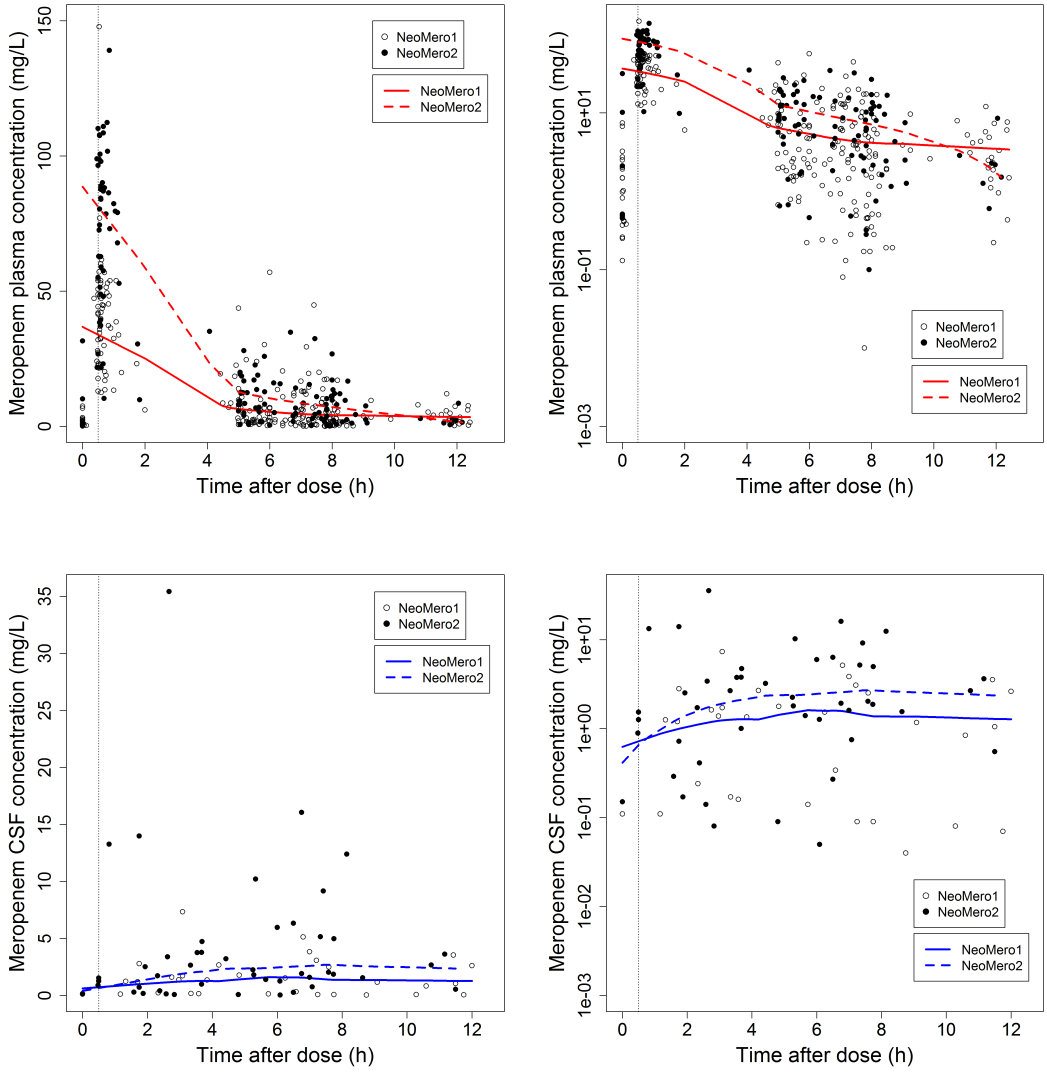

Figure 4.3: Raw plots of meropenem plasma (top) and meropenem CSF (bottom) concentration against time after dose. The y-axis on the plots on the right hand side is logarithmic. Solid and dashed lines are lowess smooth lines for data from the NeoMero-1 and NeoMero-2 studies, respectively.

tration and CSF markers of infection (i.e. CSF protein, glucose, lactate, white blood cell count) is presented in Figure 4.4. There is a positive relationship between meropenem CSF concentration and CSF lactate concentration; other trends are not that obvious, but there appears to be a slight upward trend with CSF total proteins and WBC count, and a downward with CSF glucose (Figure 4.4).

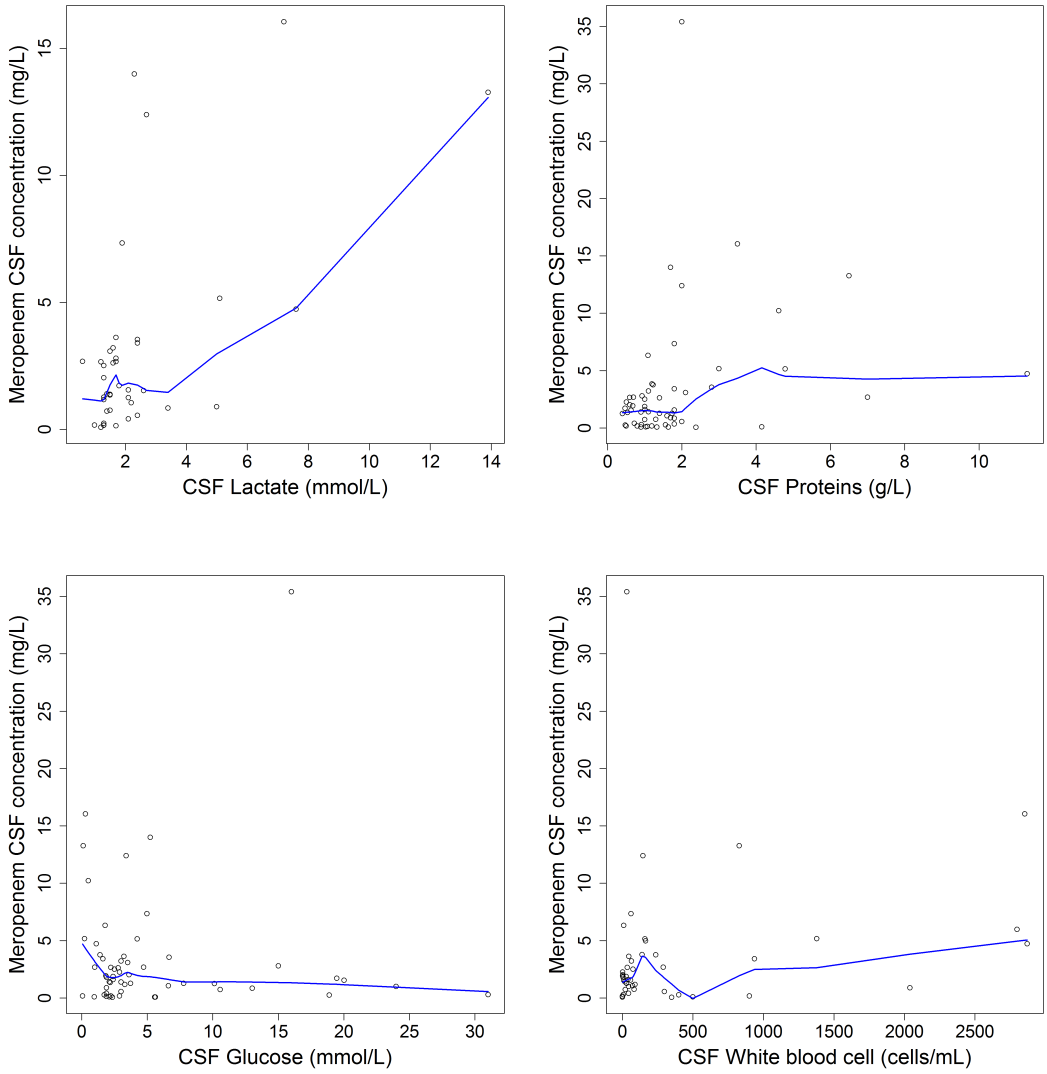

Figure 4.4: Raw plots of CSF meropenem concentration versus CSF markers of infection. Blue lines are lowess smooth lines.

4.4.2 Non-linear mixed-effects model building

The structural model that provided the best fit to the data was initially a 1-compartment model (the drop in OFV when using a 2-compartment model was only 1.6 points). The residual error was best described with a combination of proportional and additive model. Weight and postmenstrual age were included in the NLME model *a priori*, and an additional covariate that had a significant effect on meropenem clearance was standardised serum creatinine. Postnatal age was found not to further improve the fit. After all covariates were included in the model, the structural model was re-tested and then, a 2-compartment model was found to describe the data better (ΔOFV=12.1; corresponding to a p-value for two additional degrees of freedom of 0.002). The drop in the OFV between the initial model and the model with covariates (i.e. the final plasma PK model) was 199.4 units. The covariates remained significant with a 2-compartment model (p-value retention cut-off=0.005).

A CSF compartment was then added to the final plasma PK model, facilitating the description of the CSF pharmacokinetics (and penetration) of meropenem in infants. Two different parameterisations were tested, and the model, described with Equations 4.1, was selected as it provided a lower value of the objective function (ΔAIC=42.6 units); and a better fit was also observed in the diagnostic plots.

The best model for the CSF residual error proved to be a proportional model. The influence of CSF markers of inflammation on meropenem CSF penetration was also investigated, and the inclusion of CSF lactate and CSF protein concentration resulted in a similar OFV drop (ΔOFV=24.7 and 28.3, respectively). When both were included in the model, this did not provide a further improvement in the fit. Although the drop in the OFV was slightly bigger with CSF proteins, the difference was small (3.6) when compared to CSF lactate; furthermore, the

uncertainty on parameters was smaller, and GOF plots showed better agreement with the data, when CSF lactate was included. Consequently, CSF lactate concentration was included in the final model. NONMEM code for the final model is given in Appendix F.

Equations 4.4 describe the final model.

$$
\begin{aligned}
CL &= \theta_{CL} \cdot \left(\frac{WT}{70}\right)^{0.632} \cdot \left(\frac{PMA^{3.33}}{55.4^{3.33} + PMA^{3.33}}\right) \cdot \left(\frac{SCr}{TSCr}\right)^{\theta_{SCr}} \cdot e^{\eta_{CL}}, \\
V_C &= \theta_V \cdot \left(\frac{WT}{70}\right) \cdot e^{\eta_V}, \\
Q &= \theta_Q \cdot \left(\frac{WT}{70}\right)^{0.75}, \\
V_P &= \theta_V \cdot \left(\frac{WT}{70}\right), \\
Q_{CSF} &= \theta_{Q_{CSF}} \cdot \left(\frac{WT}{70}\right)^{0.75}, \\
V_{CSF} &= 0.15 \cdot \left(\frac{WT}{70}\right), \\
f_{CSF} &= \frac{1}{1 + e^{\theta_{uptake} \cdot (1 + \theta_{lactate} \cdot (lactate - 1.8))}}, \\
k_{PL-CSF} &= \frac{Q_{CSF}}{V_C} \cdot 0.98 \cdot f_{CSF}, \\
k_{CSF-PL} &= \frac{Q_{CSF}}{V_{CSF}},
\end{aligned}
\tag{4.4}
$$

where CL is clearance, V_C and V_P are central and peripheral volumes of distribution, respectively, Q is inter-compartmental clearance, f_{CSF} represents the proportion of meropenem that penetrates into the CSF, and k are rate constants.

The final estimates for model parameters, with uncertainty from the NONMEM covariance step, and bootstrap analysis are given in Table 4.2 (η-shrinkage was calculated as described in Chapter 3, Equation 3.9). Internal evaluation of the model showed good fit to the data, i.e. predictions agreed with the observed concentrations and no particular trend was seen in residual plots, for both plasma, and CSF (Figures 4.5 and 4.6, respectively). A prediction-corrected VPC performed using 1,000 replicates is presented in Figure 4.7.

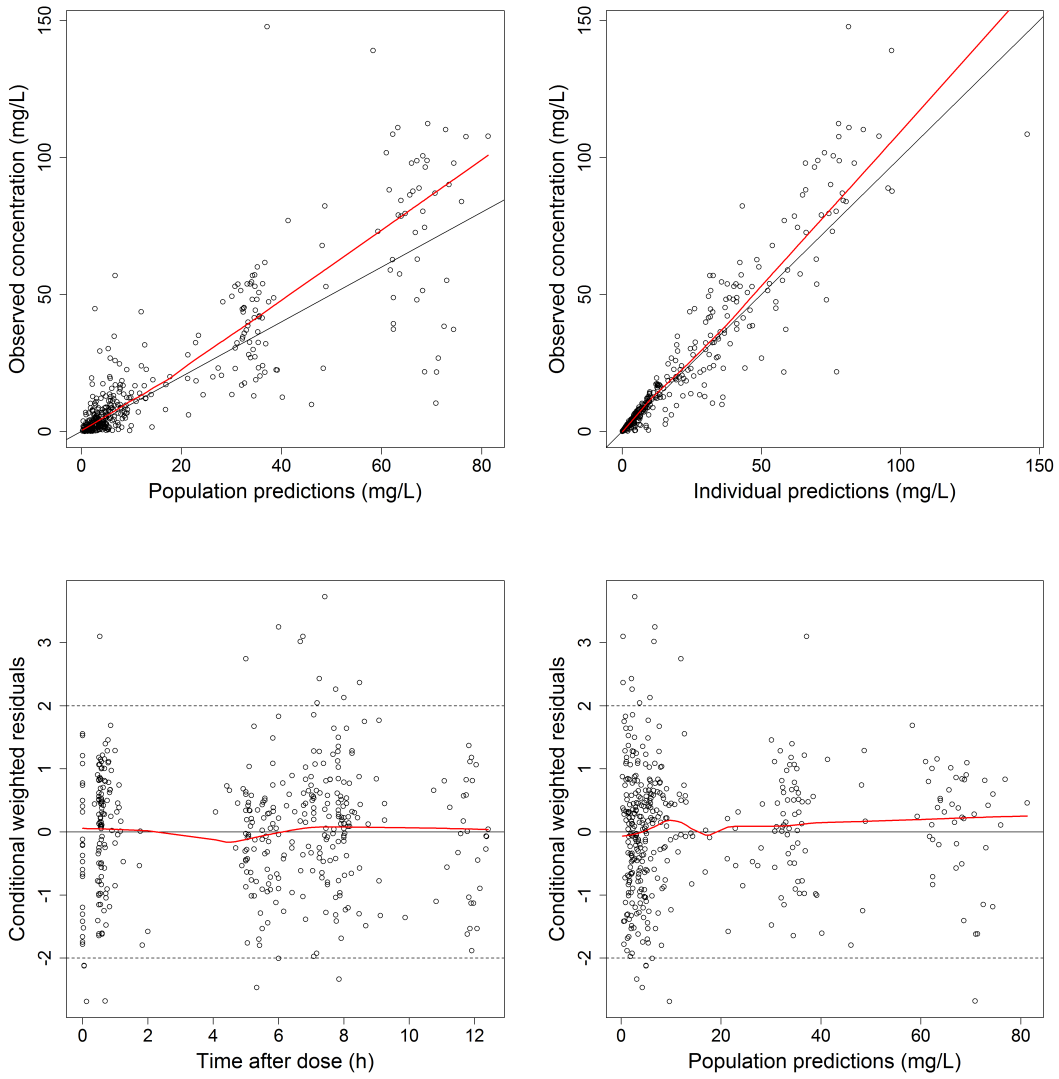

Figure 4.5: Diagnostic plots showing observed versus predicted meropenem plasma concentration (top row), and conditional weighted residuals against time after dose and population predictions (bottom row). Red line is a lowess smooth line.

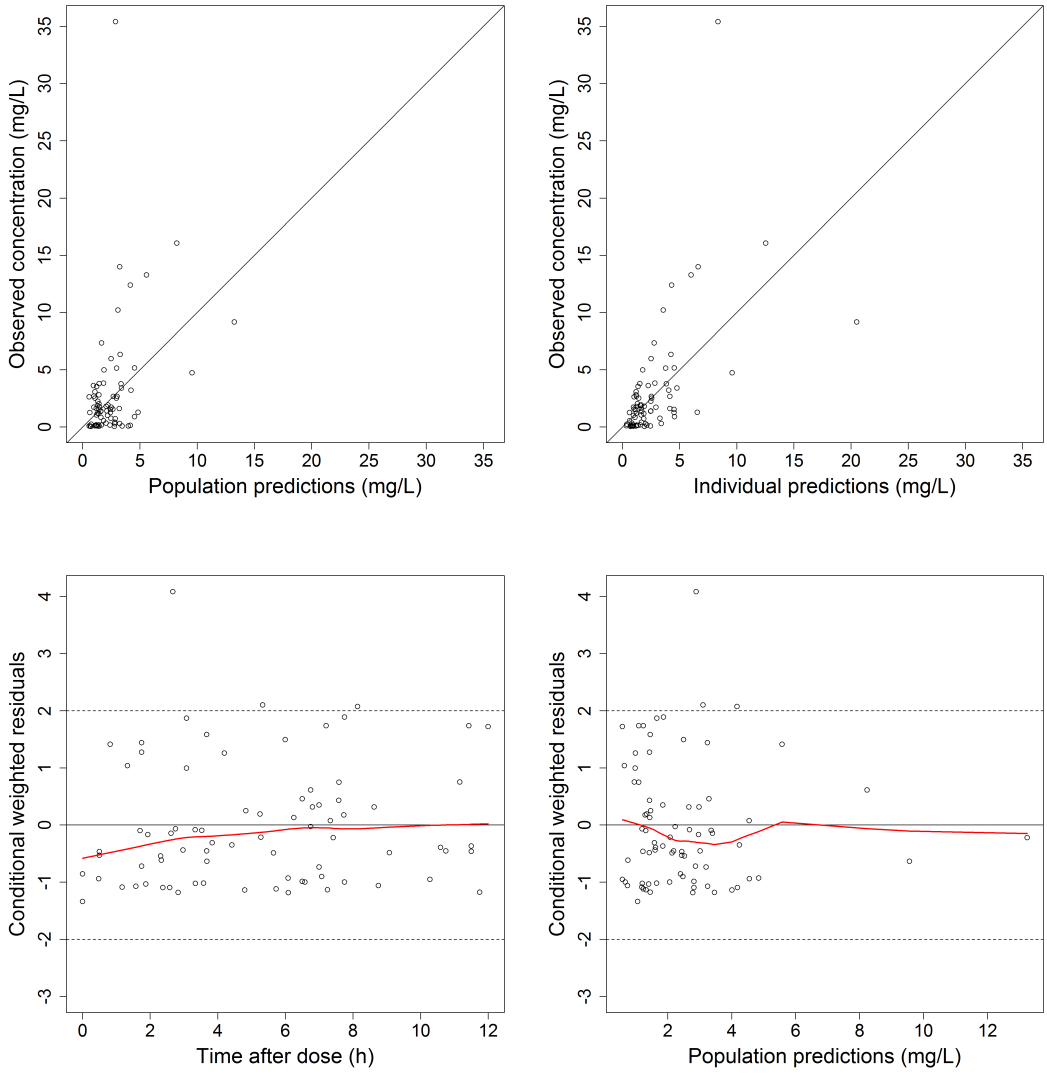

Figure 4.6: Diagnostic plots showing observed versus predicted meropenem concentration in the cerebrospinal fluid (top row), and conditional weighted residuals against time after dose and population predictions (bottom row). Red line is a lowess smooth line.

Table 4.2: Parameter estimates with uncertainty from the final model

	Parameters from the final model				Bootstrap analysis		
	mean	SE	%CV	η-shrinkage (%)	median	2.5%ile	97.5%ile
CL (L/h/70kg)	16.6	2.27	-	-	16.6	13.6	19.8
θ creatinine	-0.24	0.11	-	-	-0.24	-0.43	-0.06
V (L/70kg)	37.8	4.48	-	-	37.4	32.9	44.3
Q (L/h/70kg)	0.69	0.41	-	-	0.66	0.10	1.42
V2 (L/70kg)	124	61.4	-	-	114.6	14.8	331.0
CLCSF (L/h/70kg)	0.013	0.004	-	-	0.013	0.008	0.040
θ uptake*	1.90	0.16	-	-	1.87	1.40	2.22
θ lactate*	-0.167	0.11	-	-	-0.18	-1.09	-0.04
BSV on CL	0.28	0.09	52.9	7.26	0.28	0.15	0.46
BSV on V	0.09	0.13	30.5	32.3	0.09	0.001	0.35
cov BSV CL-V	0.13	0.11	-	-	0.13	-0.001	0.34
ε (prop)	0.15	0.03	38.7	-	0.14	0.10	0.19
ε (add)	0.008	0.003	-	-	0.007	$8 \cdot 10^{-7}$	0.015
ε (prop) CSF	0.85	0.16	92.2	-	0.80	0.58	1.19

CL is clearance, V is volume of distribution, Q is intercomparmental CL, CSF is cerebrospinal fluid, *indicates that values are from a logit function, BSV is between-subject variability, CV is coefficient of variation, ε is residual error: proportional (prop) or additive (add).

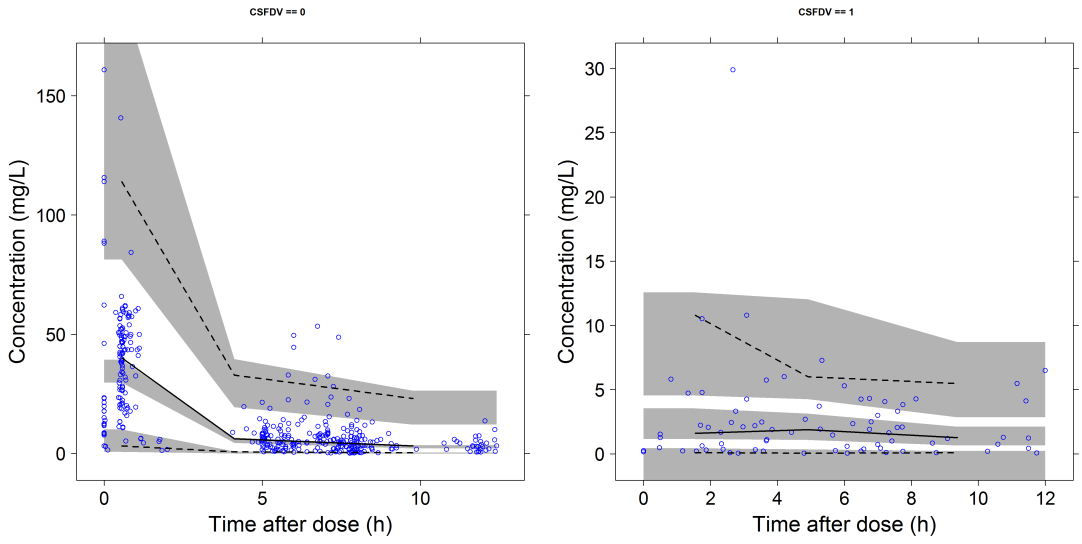

Figure 4.7: Visual predictive check (n=1000) of meropenem plasma (right) and cerebrospinal fluid (left) concentration versus time after dose; blue points are observations, black lines are the 2.5$^{\text{th}}$, 50$^{\text{th}}$ and 97.5$^{\text{th}}$ percentiles of the observed data, and the shaded area is a non-parametric 95% confidence interval for the corresponding predicted concentrations.

Table 4.3: Summary of demographic characteristics of subjects from the original and simulated dataset

	Original dataset	Simulated dataset
n	167	1,000
weight (kg)	2.12 (0.48-6.32)	2.36 (0.74-4.83)
gestational age (weeks)	33.3 (22.6-41.9)	32.0 (23.1-41.9)
postnatal age (days)	17 (1-105)	17 (2-95)
postmenstrual age (weeks)	37.4 (23.7-51.3)	36.0 (24.2-51.4)

All values are median (range).

4.4.3 Probability of target attainment

Monte Carlo simulations was performed for 1,000 virtual infants for eight different MIC values (ranging from 0.25 to 32 mg/L). A comparison of demographic characteristics of the subjects from the original and simulated datasets is given in Table 4.3.

To assess meropenem dose (and infusion length) - response relationship, different combinations of both were tested, and based on the simulations performed, probability of target attainment (PTA) plots were generated. Pharmacodynamic targets were defined as 40%T>MIC or 70%T>MIC (PTA40% or PTA70%, respectively), and the results of the simulations are presented in Figures 4.8 and 4.9, respectively.

The current dosing regimen for late-onset sepsis (i.e. 20 mg/kg, given over 30 minutes) enabled approximately 100% of simulated subjects (from all four age groups) to reach PTA40% target for an MIC of 2 mg/L (Figure 4.8), which is the highest susceptibility breakpoint for bacteria treated with meropenem, as given in the EUCAST breakpoint tables [188]. The majority of infants reached PTA70% with the same dosing regimen. However, for an MIC of 8 mg/L (i.e. resistance breakpoint for meropenem [188]), a higher dose was shown to be needed - for example 40 mg/kg, or even 80 mg/kg if the target was PTA70%, and the goal

was that the majority of patients reaches this target (Figure 4.9).

With the current dosing regimen for treating bacterial meningitis - i.e. 40 mg/kg, infused over 30 minutes - over 75% of infants reached a target of 70%T>MIC for an MIC of 1 mg/kg (Figure 4.9), which is the highest resistance breakpoint for most common pathogens that cause bacterial meningitis, according to EUCAST [188].

Boxplots, showing how the distribution of %T>MIC is changing according to the MIC value, are presented in Figure 4.10.

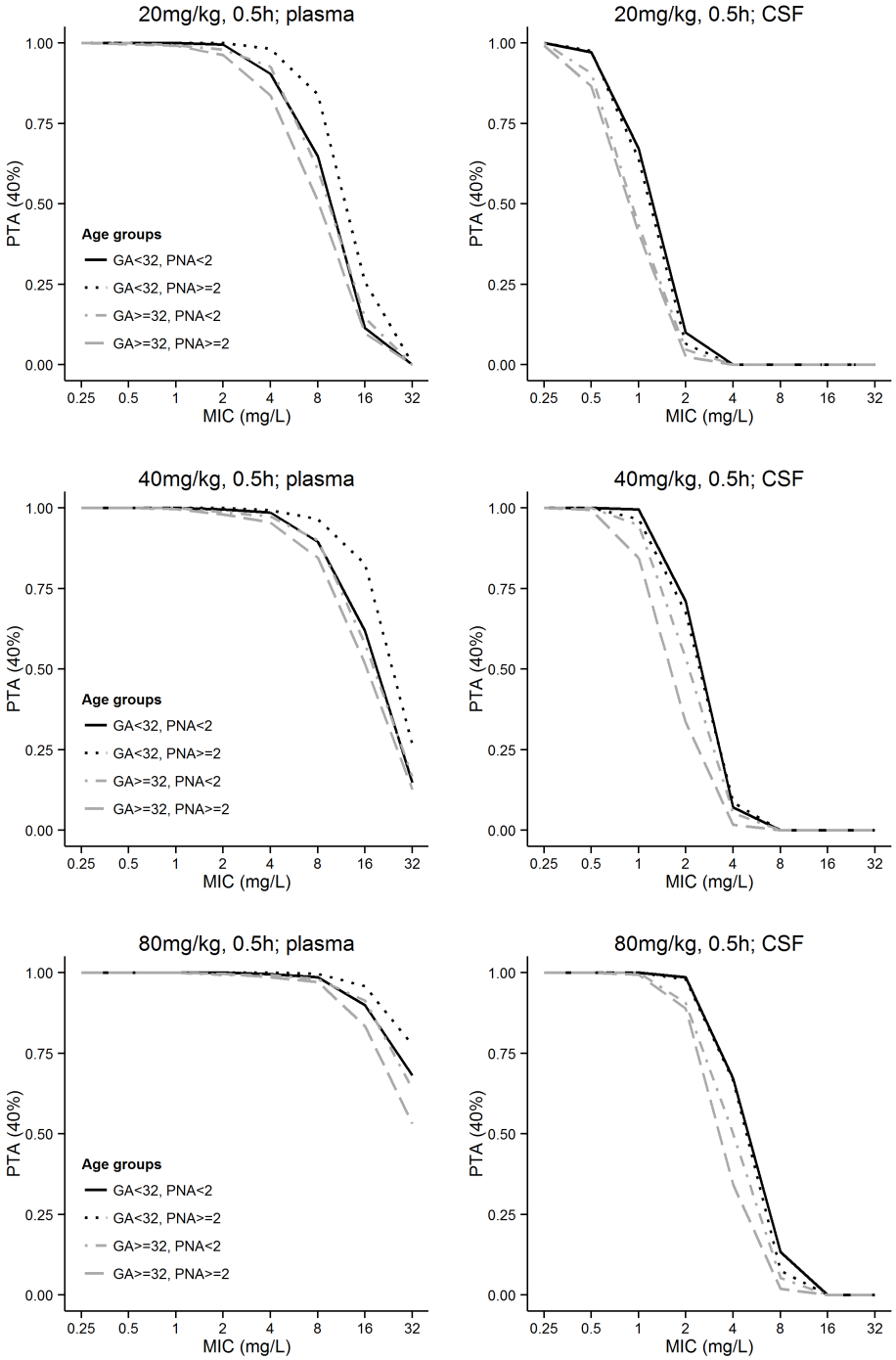

Figure 4.8: Probability of target attainment (with target defined as 40%T>MIC) relationship with MIC values for 4 different age groups. Both gestational age (GA) and postnatal age (PNA) are in weeks. The dosing interval was assumed 8 hours for all four groups, except for group 1 (12 hours). CSF is cerebrospinal fluid.

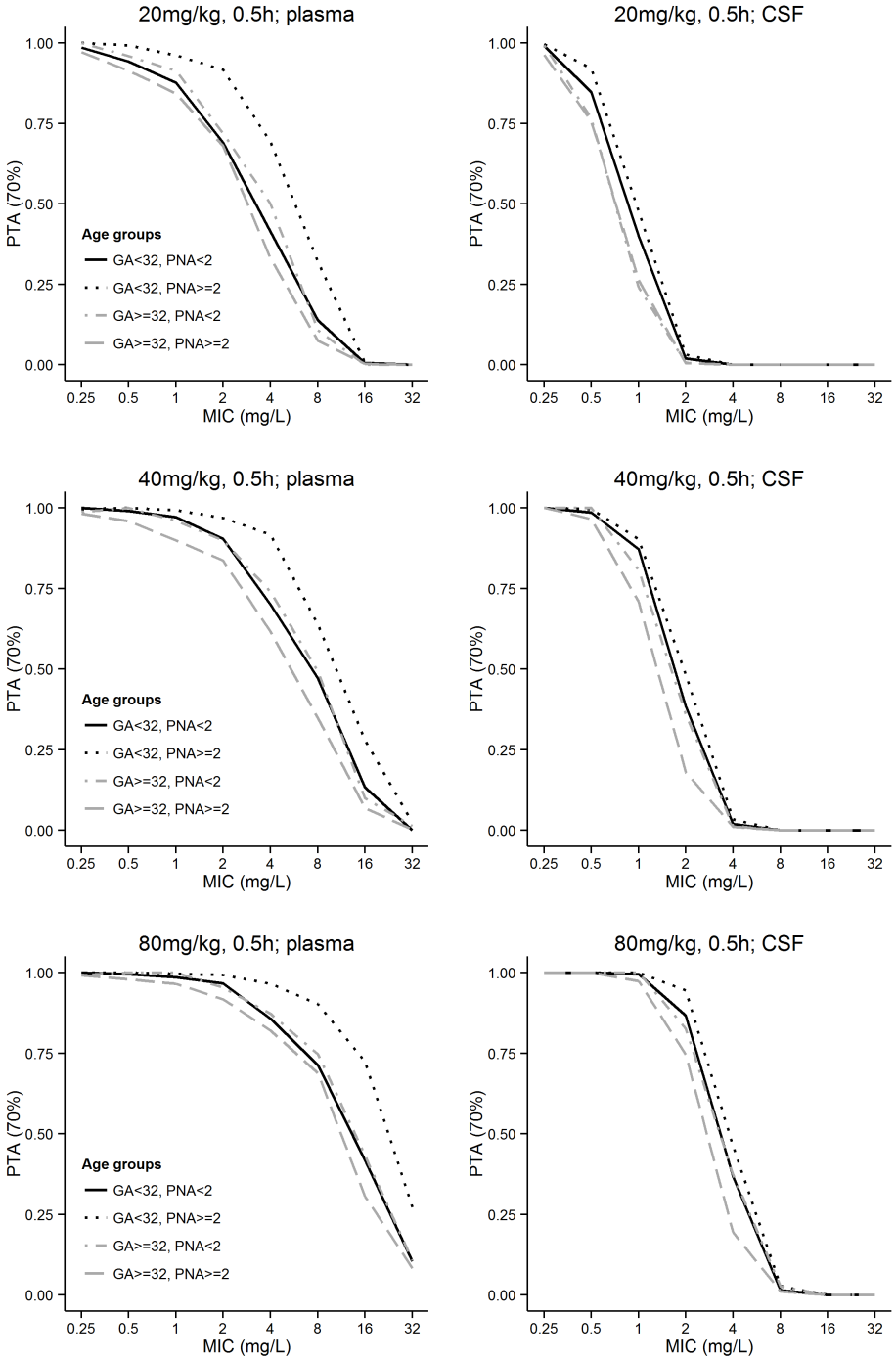

Figure 4.9: Probability of target attainment (with target defined as 70%T>MIC) relationship with MIC values for 4 different age groups. Both gestational age (GA) and postnatal age (PNA) are in weeks. The dosing interval was assumed 8 hours for all four groups, except for group 1 (12 hours). CSF is cerebrospinal fluid.

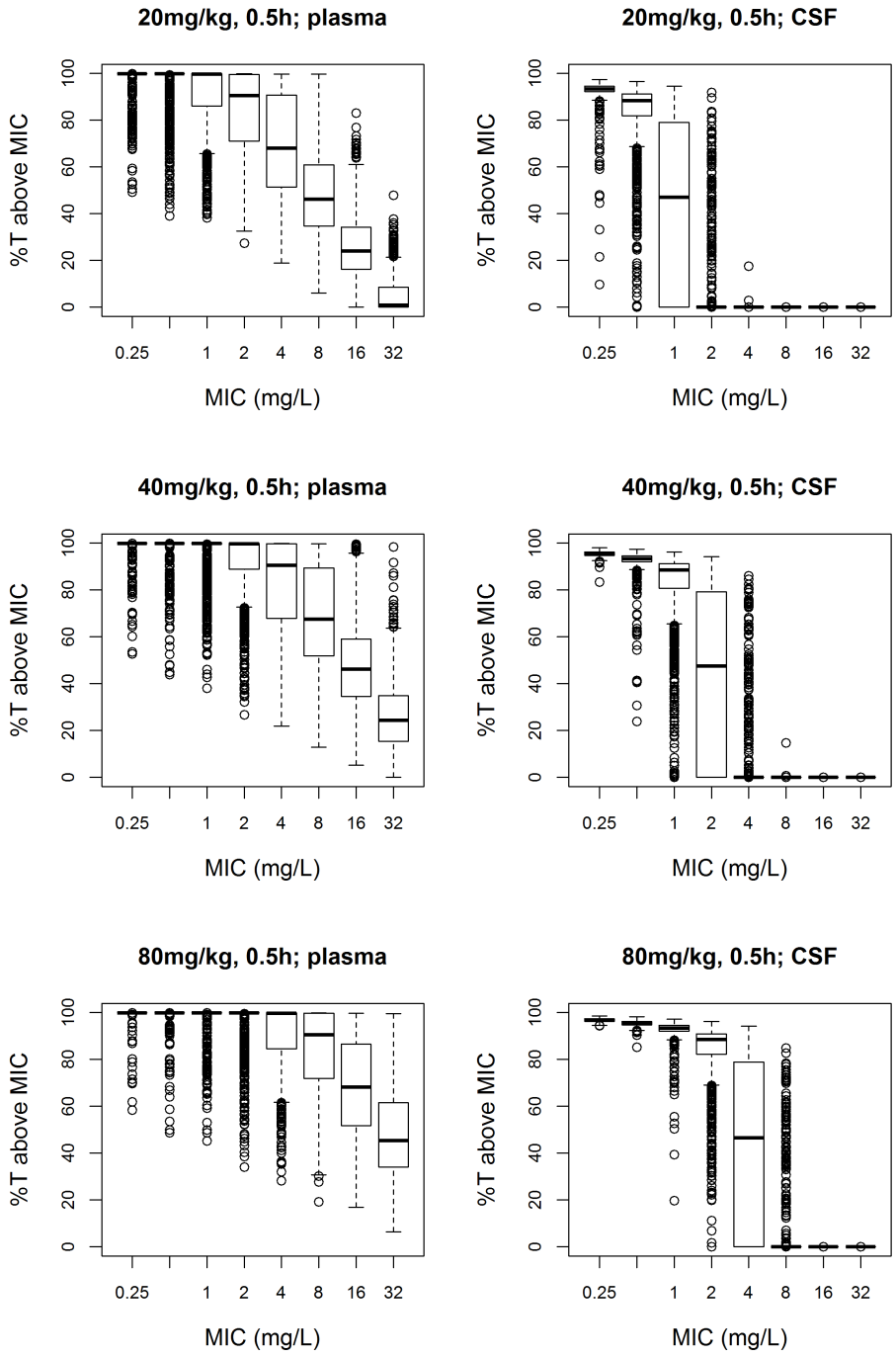

Figure 4.10: Boxplots showing time above MIC for 8 different MIC values; for both plasma (left) and cerebrospinal fluid (right). The dosing interval was assumed 8 hours for all infants, except for infants with gestational age <32 weeks, and postnatal age <2 weeks (12 hours).

4.5 Discussion

A non-linear mixed-effects model that described plasma and CSF pharmacokinetics of meropenem in infants with late-onset sepsis or bacterial meningitis younger than 90 days was developed using the largest meropenem dataset to have been collected in this population. The model was then used to perform Monte Carlo simulations and the results showed that the current standard dosing regimens are appropriate for treatment of both LOS and meningitis, if the causative pathogen has an MIC that corresponds to the EUCAST susceptibility breakpoints [188] and the PD target is 40%T>MIC.

The model described by Equations 4.1 was chosen for describing the PK of meropenem in the CSF and the relationship between plasma and CSF PK. This model provided a lower value of the objective function, and the diagnostic plots showed a better fit. Additionally, the mass balance is preserved in this model, compared to the model described by Equations 4.2.

The uptake of meropenem into the CSF (i.e. the ratio between CSF and plasma meropenem concentration at steady state) was estimated to be 13%, which is at the lower end of what was reported in the literature, where values for penetration range from approximately 10% to 40% [281, 271, 48, 282] (not including one study [265] that is discussed below). The reason for poorer penetration might be that the meninges of the infants in this study were not that inflamed, which is shown by low median CSF protein (1.2 g/L) and CSF lactate (1.8 mmol/L) concentrations. This could be because infants with both confirmed and suspected bacterial meningitis were treated. Also, 32 out of 78 CSF meropenem samples were collected from patients in NeoMero-1 trial (which was a study of LOS, and subjects were not assumed to have meningitis), and could also explain lower values of meropenem penetration.

Both CSF lactate and CSF protein concentration were significant covariates

on the parameter corresponding to meropenem penetration into the CSF, but due to smaller relative standard errors, and a better fit observed on the diagnostic plots, lactate was included in the final model. The final estimate of the effect of CSF lactate concentration was -0.17 (Table 4.2), meaning that an increase in CSF lactate of 1 mmol/L (e.g. from 1.8 mmol/L (median) to 2.8 mmol/L), would cause meropenem uptake to increase from 0.13 to 0.17 (a 31% increase). The final estimate of the parameter corresponding to CSF proteins was -0.30, meaning that CSF/plasma ratio would increase to 0.21 if CSF protein concentration increased for 1 g/L (from 1.2 to 2.2 g/L). This agrees with what has been reported in the literature, i.e. that the penetration of meropenem into the CSF increases when the meninges are inflamed, which is shown by both elevated CSF lactate and protein concentration [48].

Diagnostic plots (Figures 4.5 and 4.6) and the VPC (Figure 4.7) showed the model was able to describe the CSF and plasma meropenem data (there was no significant bias seen) and had good predictive performance. Serum creatinine (standardised using typical serum creatinine for PMA), which is a marker of renal function, had a significant effect on meropenem plasma clearance, which is expected since meropenem is predominantly renally eliminated. The values for a typical infant from this study (weight=2.12 kg, PMA=37.4 weeks, SCr=32 μmol/L, typical SCr=58.9 μmol/L) of meropenem clearance and central volume of distribution were 0.45 L/h and 1.14 L, respectively. This agrees closely with what was found by van den Anker *et al* [266] for a population with similar demographics. However, studies that involved premature neonates only, e.g. a study by Padari *et al* [264] and van Enk *at al* [262] found lower values of CL (0.06 L/h and 0.145 L/h, respectively). This is not surprising, because renal function is more immature in the premature neonates, and the median weight for subjects in their study was only approximately 1 kg, compared to >2 kg in this (i.e. the NeoMero) study. Smith *et al* [265] found that CL in their population of both premature

and mature neonates was approximately 0.13 L/h, which might seem much lower than what was found in the NeoMero study (0.45 L/h), but again, their median GA was 28 weeks, and weight 1.1 kg; which could explain the lower value of CL.

According to EUCAST [188], the highest resistance breakpoint for meropenem (for all listed pathogens in the EUCAST breakpoint tables) is 8 mg/L, and susceptibility breakpoint is 2 mg/L. For pathogens that cause meningitis, the reported breakpoints are 1 mg/L and 0.25 mg/L for resistant and susceptible bacteria, respectively. These MIC values were considered when selecting the optimal dosing regimen for meropenem in infants. Based on the results of Monte Carlo simulations, the current dosing regime for both bacterial meningitis (i.e. 40 mg/kg, over 30 minutes), and late-onset sepsis (i.e. 20 mg/kg, over 30 minutes) seem adequate, as all subjects reach the target of 40%T>MIC for MICs of 2 and 0.25 mg/L, respectively. The current dosing regime for meningitis appears appropriate for a higher target (70%T>MIC) and MIC of 1 mg/L, as >75% of infants achieve the target (Figure 4.9). But, in order for the majority of infants to reach a target of 70%T>MIC and MIC of 8 mg/L in plasma, a higher dose (e.g. 80 mg/kg) would be needed (Figure 4.9).

The dosing recommendations above were made for a worst case scenario, most pathogens will have an MIC below the resistance (or even susceptibility) breakpoints, as Figure 4.1 shows for pathogens causing bacterial meningitis. Also, the probability of target attainment was determined after the first dose, so if any accumulation of meropenem was present, it would result in a higher PTA. Ideally, the MIC distribution of the bacteria in the environment in which meropenem is intended to be used would need to be determined in order to recommend an optimal dose for that environment.

Meropenem showed low potential for nephrotoxicity [259, 247], and it has been reported that a higher dose does not relate to greater toxicity [271], but this might not be true for a much higher than currently used doses (80 versus

20 or 40 mg/kg, respectively), therefore perhaps the infusion duration could be prolonged. But when infusion durations of 1, 2, and 6 hours were tested for a dose of 20 mg/kg, this only slightly improved target attainment for plasma, but not for CSF. Moreover, a duration of 6 hours resulted in a lower target attainment for CSF, probably due to the fact that peak plasma concentration was lower with this dosing regime. Longer durations than 6 hours were not tested, as meropenem is unstable at room temperature (e.g. when kept at room temperature as 6% solution it degrades up to the allowable limit of 10% in 6 hours; but when a 4% solution is used, the time is increased to 12 hours [283]).

The pharmacodynamic targets of 40% and 70% of the dosing interval above the MIC of a pathogen were selected, because it is thought that 40%T>MIC is an adequate target for a bactericidal effect of carbapenems [17]. Furthermore, a study of β-lactam antibiotics showed that 40%T>MIC provided a bacteriological cure in 85-100% patients with otitis media [284]. A PD target of 70%T>MIC was used because it has been suggested that this target might be appropriate [64] for neonates, who have immature immune system. However, this target was not determined based on evidence, thus, clinical studies are needed to define the exact percentage of T>MIC needed for a bactericidal effect and clinical cure in neonates.

The only neonatal study [265] that reported the uptake of meropenem into the CSF, used only nine CSF samples from six patients to determine the penetration – it was reported as 70%. This value was not correctly determined, since β-lactam antimicrobial agents enter the CSF through the paracellular pathways [271], therefore the peak CSF concentration is delayed, and one cannot simply measure plasma and CSF concentation at the same time points to determine the penetration (which was what was done in the above mentioned study [265]). Instead, CSF sampling should be performed at different times in different patients (as the number of CSF samples per patient is usually very limited) [271], and then

modelling can be used to describe the penetration; as highlighted in this chapter.

It has been suggested that CL_{CSF} could be used to approximate the rate of CSF formation [285], and the CSF clearance was estimated as 0.013 L/h (for an adult of 70 kg) (Table 4.2), which is within the range of reported values for CSF formation in the literature (0.012-0.036 L/h) [267, 272, 286, 287].

On average <1 CSF sample was collected per patient, hence the between-subject variability was not estimated for the CSF compartment. This means that residual variability incorporates some of the possible BSV, which could explain the large value of the proportional residual error for the CSF compartment (0.85) (Table 4.2).

Typical serum creatinine for a specific PMA was used to standardise measured serum creatinine, and tested as a covariate when developing the plasma PK model. The equation used for typical SCr was derived using data from neonates up to 44 weeks of PMA; but, in the dataset used in this study, infants were up to 51 PMA weeks old (there were 12 infants with PMA>44 weeks). To address this, the value of the typical SCr was capped at 1 month for those 12 infants, according to what was reported in the literature – that SCr reaches a plateau around 1 month of age [224, 214, 233].

The Monte Carlo simulations showed that the current dosing regime for infants with sepsis or meningitis is appropriate for pathogens with MIC values close to the susceptibility breakpoint [188], but higher doses are needed when dealing with pathogens with higher MICs. Higher dosing recommendations would need to be prospectively evaluated in a clinical study, but as already mentioned, they were made for the worst case scenario of all pathogens having an MIC that corresponds to the meropenem resistance breakpoint, meaning that if an actual MIC distribution was used, most likely much lower doses than 80 mg/kg would be needed.

4.6 Summary

An extensive dataset from a total of 167 infants younger than 3 months (in treatment for confirmed or suspected late-onset sepsis or bacterial meningitis) was used to develop a non-linear mixed-effects model to describe the relationship between meropenem plasma and CSF pharmacokinetics. This was the largest dataset so far, and contained 401 plasma and 78 CSF samples. The evaluation showed the model was able to describe the data and had good predictive properties, therefore it was used in Monte Carlo simulations to determine an optimal dose. The results showed that current dosing regimes (20 and 40 mg/kg, over 30 minutes, for late-onset sepsis, and meningitis, respectively) are appropriate when treating infections caused by pathogens with low MIC values, i.e. MICs that corresponds to the susceptibility breakpoint for meropenem. The results from this study might provide the information needed for meropenem to be licensed in infants <3 months of age. Future work could focus on also including the available pharmacodynamic data into the model, and using the actual MIC distribution to define an optimal dose.

Chapter 5

Pharmacodynamics of neonatal sepsis

5.1 Introduction

Newborn infants admitted to NICU often start antimicrobial therapy immediately [5] to avoid the development of sepsis, which is one of the most common causes of morbidity in this population [2]. As treatment often starts before the result of the blood cultures is known [55], and/or the result can be falsely negative [288], it is imperative that an informative clinical symptom or laboratory sign (or a set of them) is also used. However, there is currently no agreement on which biomarker(s) or symptoms of infection to use to determine neonatal sepsis [55, 289]. Therefore, a proof-of-concept study (presented in this chapter), using item response theory (IRT) models, was performed to facilitate the selection of the laboratory test that provides the most information about the sepsis status.

5.1.1 Item response theory models

The development of the IRT models originates from psychology [290], and a method, similar to IRT, was first utilised in the 1920s for analysing data from

psychological and educational tests [291]. Recently, the IRT framework has been introduced into pharmacometrics [19, 292], where it was, for example, used to describe efficacy of morphine by analysing neonatal multiple pain scales data [20].

IRT involves mathematical models that specify the relationship between the probabilities for a specific response to an item (e.g. a result of a laboratory test in the current example) and the underlying hidden or latent variable of interest (Ψ) (e.g. sepsis status) [293]. The set of items represents a proxy for the hidden variable, which cannot be directly measured or observed [19].

The change in the probability for a certain response to an item with the latent trait is described by an item characteristic function (ICF) and its graphical representation, item characteristic curve (ICC). ICF puts both item characteristics and the subject-specific hidden variable on the same scale and so represents the main concept of IRT. The scale of the hidden variable is hypothetical (going from -∞ to +∞), but usually assumed to be normally distributed (in the population of interest) with a zero mean and variance of 1 [293, 294].

Logistic models are used (to characterise the relationship between the hidden variable and the response to an item) when dealing with binary items. These models differ according to the number of parameters used in the function, and the most commonly used are: one-parameter logistic model (1PL), two-parameter logistic model (2PL), and three-parameter logistic model (3PL), where 1PL and 2PL models are a simplified, or constrained, version of the 3PL [293, 295].

A 3PL model can be mathematically represented by Equation 5.1.

$$P(Y_{ij}=1) = c_j + (1-c_j)\cdot\frac{e^{a_j\cdot(\Psi_i-b_j)}}{1+e^{a_j\cdot(\Psi_i-b_j)}}, \tag{5.1}$$

where $P(Y_{ij}=1)$ is the probability of the ith subject's response to the item j being 1, b is the difficulty parameter, indicating location on the latent variable (Ψ) scale

(where there is 50% probability of Y_{ij} being 1; when c=0), a is the discrimination parameter (where items with higher values of a are more discriminatory), or the slope, and c is the guessing parameter, or the lower asymptote, and assumes a value between 0 and 1 [293, 294]. All three parameters, b, a, and c are properties of the item and define the ICC.

By fixing the guessing parameter c to zero, the model becomes a 2PL model (Equation 5.2), and the items are only allowed to differ in a or b parameters.

$$P(Y_{ij} = 1) = \frac{e^{a_j \cdot (\Psi_i - b_j)}}{1 + e^{a_j \cdot (\Psi_i - b_j)}}. \tag{5.2}$$

The most constrained version is a 1PL model, where c parameter is fixed to zero and a parameter is fixed to 1 (Equation 5.3), therefore the ICC is only allowed to shift left or right.

$$P(Y_{ij} = 1) = \frac{e^{(\Psi_i - b_j)}}{1 + e^{(\Psi_i - b_j)}}. \tag{5.3}$$

The IRT models are based on assumptions. One of the assumptions is that the probability of a subject's response to an item depends on the latent variable, i.e. it is assumed that the item follows the IRT model used [293, 296]. Another assumption is unidimensionality, meaning that the items measure only one hidden variable, or, that only one latent variable accounts for the majority of the correlations between items [297]. And, IRT models also assume that the items are locally or conditionally independent, meaning that there is no relationship between subject's responses to any pair or items after controlling for the latent variable [293].

5.1.2 Efficacy of gentamicin

The focus of Chapter 3 of this thesis was mostly on toxicity involved with gentamicin use in neonates. However, gentamicin is also an effective broad-spectrum antibacterial agent, and therefore one of the most widely used antimicrobials for the (empirical) treatment of the neonatal sepsis [161]. Gentamicin is a concentration-dependent agent, meaning that high peak concentrations are needed for it to be effective [153]. But, whilst empirical therapy should not be unnecessarily prolonged [298, 299], it can prove difficult to relate gentamicin C_{max} to the resolution of sepsis when only examining microbiological results, due to reasons described in the following section (5.1.3).

5.1.3 Defining neonatal sepsis

Whilst the standard test for confirming bacterial sepsis is a positive blood culture from an otherwise sterile site, Blackburn *et al* found that from 8904 blood cultures taken from neonates, there were only 12% culture positive, and the percentage of the positive samples was the lowest at birth [300]. A possible reason for the low numbers of culture positive microbiological results might be that a substantial number of blood cultures are actually falsely negative. This could be due to a variety of reasons, such as: the volume of the blood sample might be insufficient to detect bacteria [301], the levels of bacteria in the sample might be too low [289], the neonate might have been exposed to prior antibiotic treatment, non-typical bacteria that do not grow in the usual media are present [55], or the infection was not caused by bacteria. Additionally, the culture positive blood samples might also be falsely positive – due to a contamination [288]. These reasons are why microbiological results alone are not sufficient for the sepsis diagnosis, and different clinical and/or laboratory signs also have to be used.

However, in a recent review of 15 neonatal clinical trials, where antimicrobials were used for treating early- and late-onset sepsis, Oeser *et al* [55] found that

a variety of different clinical and laboratory signs were used to define sepsis. Wynn *et al* [289] reviewed the literature and also found considerable heterogeneity concerning the definition of sepsis in neonates, more specifically, within 42 studies or guidelines 12 of them used different combinations of 10 laboratory tests; and 62% of them used at least one clinical sign to define sepsis.

Currently, definitions for neonatal sepsis that were agreed on by a panel of experts are mainly used, such as for example, a definition according to the EMA [276], or a (different) sepsis criteria defined at the International Pediatric Sepsis Consensus Conference [275]. Therefore, there is a need for a standardised and objective definition of neonatal sepsis that is based on evidence rather than experts' opinion alone, which would then also facilitate comparison of results of different clinical trials [55].

5.2 Objective

The objective of the study described in this chapter was to develop an IRT model (using neonatal pharmacodynamic data) and then use it to define which laboratory test (from a set of laboratory sepsis signs) is the most informative regarding the sepsis status. Furthermore, the aim was also to investigate possible effects of gentamicin C_{max} on the rate of the resolution of sepsis.

5.3 Methods

5.3.1 Study population

Data used for the IRT modelling were collected in a prospective multicentre study of gentamicin in neonates (the neoGent study), and were in detail described in Chapter 3. However, the datasets were not exactly the same, as not all neonates provided PK samples; whilst all of them had pharmacodynamic data collected.

Table 5.1: Description of the items used in the analysis

item	description	thresholds
1	white cell count	<4 or >20 $\cdot 10^{12}$
2	platelet count	<100$\cdot 10^{12}$
3	C-reactive protein (CRP) concentration	>15 mg/L
4	glucose concentration	>10 or <2.5 mMol/L
5	lactate concentration or base excess (BE)	lactate >2 mMol/L or BE <-10 mEq/L

This dataset therefore included a total of 195 neonates (i.e. 32 neonates more than the dataset described in Chapter 3).

There were many (n>100) different potential markers of sepsis collected in the neoGent study, but in this proof-of-concept study the focus was only on the laboratory signs of sepsis – as described by the EMA criteria for defining neonatal sepsis [276]. This criteria is widely used and was also suggested in a recent review [55]. Furthermore, laboratory results are potentially less subjective and thus more reliable than clinical symptoms [26]. There was no information on the immature-to-total neutrophil ratio available in the data, thus a total of five items was used in the analysis (Table 5.1).

The results of the tests listed above were then dichotomised according to the thresholds indicating meeting the sepsis criteria according to the EMA, so that a value of 1 indicated meeting the criteria, and 0 meant that the criteria was not met. However, not all laboratory tests were done at each treatment day, and the missing data were assigned a value of -1. The same was done if there were no measurements for a whole treatment day - there were 26 such days from 24 subjects (which represents 12.3% of subjects).

5.3.2 Non-linear mixed-effects model building

A logistic function was used to model the binary data. Both, a 2PL and a 1PL model (Equations 5.2 and 5.3, respectively) were tested in order to describe the relationship between the probability for a specific response in an item (i.e. labo-

ratory test) and the latent variable (i.e. sepsis status).

The change in the subject-specific latent variable (Ψ_i) with time was described using a linear function (Equation 5.4) [19]:

$$\Psi_i(t) = \Psi_i^0 + s_i \cdot t, \tag{5.4}$$

where Ψ_i^0 is baseline, and s_i is slope. Both baseline and slope were allowed to differ between subjects, and the variability was described using an additive random effects model. Random effects (ηs) were assumed to follow a normal distribution. The baseline and slope were allowed to be correlated, and the correlation was estimated.

The IRT model was implemented in NONMEM 7.3 (ICON Development Solutions, Ellicott City, Maryland), and the estimates of the model parameters (both item and subject-specific parameters) were obtained using the stochastic approximation expectation maximisation (SAEM) method with Laplace approximation, followed by the importance sampling (IMP) method to obtain the OFV value.

Since data were not missing at random (i.e. usually fewer laboratory tests are done when a neonate is more stable), it was assumed that the probability for a laboratory test result to be missing was dependent on the sepsis status; therefore, missingness was treated as an additional item with a separate ICF. The following probabilities were estimated: the probability that the data is non-missing (P(Y=NM)), and the probabilities that given that the data is not missing a laboratory test met the sepsis criteria (P(Y=1|NM)), or did not meet the criteria (P(Y=0|NM)). This conditional probability model is presented in Figure 5.1.

A 2PL model for missingness would assume that whether a test is missing or not was completely dependent on the sepsis status. However, tests are also performed routinely, not depending on the sepsis status. This can be modelled

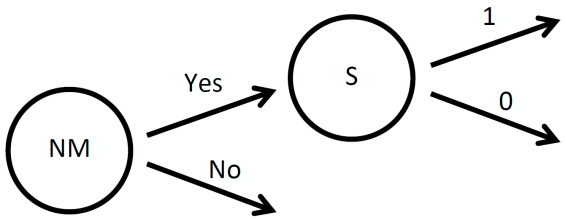

Figure 5.1: Probability diagram. NM is non-missing, S is sepsis.

with a 3PL model (Equation 5.1), where the c parameter describes the probability of a test being done independent of the sepsis status.

To describe different patterns in missingness for different items, several covariates were introduced into the model. For example, based on visual examination of the raw data, a different guessing parameter for the missing data (c_{MISS}) was assumed for the first day of therapy, for days of therapy >6, and for the last day of treatment. Additionally, an item 3 specific c_{MISS}, and a c_{MISS} for items 1&2, and for items 4&5 were tested.

The assumption of missingness being time-dependent, i.e. that with greater time on therapy it depends more on the disease whether the data is missing or not (since at the start of treatment laboratory tests would be done regardless of the disease state), was also investigated. An exponential and a sigmoidal model (Equations 5.5 and 5.6, respectively) were used to test this assumption.

$$c_{MISS} = \theta + (1-\theta) \cdot e^{-\theta_{time} \cdot t}, \tag{5.5}$$

$$c_{MISS} = 1 - (1-\theta) \cdot \frac{t}{\theta_{time} + t}, \tag{5.6}$$

where θ_{time} represents the time effect on c_{MISS}.

Additionally, it was hypothesised that the probability of data being missing decreases with increasing time since the last laboratory test. However, this trend was not observed on the plots, therefore this assumption was not tested.

Gentamicin is a concentration-dependent antimicrobial agent, thus the effect of C_{max} was investigated on the slope corresponding to the change in the sepsis status. Empirical Bayes estimates of gentamicin peak concentrations (for n=163 subjects) were obtained using the final population PK model, described in Chapter 3, and assuming that "C_{max}" occurs 1 hour after the dose [186] (C_{1h}). The highest C_{1h} per patient was selected. For 32 subjects that were not in the PK dataset, a mean C_{1h} of 9.4 mg/L was imputed.

The information about the reliability of each of the laboratory tests for discriminating between patients with different sepsis statuses was calculated analytically (as the second derivative of the log likelihood (i.e. Fisher information) with respect to the sepsis status), which was possible because the random effects in the model were only associated with the latent variable [19]. The items were then ranked according to the average information they provided, and a plot of the relationship between the information and the latent variable was produced.

5.3.3 Evaluation

To assess the uncertainty of the model parameter estimates, standard errors were obtained from the NONMEM covariance step, and a non-parametric 95% confidence interval was determined based on n=1000 bootstrap replicates.

Additionally, a visual evaluation of the IRT model was performed by producing a categorical VPC [302] with n=1000 simulations using the parameter estimates from the final model. The proportions of specific responses to an item in the simulated (n=100) and the observed data were compared using mirror plots.

Table 5.2: A summary of the dataset

item	n	DV=0	DV=1
1	789	663	126
2	788	677	111
3	990	625	365
4	957	809	148
5	930	614	316

DV=1 indicates that the item, i.e. result of a laboratory test, was below/above the threshold indicating meeting the sepsis criteria; and DV=0 indicates the opposite. Items are specified in Table 5.1.

5.4 Results

5.4.1 Study population

The dataset used in this study included pharmacodynamic data from 195 neonates and infants that were prospectively collected during the neoGent study in five UK hospitals. The PNA of subjects ranged from 1 to 83 days (with day 1 defined as the day of birth), with the median PNA of 5 days (the median PNA at treatment initiation was 1 day). The patients stayed on therapy for median 6 days (range: 2-21 days). Fifteen subjects (7.7%) were culture positive.

Laboratory signs of sepsis (according to the EMA [276]) were selected from the available data, and the dichotomised values for each item are presented in Table 5.2. When the missing data were added in, there was a total of 1163 values for each item.

Figure 5.2 shows the number of subjects at each treatment day, and Figure 5.3 the patterns of missingness for each item with treatment day.

5.4.2 Non-linear mixed-effects model building

A 2PL model provided a better fit to the data than a 1PL model (ΔOFV=92.8). The missing data was analysed using a 3PL model. From all of the tested effects

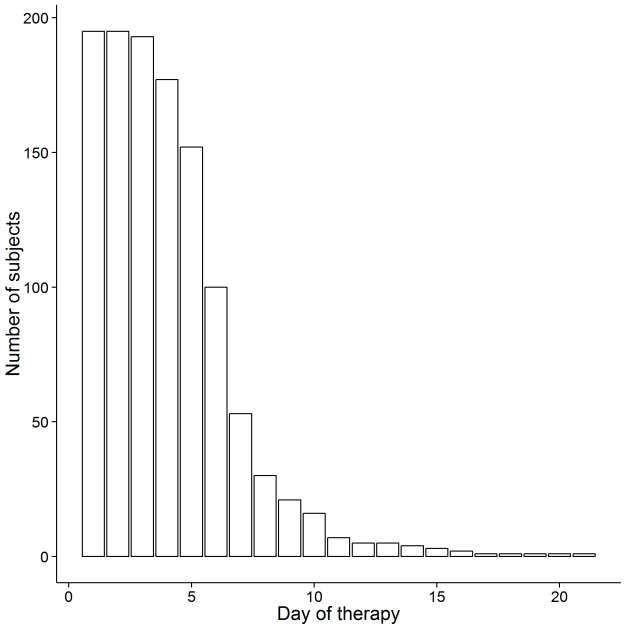

Figure 5.2: Number of subjects at each treatment day.

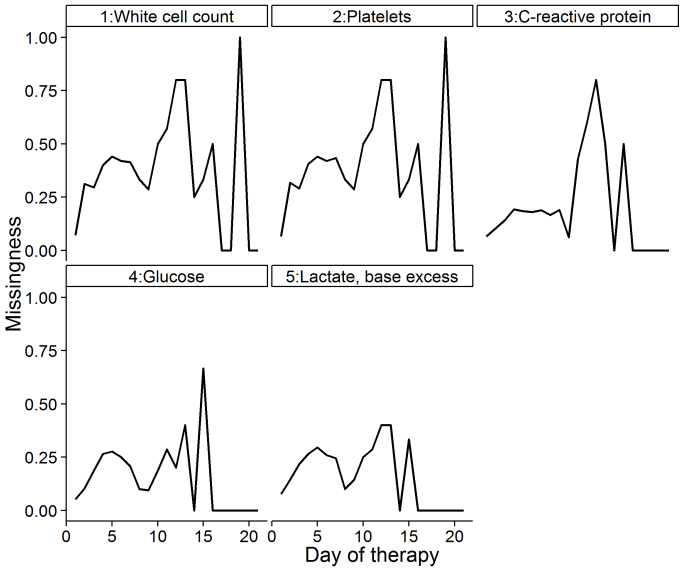

Figure 5.3: Patterns of missingness depending on the treatment day for each item.

on the guessing parameter (described in Section 5.3.2), only a separate c_{MISS} for item 3, items 1&2, and items 4&5, and the effect of the first day of treatment proved significant (i.e. the drop in the OFV between two nested models was >3.84). The ΔOFV between the initial and the model with covariates was 217.2 units.

The correlation between the baseline and the slope was not included in the model, as it was only -0.01, and it produced a non-significant decrease in the OFV (ΔOFV=0.1). Furthermore, with correlation included, the covariance step was no longer successful.

Including peak gentamicin concentration (C_{1h}) as a covariate on the slope relating to the rate of the change in the latent variable also did not proved significant.

The final parameter estimates and the uncertainty associated with them are presented in Table 5.3, and the NONMEM code for the final model is given in Appendix G.

Figure 5.4 shows the relationship between the informativeness of each item (about the sepsis status of an individual) and the latent variable. Item 5 (lactate concentration or base excess) appears to be the most informative, as seen from the highest magnitude of the information, indicating that an item is more reliable for differentiating between individuals at a point on the latent variable scale. Conversely, item 3 (CRP concentration) does not seem to contain much information. Ranking items by their average information content confirms that item 5 is the most informative item (Table 5.4).

5.4.3 Evaluation

Both item-level categorical VPCs (Figures 5.5 and 5.6) and mirror plots (Figure 5.7) showed that the model fits the data and has adequate predictive power.

Table 5.3: Parameter estimates with uncertainty from the final model

	Parameters from the final model			Bootstrap analysis		
	mean	SE	%CV	median	2.5%ile	97.5%ile
slope	-0.61	0.15	-	-0.64	-25.0	-0.17
Item 1: dis	0.48	0.2	-	0.45	0.00	20.3
Item 1: dif	2.97	1.39	-	3.01	$-1 \cdot 10^6$	$9 \cdot 10^3$
Item 2: dis	0.73	0.45	-	0.66	0.00	38.8
Item 2: dif	2.17	1.34	-	2.28	$-1 \cdot 10^6$	$1.6 \cdot 10^5$
Item 3: dis	0.29	0.09	-	0.27	0.00	$1 \cdot 10^6$
Item 3: dif	0.85	0.62	-	0.90	$-6 \cdot 10^5$	$1 \cdot 10^6$
Item 4: dis	0.91	0.19	-	0.88	0.00	$1 \cdot 10^6$
Item 4: dif	1.44	0.37	-	1.45	$-9 \cdot 10^3$	$2.5 \cdot 10^5$
Item 5: dis	1.00	0.17	-	0.96	0.00	$1 \cdot 10^6$
Item 5: dif	0.06	0.24	-	0.02	$-7 \cdot 10^5$	$1 \cdot 10^6$
Missing dis	1.04	0.21	-	1.00	0.00	$1 \cdot 10^6$
Missing dif	-2.12	0.44	-	-2.23	$-7 \cdot 10^5$	$1 \cdot 10^6$
MGUE I1and2	0.07	0.05	-	0.07	0.00	0.54
MGUE I3	0.58	0.04	-	0.58	0.00	0.72
MGUE I4and5	0.38	0.08	-	0.39	0.21	0.80
MGUE OCC1	0.51	0.1	-	0.51	0.23	0.83
η slope	0.23	0.11	47.6	0.25	0.03	781

Dis is the discrimination parameter (a), dif is the difficulty parameter (b), and gue is the guessing parameter (c), M indicates missing data, OCC1 is the first day of treatment, I is item; SE is standard error, CV is coefficient of variation. Items are specified in Table 5.1.

Table 5.4: Items, ranked by the average information content

item	average information
lactate concentration or base excess	0.205
glucose concentration	0.134
platelet count	0.076
white cell count	0.037
C-reactive protein concentration	0.020

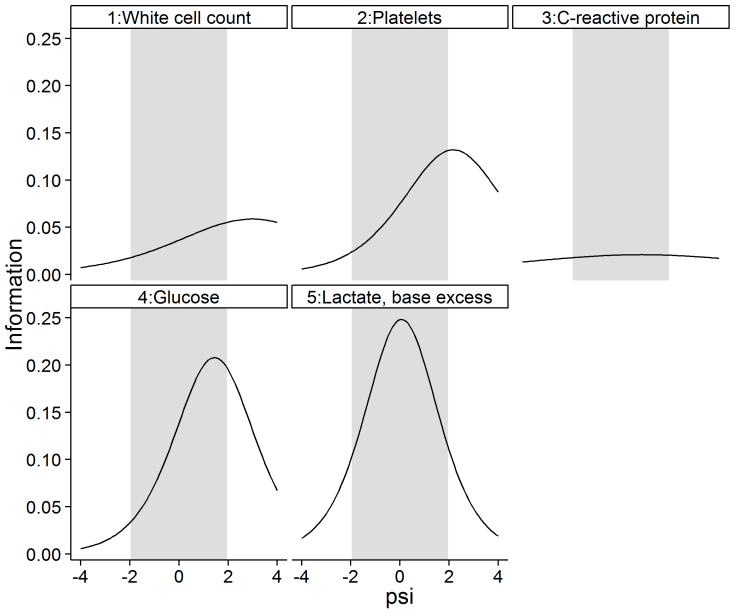

Figure 5.4: Graphs showing the informativeness of each item as a function of the latent variable (i.e. sepsis status). Grey area indicates the 95% prediction interval for disease severity at baseline.

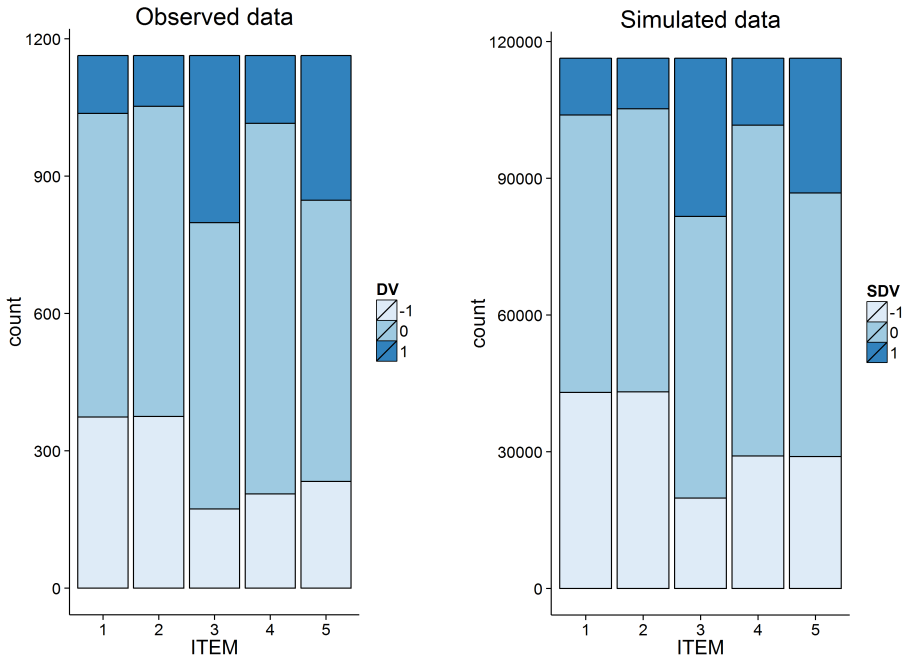

Figure 5.7: Mirror plots, for original (left) and simulated data (right), performed using 100 simulations. DV=1 indicates meeting criteria for sepsis, DV=0 not meeting the sepsis criteria, and DV=-1 indicates missing data. Items are defined in Table 5.1.

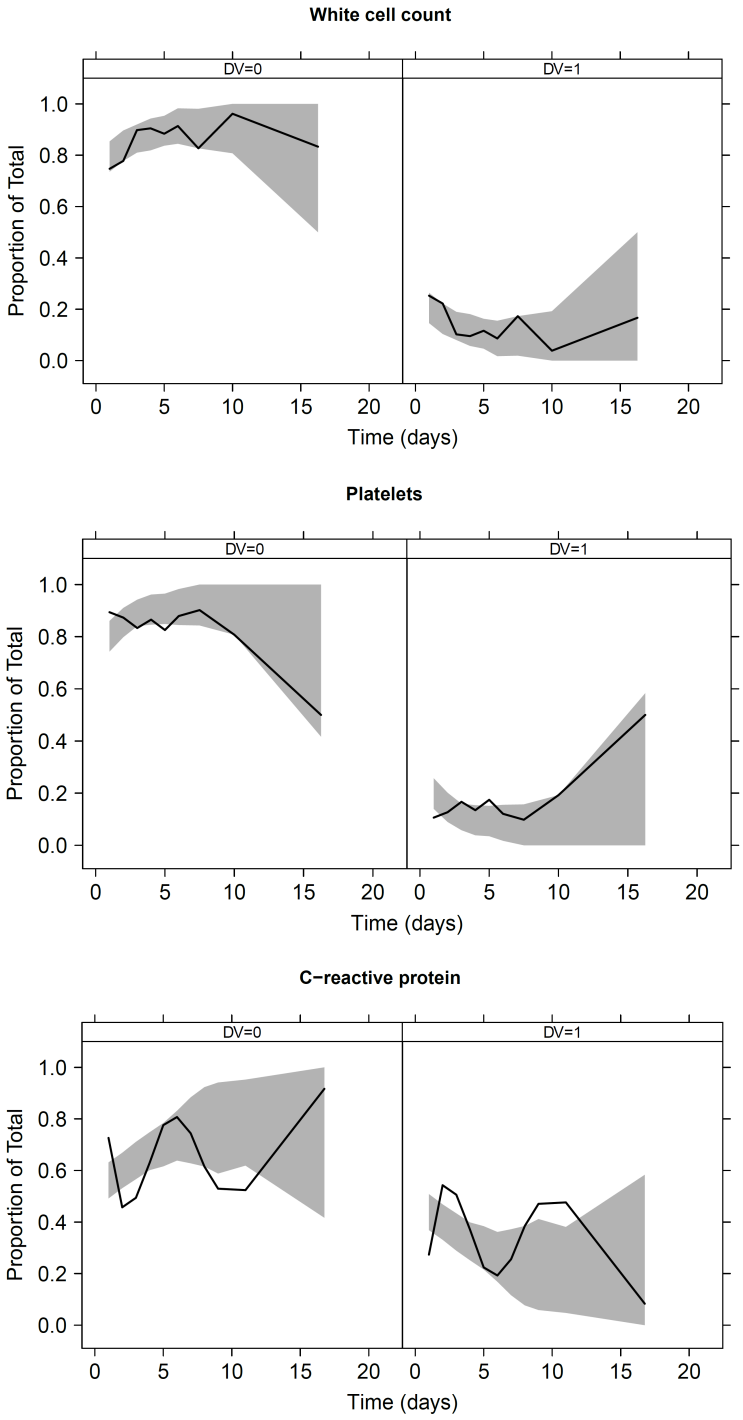

Figure 5.5: Visual predictive check (n=1000) for items 1, 2 and 3, showing the observed fraction of each response to an item against time (black line) and the corresponding model-based 95% CI (grey area).

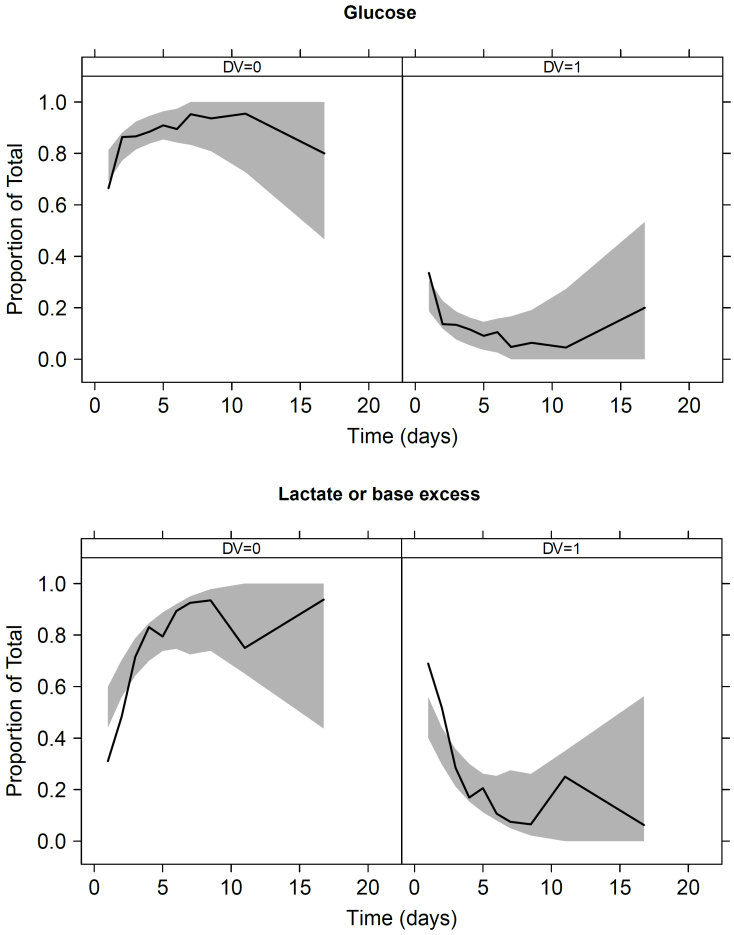

Figure 5.6: Visual predictive check (n=1000) for items 4 and 5, showing the observed fraction of each response to an item against time (black line) and the corresponding model-based 95% CI (grey area).

5.5 Discussion

The IRT framework was used in this proof-of-concept study to determine which is the most informative laboratory test for determining neonatal sepsis (from a set of laboratory tests recommended by the EMA [276]), and to find possible effects of gentamicin peak concentration on the rate of the resolution of sepsis.

The results of the IRT modelling showed that at baseline, in this population of neonates, metabolic acidosis (i.e. base excess <10 mEq/L or serum lactate concentration >2 mMol/L) provided the highest precision in distinguishing whether a neonate had sepsis or not. The potential importance of serum lactate in neonates was also found by Fitzgerald *et al* [303] who compared data from 23 culture negative and 6 culture positive premature neonates in their first 48 hours of life, and found that lactate concentrations were significantly higher in culture positive newborns. Based on that they concluded that increased serum lactate could be a potential marker of neonatal sepsis [303]. However, they used a small sample size, and the variability in lactate concentrations in septic newborns was large. A prospective study in the neonatal setting is needed to confirm the clinical significance of serum lactate for defining sepsis. Additionally, although metabolic acidosis proved to be the most informative indicator about the sepsis status, serum lactate is not a specific marker of sepsis, since it can also be increased in other conditions such as trauma, again highlighting the need for further research in this area.

An interesting result of the current study was also that C-reactive protein contains very little information about the sepsis status at baseline. However, this might not be so surprising, since CRP is an acute phase protein, and inflammatory response needs to be triggered for CRP to increase [299]. It is thus not an early marker of infection [301].

To avoid the emergence of resistance, empirical treatment should not be un-

necessarily used, and should be discontinued as soon as it is confirmed that the sepsis has resolved [298]. Therefore it is important to determine (based on evidence) which signs or what sepsis criteria to use. IRT models could prove useful as shown in this example. Additionally, IRT models could facilitate the selection of thresholds for a laboratory test, as it was found that there is no agreement on which thresholds to use [55]. It would not be too difficult to change the thresholds in the data and compare which is more informative.

In this analysis gentamicin peak concentration was included as the highest C_{1h} for a particular neonate, and did not prove significant on the slope, describing the change in the latent variable. However, peak concentrations could also be obtained differently - for example, the highest C_{1h} in a treatment day would possibly relate to the rate of clinical improvement more. But as premature newborns were included in this study too, the gentamicin dosing intervals were in some cases greater than 24 hours, meaning that if this approach was used, "peak" concentration for some days would be very low.

5.6 Summary

An item response theory framework was applied to PD data from the neoGent study and a model was developed. In this proof-of-concept study five laboratory sepsis signs were selected and dichotomised, according to a widely used sepsis criteria [276]. Out of these items (i.e. laboratory tests), metabolic acidosis (base excess deficit or increased serum lactate concentration) was shown to provide the most information about the sepsis status of the neonates in this population at baseline. Peak gentamicin concentration did not have a significant effect on the rate of the resolution of sepsis, which might mean that the current practice on focusing on toxicity and not efficacy when performing therapeutic drug monitoring is appropriate. Further work could focus on including other possible markers of neonatal sepsis into the model, and using continuous instead of binary data. The

focus should also be on obtaining a more appropriate dataset (i.e. with fewer missing data) to facilitate investigation of sepsis resolution, and hidden Markov models could instead be applied.

Chapter 6

Conclusions

Although antenatal care has improved dramatically in the last decades, bacterial infections, namely sepsis and meningitis, still remain a major cause of neonatal deaths and morbidity [244, 245]. An additional problem is that due to a large proportion of false negative culture results [288], these results cannot be examined separately, but need to be combined with other clinical or laboratory markers, which lack specificity, and furthermore, there is no agreement on which exact marker(s) to use [55]. Antibacterial agents are therefore often used empirically, and off-label [10], indicating that more research is needed to provide evidence-based guidelines, as also shown by a considerable variability in their prescribing and monitoring regimens [8, 9].

With the work done and described here, I aimed to address some of the problems mentioned above by firstly selecting an appropriate model for scaling clearance in the paediatric population (by comparing several distinct models on the same dataset). For a renally excreted drug (gentamicin) allometric weight scaling (with a single fixed allometric exponent) and a postmenstrual age driven sigmoidal maturation function proved to have the lowest AIC value, hence this model was then used when describing the change in clearance with size and age in the following chapters (3 and 4). Having a standard model for scaling clearance

would enable comparison of similar compounds, and make meta-analyses easier. This model also facilitates the idea that maturation and growth are continuous not dichotomous processes and so more can be understood about scaling for size and age and more can be learnt about clearance maturation. Using an appropriate scaling method ensures that the models are applicable to all ages, and so for example the neoGent model could be readily extendible to be used for children of all ages (subject to evaluation).

One of the interesting findings of performing the non-linear mixed-effects modelling in Chapters 3 and 4 was that the structural model should be re-tested after the inclusion of the covariates. This should particularly be done where covariates are important, for example in neonates due to their high variability in the pharmacokinetic parameters. In both cases, following covariate addition, a further distribution compartment significantly improved model fit, and in the case of the neoGent model may have contributed to its superior predictive performance over other published models (see Figure 3.16).

The modelling that was undertaken using published gentamicin data and evaluated on external dataset originating from the neoGent study showed that a more mechanistic model (compared to previously published models), which contains biological prior information, can provide better individual predictions when applied to an external dataset. The results (presented in Chapter 3) also showed that the model is able to predict trough gentamicin concentrations from a previously taken sample for other clinical purposes. Using this model could enable prediction of trough levels from samples taken at earlier time points, therefore eliminating the need for "trough" levels to be collected exactly before the next dose, which would help address some of the safety concerns raised by the NPSA [149]. The preliminary work presented in Chapter 5 also showed that peak gentamicin concentration did not significantly affect the rate of the resolution of sepsis, which could indicate that the current practice on focusing on toxicity and

not efficacy when performing gentamicin therapeutic drug monitoring in neonates is appropriate.

Another example of using population modelling was described in Chapter 4, where treatment (specifically, dosing regimen) was optimised on a population level using data from the largest so far meropenem pharmacokinetic study in neonates and infants (i.e. the NeoMero study). A dose needed to reach a specific pharmacodynamic target for treatment of late-onset sepsis and meningitis, has been defined, and it appears that the current dosing regimen for these two infectious diseases is appropriate when dealing with susceptible pathogens with low MIC values; but higher doses would be needed for resistant microorganisms. Knowing what dose is sufficiently high would also help prevent the emergence of resistance.

The problem of which (laboratory) marker of sepsis to use was addressed in Chapter 5, where preliminary work using item response theory models was carried out, using a gentamicin neonatal dataset as an example. Choosing from a set of five laboratory tests [276], metabolic acidosis (namely base excess deficit or increased serum lactate concentration) was shown to be the most informative about the sepsis status at treatment initiation. Interestingly, CSF lactate was also shown to have a significant effect on the proportion of meropenem that penetrates into the CSF. This is perhaps not surprising, given that it is a marker of the blood-brain barrier permeability, however, CSF lactate concentrations are currently not routinely measured in all neonatal wards.

6.1 Further work

Although some work has been done in order to help improve antimicrobial therapy in neonates, there is still potential for future investigations that would further improve the current clinical practice.

For example, the provisional software tool neoGent that was developed cur-

rently does not have a user-friendly interface, which would probably limit its usefulness. Also, a clinical study evaluating the model is needed before it could be used in routine neonatal care. But since much more work is needed to develop the neoGent software (i.e. collecting more data of good quality, and developing a front-end), it could be in the meantime applied to, for example, a nomogram. This would still improve the dose individualisation since it is presently often only based on clinical judgement. A nomogram based on predictions from the developed gentamicin pharmacokinetic model that would allow for inclusion of covariates (such as postmenstral age, postnatal age, serum creatinine) could prove useful, especially as preliminary work presented here showed that not focusing on peak concentrations might be appropriate.

The investigation of how clearance scales from the paediatric population to adults was performed for a renally cleared drug. Therefore, it should be tested whether the 0.75 fixed allometric exponent with a sigmoidal maturation function is also appropriate for drugs that are cleared through the liver, or have mixed clearance.

The probability of target attainment for different pharmacodynamic targets was explored, however, future work is needed to determine exactly what percentage of T>MIC is needed in neonates for a clinical and microbiological effect. Also, in the work presented here simulations were done using fixed MIC values, whilst ideally the MIC distribution should be determined in the environment where meropenem is intended to be used for, to then correctly define an optimal dose. Future work should also involve including more pharmacodynamic data into the model, to help gain more insights into the underlying biological system.

Concerning the work involving item response theory models, more data (with fewer missing values) is needed, and perhaps actual laboratory values, instead of binary data could be included.

In summary the work presented in this thesis has shown how pharmacokinetic-pharmacodynamic modelling can help understand and improve the management of neonatal infections. Models allow for a potentially more nuanced understanding of dosing beyond simple MIC targets, and as new and better diagnostics are developed, PKPD models will be useful in understanding their significance. Although there are few antimicrobials currently in clinical development, as new agents are developed their use in neonates will need to be investigated; and PKPD modelling will be crucial in defining their dosing. In an era of antimicrobial resistance, optimising treatment of neonatal infections with PKPD modelling will be vital.

Appendix A

Search and screening procedure

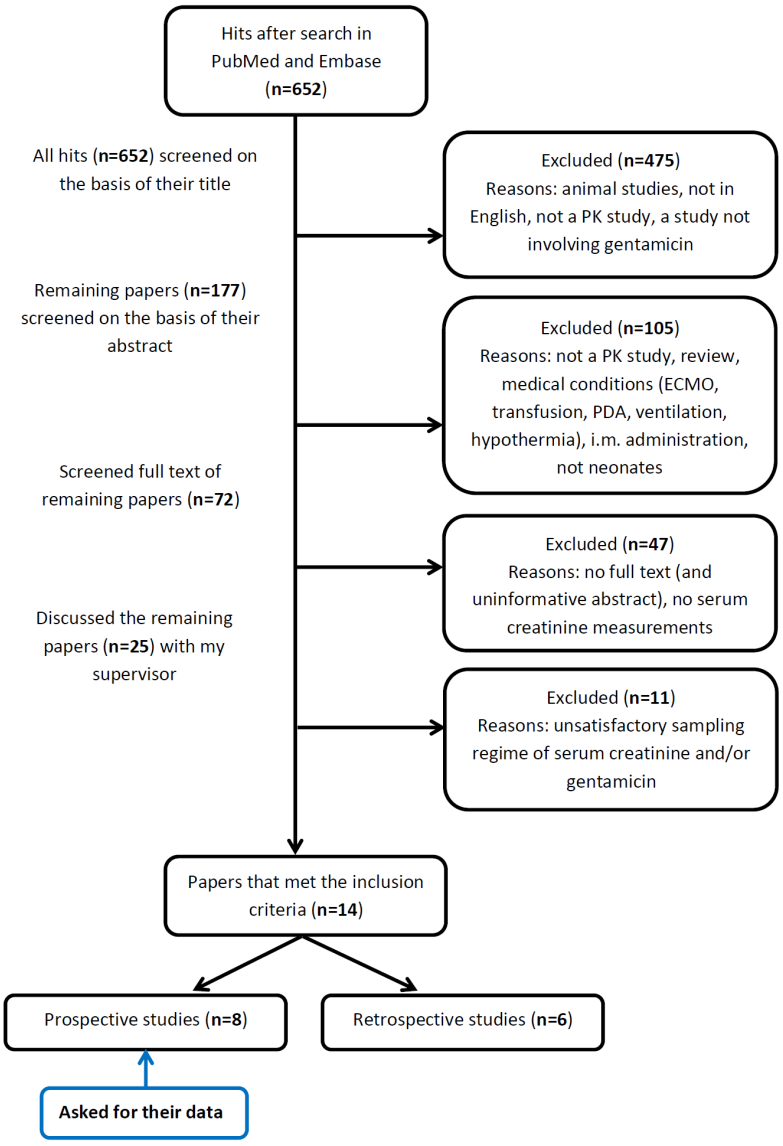

Figure A.1: A flow chart illustrating the search strategy (performed in April 2013) in order to find data for gentamicin PK model building.

Appendix B

NONMEM control file for the final gentamicin model

```
$PROBLEM neoGent model Germovsek 2014
$INPUT ID GA GIRL TIME PNA PMA WT CREA TCRE RATE AMT DV EVID OCC MDV
;GA (days), PNA (days), PMA (weeks)
;GIRL: 0=male, 1=female
;TIME (hrs, time after the first dose)
;RATE (mg/h), AMT (mg), DV=genta conc (mg/L)
;EVID: 0=DV measurement, 1=dose given, 2=dummy time point
;WT (g)
;CREAT (umol/L)
;
$DATA Patient_data-NM.csv IGNORE=@
$SUBROUTINE ADVAN6 TOL=6
;
$MODEL
COMP=(CENTRAL)
COMP=(PERIPH1)
COMP=(PERIPH2)
COMP=(COVCMT1)           ; PNA time-var. covariate compartment
COMP=(COVCMT2)           ; CREATININE t-v. cov. compartment
;
$PK
; Three-comp model
; -------- Parameterization for time-varying covariates --------
IF(NEWIND.NE.2)OTIM1=0
IF(NEWIND.NE.2)OCOV1=0
IF(NEWIND.NE.2)OTIM2=0
IF(NEWIND.NE.2)OCOV2=0
;
WTKG = WT/1000
T50  = 55.4
HILL = 3.33
MF   = PMA**HILL/(PMA**HILL+T50**HILL)
;
SECR = CREA
IF(SECR.LE.0) SECR = TCRE
;
P50  = THETA(8)  ; postnatal age at 50% of adult's clearance
;
```

```
CRPWR = THETA(7)  ; power exponent on the creatinine function
;
; -------- Inter-occasion variability code ----------------------
BOVC = 0
IF(OCC.EQ.1)  BOVC = ETA(7)
IF(OCC.EQ.2)  BOVC = ETA(8)
IF(OCC.EQ.3)  BOVC = ETA(9)
IF(OCC.EQ.4)  BOVC = ETA(10)
IF(OCC.EQ.5)  BOVC = ETA(11)
IF(OCC.EQ.6)  BOVC = ETA(12)
IF(OCC.EQ.7)  BOVC = ETA(13)
IF(OCC.EQ.8)  BOVC = ETA(14)
IF(OCC.EQ.9)  BOVC = ETA(15)
IF(OCC.EQ.10) BOVC = ETA(16)
IF(OCC.EQ.11) BOVC = ETA(17)
IF(OCC.EQ.12) BOVC = ETA(18)
IF(OCC.EQ.13) BOVC = ETA(19)
IF(OCC.EQ.14) BOVC = ETA(20)
IF(OCC.EQ.15) BOVC = ETA(21)
IF(OCC.EQ.16) BOVC = ETA(22)
IF(OCC.EQ.17) BOVC = ETA(23)
IF(OCC.EQ.18) BOVC = ETA(24)
IF(OCC.EQ.19) BOVC = ETA(25)
IF(OCC.EQ.20) BOVC = ETA(26)
IF(OCC.EQ.21) BOVC = ETA(27)
IF(OCC.EQ.22) BOVC = ETA(28)
;
TVCL = THETA(1)*MF*(WTKG/70)**(0.632)   ; typical value of CL
TVV1 = THETA(2)*(WTKG/70)               ; typical value of V1
TVQ  = THETA(3)*(WTKG/70)**(0.75)       ; ty. value of Q
TVV2 = THETA(4)*(WTKG/70)               ; ty. value of V2
TVQ2 = THETA(5)*(WTKG/70)**(0.75)       ; ty value of CL3
TVV3 = THETA(6)*(WTKG/70)               ; ty value of V3
;
CL   = TVCL*EXP(ETA(1)+BOVC)            ; individual value of CL
V1   = TVV1*EXP(ETA(2))                 ; individual value of V1
Q    = TVQ*EXP(ETA(3))                  ; individual value of Q
V2   = TVV2*EXP(ETA(4))                 ; individual value of V2
Q2   = TVQ2*EXP(ETA(5))                 ; individual value of Q2
V3   = TVV3*EXP(ETA(6))                 ; individual value of V3
;
K    = CL/V1                            ; rate constants
K12  = Q/V1
K13  = Q2/V1
K21  = Q/V2
K31  = Q2/V3
;
; -------- Code to calculate time after dose ----------------------
IF(EVID.EQ.1) TM=TIME
IF(EVID.EQ.1) TAD=0
IF(EVID.NE.1) TAD=TIME-TM
;
; -------- Parameterisation for time-varying covariates -----------
SL1 = 0
IF(TIME.GT.OTIM1) SL1 = (PNA-OCOV1)/(TIME-OTIM1)
A_0(4) = PNA
;
```

```
SL2 = 0
IF(TIME.GT.OTIM2) SL2 = (SECR-OCOV2)/(TIME-OTIM2)
A_0(5) = SECR
;
; -------- Differential equations ---------------------------------
$DES
DADT(4)= SL1
TCOV1 = A(4)
;
DADT(5)= SL2
TCOV2 = A(5)
;
PNAF = TCOV1/(P50+TCOV1)
OF = (TCOV2/TCRE)**CRPWR
DADT(1) = A(3)*K31+A(2)*K21-A(1)*(K*PNAF*OF+K12+K13)
DADT(2) = A(1)*K12-A(2)*K21
DADT(3) = A(1)*K13-A(3)*K31
;
$ERROR
CP=A(1)/V1
IF (CP.LE.2) TLE2=TAD
; -------- Statistical model ---------------------------------------
Y = CP*(1+EPS(1)) + EPS(2)
;
OCOV1 = PNA
OTIM1 = TIME
;
OCOV2 = SECR
OTIM2 = TIME
;
$THETA  6.71034 FIX       ; 1. TVCL
$THETA  27.5169 FIX       ; 2. TVV1
$THETA  0.301033 FIX      ; 3. TVQ
$THETA  156.775 FIX       ; 4. TVV2
$THETA  2.19567 FIX       ; 5. TVQ2
$THETA  21.2259 FIX       ; 6. TVV3
$THETA  -0.173523 FIX     ; 7. power exponent on creatinine
$THETA  1.77352 FIX       ; 8. P50 = PNA50

$OMEGA  0.0656879 FIX         ; 1. IIV_CL
$OMEGA  0.00922249 FIX        ; 2. IIV_V1
$OMEGA  0  FIX                ; 3. IIV_Q
$OMEGA  0.0216515 FIX         ; 4. IIV_V2
$OMEGA  0.0190804 FIX         ; 5. IIV_Q2
$OMEGA  0.0208852 FIX         ; 6. IIV_V3

$OMEGA  BLOCK(1) 0.0240382 FIX  ; 7. IOV_CL
$OMEGA  BLOCK(1) SAME
$OMEGA  BLOCK(1) SAME
$OMEGA  BLOCK(1) SAME
$OMEGA  BLOCK(1) SAME
$OMEGA  BLOCK(1) SAME
$OMEGA  BLOCK(1) SAME
$OMEGA  BLOCK(1) SAME
$OMEGA  BLOCK(1) SAME
$OMEGA  BLOCK(1) SAME
$OMEGA  BLOCK(1) SAME
```

```
$OMEGA  BLOCK(1) SAME
$OMEGA  BLOCK(1) SAME
$OMEGA  BLOCK(1) SAME
$OMEGA  BLOCK(1) SAME
$OMEGA  BLOCK(1) SAME
$OMEGA  BLOCK(1) SAME
$OMEGA  BLOCK(1) SAME
$OMEGA  BLOCK(1) SAME
$OMEGA  BLOCK(1) SAME
$OMEGA  BLOCK(1) SAME
$OMEGA  BLOCK(1) SAME

$SIGMA  0.024069 FIX   ; variance PROP res error, initial estimate
$SIGMA  0.0100037 FIX  ; variance ADD res error, initial estimate

$ESTIMATION METHOD=1 INTER MAXEVAL=0 PRINT=1      ; estimation method

$TABLE ID TIME CWRES GA PMA AMT TAD TLE2 CP OCC EVID TCRE SECR PNA
NOPRINT ONEHEADER FILE=sdtab-nG
```

Appendix C

Individual plots of observed and predicted gentamicin trough concentration

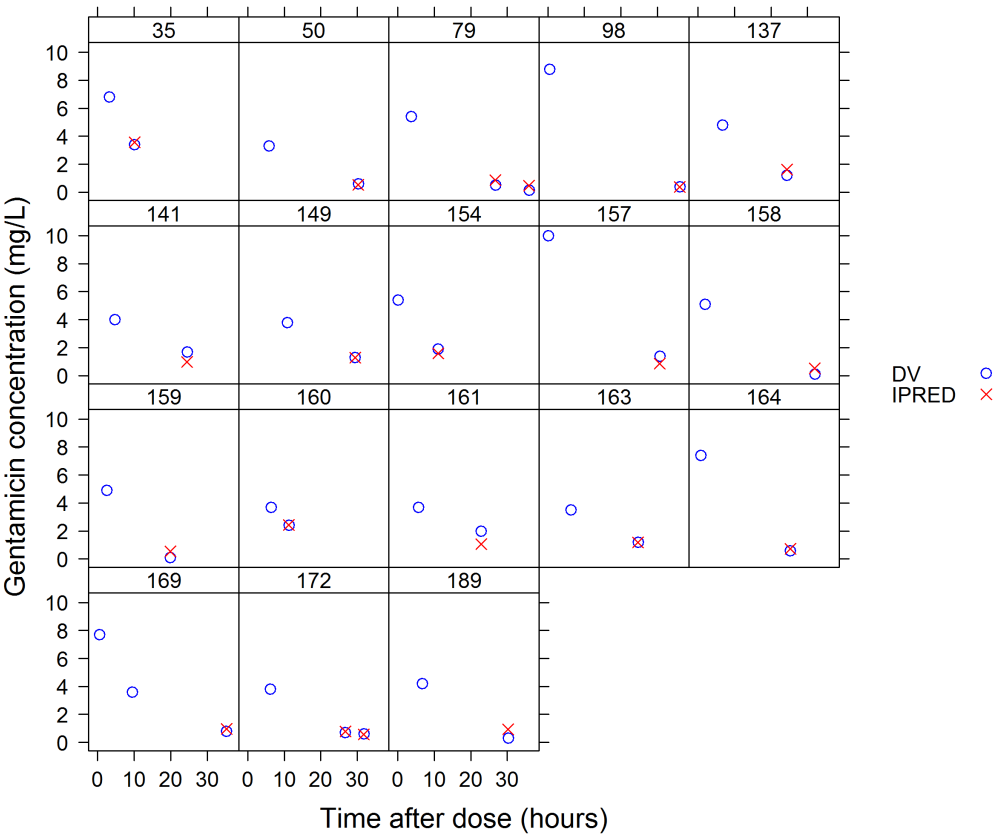

Figure C.1: Individual plots of observed (DV) and predicted (IPRED) gentamicin concentration versus time after dose from dataset of study-routine paired samples with the earlier (study) sample $\geq$3 mg/L. In some cases there were more than two samples in a "pair". Only the information from the study sample (i.e. first sample) was used to predict the later, i.e. routine concentration(s).

Appendix D

R code for predicting the time when plasma concentration of gentamicin goes below 2 mg/L

```
#(everything after the "#" is a comment)

######################################################################
## R script for the neoGent software
# developed by Eva Germovsek
# 2014
######################################################################
#
#clean workspace
rm(list=ls())
#
#set working directory
setwd("C:/neoGent/RShell")
#
##### read in a .csv file (from e.g. hospital)
## information needed (with order and names of the columns):
# ID,GA(days),GIRL(1=female),DATE(DD/MM/YYYY),TIME(HH:MM),PNA(days),
# WT(g),CREAT(umol/L),RATE(dose/infusion duration,mg/h),AMT(mg),
#   DV(mg/L), OCC(=a dose with subsequent gentamicin samples taken)
# e.g.
# ID  GA    GIRL  DATE        TIME  PNA   WT  CREAT RATE AMT DV  OCC
# 1   226    1    03/09/2013  12:00  1   1770  59   240   8  0    1
# 1   226    1    05/09/2013  00:15  3   1710  59   240   8  0    1
# 1   226    1    05/09/2013  10:11  3   1710  59   0     0  3.4  1
# 1   226    1    06/09/2013  12:29  4   1710  50   240   8  0    2
# 1   226    1    06/09/2013  15:45  4   1710  50   0     0  6.8  2
#
data1 <- read.csv("Patient_data.csv",head=T,skip=0)
#
#################### change the datafile ##########################
#
####### change date and time to time in decimal hours
colnames(data1)[5]<-"TIMEX"
data1$DT <- do.call(paste,c(data1[c("DATE","TIMEX")],sep=" "))
data1$DT <- as.POSIXct(strptime(data1$DT,format="%d/%m/%Y %H:%M",
tz="UTC"))
```

```
TIME2 <- NA
data1$TIME2<-data1$DT[1]
data1$TIME <- as.numeric(difftime(data1$DT,data1$TIME2,units="hours"))
data1<-data1[,-c(4,5,13,14)]
last<-nrow(data1)
lastT<-data1$TIME[last]
#
####### extend the matrix (300 additional rows)
NAs<-matrix(nrow=300-nrow(data1),ncol=ncol(data1))
colnames(NAs)<-colnames(data1)
data<-rbind(data1,NAs)
#
######## TIME(add in dummy time points,every 15mins,up to 72h)
for(i in(nrow(data1)+1):nrow(data)){
 if(data$TIME[nrow(data1)]>0)
  data$TIME[(nrow(data1)+1):(length(seq((data$TIME[nrow(data1)]
  +0.25),lastT+72,0.25))+nrow(data1))]<-seq((data$TIME[nrow(data1)]
  +0.25),lastT+72,0.25)
}
#
## remove rows where TIME=NA
# (since TIME only to 72hrs,some rows TIME=NA)
data<-data[complete.cases(data$TIME),]
#
########## extend ID, GA, SEX, WT, CREAT to all columns
data$ID[2:nrow(data)]<-data$ID[1]
data$GA[2:nrow(data)]<-data$GA[1]
data$GIRL[2:nrow(data)]<-data$GIRL[1]
data$WT[2:nrow(data)]<-data$WT[last]
data$CREAT[2:nrow(data)]<-data$CREAT[last]
#
########## replace NAs with zeros
data$AMT[is.na(data$AMT)] <- 0
data$DV[is.na(data$DV)] <- 0
data$RATE[is.na(data$RATE)] <- 0
#
########## EVID
# if AMT-> EVID=1
# if DV-> EVID=0
# if extra dummy time point-> EVID=2
#
for(i in 1:nrow(data)){
if(data$AMT[i]!=0) data$EVID[i]<-1
if(data$DV[i]!=0) data$EVID[i]<-0
if((data$AMT[i]==0)&(data$DV[i]==0)) data$EVID[i]<-2
}
#
########### PNA
# if t>12 -> +1 day PNA
# if t>36 -> +1 day PNA
# if t>60 -> +1 day PNA
#
for(i in (nrow(data1)+1):nrow(data)){
 if(data$TIME[i]<(lastT+12)) data$PNA[i]<-data$PNA[last]
 if((data$TIME[i]>=(lastT+12))&(data$TIME[i]<(lastT+36)))
data$PNA[i]<-data$PNA[last]+1
 if((data$TIME[i]>=(lastT+36))&(data$TIME[i]<(lastT+60)))
```

```
data$PNA[i]<-data$PNA[last]+2
 if(data$TIME[i]>=(lastT+60)) data$PNA[i]<-data$PNA[last]+3
}
#
########### PMA
data$PMA <- (data$GA+data$PNA)/7
#
########### TCREA
# formula:Cuzzolin et al (Pediatr Nephrol.2006);
# Rudd et al (Arch Dis Child.1983)
data$TCREA <- (data$PMA*(-2.8488)+166.48)
#
########### OCC
data$OCC[data$EVID==2]<-data$OCC[last]
#
########### MDV = missing data value
data$MDV[data$EVID==0]<-0
data$MDV[data$EVID!=0]<-1
#
########### rearrange the order of the columns
data <- data.frame(data["ID"],data["GA"],data["GIRL"],data["TIME"],
data["PNA"],data["PMA"],data["WT"],data["CREAT"],data["TCREA"],
data["RATE"],data["AMT"],data["DV"],data["EVID"],data["OCC"],
data["MDV"])
#
########### write .csv file
write.csv(data,file="Patient_data-NM.csv",quote=FALSE,row.names=FALSE)
#
#
######################### run NONMEM ############################
cmd<-paste("nmfe73 neoGent.mod neoGent.lst")
shell(cmd)
#
#
############ read the results from NONMEM back into R ############
sdtab<-read.table(file="sdtab-nG",head=TRUE,skip=1)
#
#only look at the last dosing interval
sdtab<-sdtab[(sdtab$OCC>=sdtab$OCC[last]),]
#
# locate the row where CP(plasma conc) goes below 2mg/L first
dtime<-0
dtime[1]<-1
for(i in 2:nrow(sdtab)){
if((sdtab$TLE2[i]!=0) & (sdtab$TLE2[i-1]==0))
dtime[i]<-100
else
dtime[i]<-1
}
sdtab$dtime <- dtime
below2 <- sdtab[sdtab$dtime==100,]
below2 <- below2[,c("ID","TLE2","CP")]
below2$CP<-round(below2$CP,2)
below2$TLE2<-round(below2$TLE2,1)
name<-below2$ID
time<-below2$TLE2
conc<-below2$CP
```

```
names(below2) <- c("SubjectID","Time(h)","PredConc(mg/L)")
#
#
########################## results ################################
#
datestamp<-Sys.Date()
#
######### a table
write.csv(below2,file=paste("Below_2mgL_","ID",name,"_",
datestamp,".csv",sep=""),quote=F,row.names=F)
#
########## a plot
#remove the dosing rows
sdtab1<-sdtab[sdtab$EVID==2,]   # predictions
sdtab2<-sdtab[sdtab$EVID==0,]   # observations
#
pdf(paste("Below_2mgL_","ID",name,"_",datestamp,".pdf",sep=""))
plot(sdtab1$TAD,sdtab1$CP,      # predictions
 main="Prediction of time when conc<2mg/L",
 xlab="Time (h)",
 ylab="Gentamicin concentration (mg/L)",
 cex.lab=1.5,cex.axis=1.5,cex.main=1.5,
 xlim=c(0,75),
 ylim=c(0,13),
 type="n",
 )
lines(sdtab1$TAD,sdtab1$CP,col="black",lwd=2)
abline(h=2,lty=3)
par(new=T)
plot(sdtab2$TAD,sdtab2$DV,      # observations
 col="red",
 pch=4,
 lwd=2,
 axes=F,
 xlab="",ylab="",
 xlim=c(0,75),
 ylim=c(0,13),
 )
par(new=F)
# put a legend in the top right corner
legend("topright",
cex = 1.2,
      legend = c("observations","predictions"),
      col = c("red","black"),
      pch = c("x","line"),
)
# put a legend - central, right
legend(50,8,cex = 1.2,bty = "n",legend = paste("Date:",datestamp),)
legend(50,7,cex = 1.2,bty = "n",legend = paste("ID:",name),)
legend(50,6,cex = 1.2,bty = "n",legend = paste("Time =",time,"h"),)
legend(50,5,cex = 1.2,bty = "n",legend = paste("Conc =",conc,"mg/L"),)
dev.off()
######################### end code ################################
```

Appendix E

An example output of the neoGent software

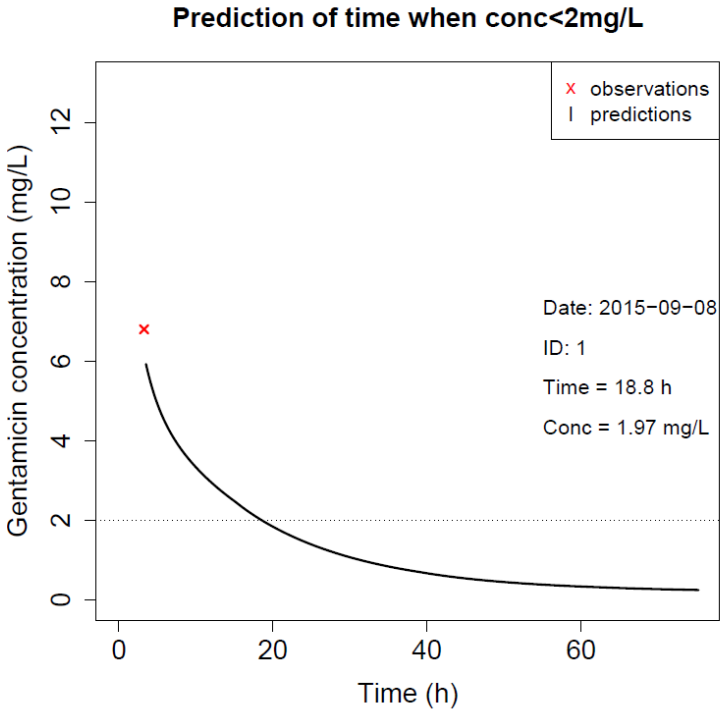

Figure E.1: An example output of the neoGent software.

Appendix F

NONMEM control file for the final meropenem model

```
$PROBLEM NeoMero model Germovsek 2015

$INPUT ID STUDY GIRL GAW BWT=DROP DUR AMT RATE DV CSF EVID
   WT CREAT CRP PCT PROT GLU LACT PNA THDAY TIME TAD CSFDV
   PMA MDV CMT TCREA FREQ ATBDOSE BEFORE HIGHER HIGHCSF
   TAD2 B4 RMV WBC NEUT NEUTP LYMPHO LYMHOP RBC
$DATA NeoMero_18092015-CSFlab2.csv IGNORE=@
;GAW (weeks), PNA (days)- day0= date of birth
;GIRL: 0=male, 1=female
;TIME (hrs, time after the first dose),
;TAD (hrs, time after the last dose)
;RATE (mg/h), AMT (mg), DV=meropenem conc (mg/L)
;EVID: 0=DV measurement, 1=dose given
;WT (kg)
;
$SUBROUTINE ADVAN7
; 3-comp model

$MODEL      COMP=(PL)  ; Plasma - central cmt
            COMP=(PERIPH) ; Peripheral cmt plasma
            COMP=(CSF) ; Cerebrospinal fluid


$PK
; Two-compartment plasma model with additional CSF compartment
PMA50 = THETA(7)
HILL  = THETA(8)
MF    = PMA**HILL/(PMA**HILL+PMA50**HILL)
SCR = CREAT
; for when SCr is NA, i.e. -99
IF(SCR.LE.0) SCR = TCREA
OF = (SCR/TCREA)**(THETA(9))

LACT2 = LACT
; for when lactate is NA, i.e. -99
IF(LACT2.LT.0) LACT2 = 1.8
; uptake into the CSF
UPTK = 1/(1+EXP(THETA(10)*(1+THETA(11)*(LACT2-1.8))))
```

```
TVCL = THETA(1)*OF*MF*(WT/70)**(0.632)  ; typical value of CL
TVV1 = THETA(2)*(WT/70)                 ; typical value of V1
TVQ  = THETA(3)*(WT/70)**(0.75)         ; ty. value of Q
TVV2 = THETA(4)*(WT/70)                 ; ty. value of V2
TVCLCSF  = THETA(5)*(WT/70)**(0.75)     ; ty. value of CL_CSF
TVVCSF = THETA(6)*(WT/70)               ; ty. value of V_CSF

CL   = TVCL*EXP(ETA(1))          ; individual value of CL
V1   = TVV1*EXP(ETA(2))          ; individual value of V1
Q    = TVQ*EXP(ETA(3))           ; individual value of Q
V2   = TVV2*EXP(ETA(4))          ; individual value of V2
CLCSF   = TVCLCSF*EXP(ETA(5))    ; individual value of CL_CSF
VCSF   = TVVCSF*EXP(ETA(6))      ; individual value of V_CSF
;
K10  = CL/V1                          ; rate constants
K12  = Q/V1
K13  = (CLCSF/V1)*0.98*UPTK           ; k into the CSF
K21  = Q/V2
K31  = CLCSF/VCSF                     ; k out of the CSF


$ERROR
; -------- Statistical model ------------------------------------
IPRED=0
; Plasma
 IF(CMT==1) IPRED  = A(1)/V1
 IF(CMT==1) Y = IPRED*(1+EPS(1)) + EPS(2)
; cerebrospinal fluid
 IF(CMT==3) IPRED  = A(3)/VCSF
 IF(CMT==3) Y = IPRED*(1+EPS(3))

$THETA  (0,16.585) ; 1. TVCL (lower bound,initial estimate)
$THETA  (0,37.7867) ; 2. TVV  (lower bound,initial estimate)
$THETA  (0,0.691854) ; 3. TVQ (lower bound,initial estimate)
$THETA  (0,124.191) ; 4. TVV2  (lower bound,initial estimate)
$THETA  (0,0.0128436) ; 5. TVCL CSF
$THETA  0.15 FIX ; 6. TVV  of CSF
$THETA  55.4 FIX ; 7. PMA50
$THETA  3.33 FIX ; 8. HILL
$THETA  -0.240546 ; 9. power exponent on creatinine
$THETA  1.90382 ; 10. uptake into CSF; logit
$THETA  -0.167076 ; 11. lactate; logit

$OMEGA  BLOCK(2)
 0.279253  ; variance for ETA(1), initial estimate
 0.125443 0.0933118  ; COvariance ETA(1)-ETA(2), var for ETA(2)
$OMEGA  0  FIX
$OMEGA  0  FIX
$OMEGA  0  FIX  ; eta5, Q:pl-csf
$OMEGA  0  FIX  ; eta6, V:csf

$SIGMA  0.152682  ; variance PROP res error, initial estimate
$SIGMA  0.00803814  ; variance add res error, initial estimate
$SIGMA  0.851054  ; variance PROP res error, initial estimate

$ESTIMATION METHOD=1 INTER MAXEVAL=9999 PRINT=1  ; estimation method
```

```
$COVARIANCE

$TABLE ID STUDY GIRL GAW AMT RATE EVID MDV TIME TAD DV CSF CSFDV PNA
PMA WT CREAT TCREA SCR CRP PCT PROT GLU LACT FREQ ATBDOSE BEFORE
HIGHER HIGHCSF CMT IPRED CWRES ETA(1) ETA(2) ETA(3) ETA(4) CL V1
Q V2 CLCSF VCSF LACT2 UPTK OF WBC NEUT NEUTP LYMPHO LYMHOP RBC
NOPRINT ONEHEADER FILE=sdtab72
```

Appendix G

NONMEM control file for the final item response theory model

```
$PROBLEM    IRT neoGent PD data
$INPUT      ID PNA TIME ITEM DV OCC FIRST TEND
$DATA       IRTdata_29.07.2015.csv IGNORE=@

$PRED

;--------------------Hidden variable model-----------------------

TIME0 = TIME - 1
MU_1=THETA(16)
MU_2=THETA(17)
BASELINE=THETA(16)+ETA(1)
SLP=THETA(17)+ETA(2)
PSI=BASELINE+SLP*TIME0

MDIS=THETA(18) ;missing DISPL3
MDIF=THETA(19) ;missing DIFPL3
MGUE = THETA(20)            ; missing MGUE for items 1 and 2
IF(ITEM.EQ.3) MGUE = THETA(21) ; missing MGUE for item 3
IF(ITEM.GT.3) MGUE = THETA(22) ; missing MGUE for items 4 and 5
IF(OCC.EQ.1) MGUE=THETA(23) ; missing MGUE for occasion 1

;---------------Item parameter selection-------------------------

IF(ITEM.EQ.1) THEN
DIS=THETA(1) ;I1DISPL3
DIF=THETA(2) ;I1DIFPL3
GUE=THETA(3) ;I1GUEPL3
ENDIF

IF(ITEM.EQ.2) THEN
DIS=THETA(4) ;I2DISPL3
DIF=THETA(5) ;I2DIFPL3
GUE=THETA(6) ;I2GUEPL3
ENDIF

IF(ITEM.EQ.3) THEN
DIS=THETA(7) ;I3DISPL3
```

```
DIF=THETA(8) ;I3DIFPL3
GUE=THETA(9) ;I3GUEPL3
ENDIF

IF(ITEM.EQ.4) THEN
DIS=THETA(10) ;I4DISPL3
DIF=THETA(11) ;I4DIFPL3
GUE=THETA(12) ;I4GUEPL3
ENDIF

IF(ITEM.EQ.5) THEN
DIS=THETA(13) ;I5DISPL3
DIF=THETA(14) ;I5DIFPL3
GUE=THETA(15) ;I5GUEPL3
ENDIF

;----------3 parameter logit model implementation------------------

P_NM = MGUE+(1-MGUE)*EXP(MDIS*(PSI-MDIF))/(1+EXP(MDIS*(PSI-MDIF)))
P1   = GUE+(1-GUE)*EXP(DIS*(PSI-DIF))/(1+EXP(DIS*(PSI-DIF)))
P0   = 1-P1

;----------------Response probability prediction-------------------

IF(DV.EQ.-1) Y=-2*LOG(1-P_NM)
IF(DV.EQ.0)  Y=-2*LOG(P_NM) -2*LOG(P0)
IF(DV.EQ.1)  Y=-2*LOG(P_NM) -2*LOG(P1)


;----------------Simulation code---------------------------------

IF(ICALL.EQ.4) THEN
    CALL RANDOM (2,R)
    IF(P_NM.LT.R) THEN
       SDV = -1
    ELSE
       CALL RANDOM (2,R)
       SDV=0
       IF(P1.GT.R) SDV=1
    ENDIF
    DV=SDV
ENDIF


$ESTIMATION METHOD=SAEM LAPLACE -2LL NOABORT PRINT=1
            MSFO=msf_run1 AUTO=1
$ESTIMATION METHOD=IMP NITER=10 EONLY=1 ISAMPLE=1000

$COV PRINT=E

$THETA  (0,0.484642) ; 1 I1DISPL3
$THETA  2.97139 ; 2 I1DIFPL3
$THETA  0 FIX ; 3 I1GUEPL3
$THETA  (0,0.726877) ; 4 I2DISPL3
$THETA  2.16772 ; 5 I2DIFPL3
$THETA  0 FIX ; 6 I2GUEPL3
$THETA  (0,0.289182) ; 7 I3DISPL3
```

```
$THETA  0.84648 ; 8 I3DIFPL3
$THETA  0 FIX ; 9 I3GUEPL3
$THETA  (0,0.912074) ; 10 I4DISPL3
$THETA  1.44461 ; 11 I4DIFPL3
$THETA  0 FIX ; 12 I4GUEPL3
$THETA  (0,0.996759) ; 13 I5DISPL3
$THETA  0.0641173 ; 14 I5DIFPL3
$THETA  0 FIX ; 15 I5GUEPL3
$THETA  0 FIX ; 16     baseline
$THETA  -0.606681 ; 17     slope
$THETA  (0,1.04032) ; 18 missing DISPL3
$THETA  -2.11862 ; 19 missing DIFPL3
$THETA  (0,0.0659003,1) ; 20 MGUEPL3 I1,2
$THETA  (0,0.579741,1) ; 21 MGUEPL3 I3
$THETA  (0,0.380483,1) ; 22 MGUEPL3 I4,5
$THETA  (0,0.509362,1) ; 23 MGUEPL3 OCC1

$OMEGA  1  FIX  ; OMbaseline
$OMEGA  0.227487  ;    OMslope

$TABLE ID PNA TIME ITEM DV OCC PSI BASELINE SLP FIRST TEND
ONEHEADER NOPRINT FILE=tab16b
```

ID	PNAD	THERD	ITEM	DV	OCC	FIRST	TEND
1	1	1	1	1	1	1	3
1	1	1	2	0	1	0	3
1	1	1	3	0	1	0	3
1	1	1	4	0	1	0	3
1	1	1	5	1	1	0	3
1	2	2	1	-1	2	1	2
1	2	2	2	-1	2	0	2
1	2	2	3	-1	2	0	2
1	2	2	4	0	2	0	2
1	2	2	5	1	2	0	2
1	3	3	1	0	3	1	1
1	3	3	2	0	3	0	1
1	3	3	3	1	3	0	1
1	3	3	4	-1	3	0	1
1	3	3	5	-1	3	0	1
1	4	4	1	0	4	1	0
1	4	4	2	0	4	0	0
1	4	4	3	1	4	0	0
1	4	4	4	-1	4	0	0
1	4	4	5	-1	4	0	0
2	1	1	1	0	1	1	6

Figure G.1: Excerpt of the data used for the IRT modelling.

Appendix H

Colophon

This document was set in Computer Modern typeface using LaTeX and BibTeX, composed with the TeXMAKER text editor.

Bibliography

[1] Vergnano S, Menson E, Kennea N, Embleton N, Russell AB, Watts T, et al. Neonatal infections in England: the NeonIN surveillance network. Arch Dis Child Fetal Neonatal Ed. 2011;96(1):F9–14.

[2] Vergnano S, Sharland M, Kazembe P, Mwansambo C, Heath P. Neonatal sepsis: an international perspective. Arch Dis Child Fetal Neonatal Ed. 2005;90(3):F220–FF224.

[3] Luck S, Torny M, d'Agapeyeff K, Pitt A, Heath P, Breathnach A, et al. Estimated early-onset group B streptococcal neonatal disease. Lancet. 2003;361(9373):1953–4.

[4] Russell AB, Sharland M, Heath PT. Improving antibiotic prescribing in neonatal units: time to act. Arch Dis Child Fetal Neonatal Ed. 2012;97(2):F141–F146.

[5] Muller-Pebody B, Johnson A, Heath P, Gilbert R, Henderson K, Sharland M, et al. Empirical treatment of neonatal sepsis: are the current guidelines adequate? Arch Dis Child Fetal Neonatal Ed. 2011;96(1):F4–F8.

[6] Spellberg B, Bartlett J, Wunderink R, Gilbert DN. Novel approaches are needed to develop tomorrows antibacterial therapies. Am J Respir Crit Care Med. 2015;191(2):135–40.

[7] Drawz SM, Papp-Wallace KM, Bonomo RA. New β-lactamase inhibitors: a

therapeutic renaissance in an MDR world. Antimicrob Agents Chemother. 2014;58(4):1835–46.

[8] Kadambari S, Heath P, Sharland M, Lewis S, Nichols A, Turner M. Variation in gentamicin and vancomycin dosage and monitoring in UK neonatal units. J Antimicrob Chemother. 2011;66(11):2647–50.

[9] Lutsar I, Chazallon C, Carducci FIC, Trafojer U, Abdelkader B, de Cabre VM, et al. Current management of late onset neonatal bacterial sepsis in five European countries. Eur J Pediatr. 2014;173(8):997–1004.

[10] Conroy S, McIntyre J. The use of unlicensed and off-label medicines in the neonate. Semin Fetal Neonatal Med. 2005;10(2):115–22.

[11] Turner MA. Clinical trials of medicines in neonates: the influence of ethical and practical issues on design and conduct. Br J Clin Pharmacol. 2015;79(3):370–378.

[12] Ette EI, Williams PJ, Lane JR. Population pharmacokinetics III: design, analysis, and application of population pharmacokinetic Studies. Ann Pharmacother. 2004;38(12):2136–44.

[13] Tod M, Jullien V, Pons G. Facilitation of drug evaluation in children by population methods and modelling. Clin Pharmacokinet. 2008;47(4):231–243.

[14] Bonate PL. Pharmacokinetic-Pharmacodynamic Modeling and Simulation. Springer; 2011.

[15] Aarons L. Physiologically based pharmacokinetic modelling: a sound mechanistic basis is needed. Br J Clin Pharmacol. 2005;60(6):581–3.

[16] Paule I, Girard P, Freyer G, Tod M. Pharmacodynamic models for discrete data. Clin Pharmacokinet. 2012;51(12):767–86.

[17] Drusano GL. Antimicrobial pharmacodynamics: critical interactions of 'bug and drug'. Nat Rev Micro. 2004;2(4):289–300.

[18] Cailes B, Vergnano S, Kortsalioudaki C, Heath P, Sharland M. The current and future roles of neonatal infection surveillance programmes in combating antimicrobial resistance. Early Hum Dev. 2015;.

[19] Ueckert S, Plan EL, Ito K, Karlsson MO, Corrigan B, Hooker AC, et al. Improved utilization of ADAS-cog assessment data through item response theory based pharmacometric modeling. Pharm Res. 2014;31(8):2152–65.

[20] Valitalo PAJ, van Dijk M, Krekels EHJ, Simons SHP, Tibboel D, Knibbe CAJ. Morphine efficacy in mechanically ventilated preterm neonates; an item response theory analysis; 2015. PAGE 24 (2015) Abstr 3388 `www.page-meeting.org/?abstract=3388`.

[21] Muir KT, Gomeni RO. Non-compartmental Analysis. In: Bonate PL, Howard DR, editors. Pharmacokinetics in Drug Development: Clinical Study Design and Analysis. vol. 1. Springer; 2005. p. 235–66.

[22] De Cock RF, Piana C, Krekels EH, Danhof M, Allegaert K, Knibbe CA. The role of population PK-PD modelling in paediatric clinical research. Eur J Clin Pharmacol. 2011;67 Suppl 1:5–16.

[23] Ette EI, Williams PJ, Ahmad A. Population Pharmacokinetics Estimation Methods. In: Ette EI, Williams PJ, editors. Pharmacometrics: The Science of Quantitative Pharmacology. Wiley; 2007. p. 265–85.

[24] Ette EI, Williams PJ. Population pharmacokinetics II: estimation methods. Ann Pharmacother. 2004;38(11):1907–15.

[25] O'Hara K, Wright IM, Schneider JJ, Jones AL, Martin JH. Pharmacokinetics in neonatal prescribing: evidence base, paradigms and the future. Br J Clin Pharmacol. 2015;.

[26] Lutsar I, Trafojer U, Heath PT, Metsvaht T, Standing J, Esposito S, et al. Meropenem vs standard of care for treatment of late onset sepsis in children of less than 90 days of age: study protocol for a randomised controlled trial. Trials. 2011;12(1):215.

[27] Boeckmann AJ, Beal SL, Sheiner LB. NONMEM Users Guide. University of California at San Francisco, San Francisco; 1999.

[28] Duffull S, Waterhouse T, Eccleston J. Some considerations on the design of population pharmacokinetic studies. J Pharmacokinet Pharmacodyn. 2005;32(3-4):441–57.

[29] Ette EI, Williams PJ. Population pharmacokinetics I: background, concepts, and models. Ann Pharmacother. 2004;38(10):1702–6.

[30] Bonate PL. Nonlinear Models and Regression. In: Bonate PL, editor. Pharmacokinetic-Pharmacodynamic Modeling and Simulation. Springer; 2011. p. 205–65.

[31] Ueckert S. Novel Pharmacometric Methods for Design and Analysis of Disease Progression Studies. Uppsala Universitet; 2014.

[32] Shafer S, Fisher D. Fisher/Shafer NONMEM Workshop: Pharmacokinetic and Pharmacodynamic Analysis with NONMEM; Basic Concepts; 2007. Het Pand, Ghent, Belgium.

[33] Lavielle M, Mentré F. Estimation of population pharmacokinetic parameters of saquinavir in HIV patients with the MONOLIX software. J Pharmacokinet Pharmacodyn. 2007;34(2):229–249.

[34] DArgenio DZ, Schumitzky A. ADAPT 5 Users Guide: Pharmacokinetic/Pharmacodynamic Systems Analysis Software. Biomedical Simulations Resource, Los Angeles; 2009.

[35] Tatarinova T, Neely M, Bartroff J, van Guilder M, Yamada W, Bayard D, et al. Two general methods for population pharmacokinetic modeling: non-parametric adaptive grid and non-parametric Bayesian. J Pharmacokinet Pharmacodyn. 2013;40(2):189–199.

[36] Plan EL, Maloney A, Mentre F, Karlsson MO, Bertrand J. Performance comparison of various maximum likelihood nonlinear mixed-effects estimation methods for dose-response models. AAPS J. 2012;14(3):420–32.

[37] Brendel K, Dartois C, Comets E, Lemenuel-Diot A, Laveille C, Tranchand B, et al. Are population pharmacokinetic and/or pharmacodynamic models adequately evaluated? A survey of the literature from 2002 to 2004. Clin Pharmacokinet. 2007;46(3):221–34.

[38] Karlsson MO, Savic RM. Diagnosing model diagnostics. Clin Pharmacol Ther. 2007;82(1):17–20.

[39] Post TM, Freijer JI, Ploeger BA, Danhof M. Extensions to the visual predictive check to facilitate model performance evaluation. J Pharmacokinet Pharmacodyn. 2008;35(2):185–202.

[40] Bergstrand M, Hooker AC, Wallin JE, Karlsson MO. Prediction-corrected visual predictive checks for diagnosing nonlinear mixed-effects models. AAPS J. 2011;13(2):143–51.

[41] Karlsson MO, Holford N. A Tutorial on Visual Predictive Checks; 2008. PAGE 17 (2008) Abstr 1434 `www.page-meeting.org/?abstract=1434`.

[42] Holford NH. The Visual Predictive Check Superiority to Standard Diagnostic (Rorschach) Plots; 2005. PAGE 14 (2005) Abstr 738 `www.page-meeting.org/?abstract=738`.

[43] Allegaert K, Velde M, Anker J. Neonatal clinical pharmacology. Paediatr Anaesth. 2014;24(1):30–8.

[44] Kearns GL, Abdel-Rahman SM, Alander SW, Blowey DL, Leeder JS, Kauffman RE. Developmental pharmacology–drug disposition, action, and therapy in infants and children. N Engl J Med. 2003;349(12):1157–67.

[45] Strolin Benedetti M, Baltes EL. Drug metabolism and disposition in children. Fundam Clin Pharmacol. 2003;17(3):281–99.

[46] Alcorn J, McNamara PJ. Pharmacokinetics in the newborn. Adv Drug Deliv Rev. 2003;55(5):667–86.

[47] van den Anker JN, Schwab M, Kearns GL. Developmental pharmacokinetics. Handb Exp Pharmacol. 2011;205:51–75.

[48] Nau R, Sörgel F, Eiffert H. Penetration of drugs through the blood-cerebrospinal fluid/blood-brain barrier for treatment of central nervous system infections. Clin Microbiol Rev. 2010;23(4):858–83.

[49] Turnidge J. Pharmacodynamics and dosing of aminoglycosides. Infect Dis Clin North Am. 2003;17(3):503–28.

[50] Moon YS, Chung KC, Gill MA. Pharmacokinetics of meropenem in animals, healthy volunteers, and patients. Clin Infect Dis. 1997;24(Supplement 2):S249–55.

[51] Alcorn J, McNamara PJ. Ontogeny of hepatic and renal systemic clearance pathways in infants: part I. Clin Pharmacokinet. 2002;41(12):959–98.

[52] Rhodin MM, Anderson BJ, Peters AM, Coulthard MG, Wilkins B, Cole M, et al. Human renal function maturation: a quantitative description using weight and postmenstrual age. Pediatr Nephrol. 2009;24(1):67–76.

[53] Engle WA. Age terminology during the perinatal period. Pediatrics. 2004;114(5):1362–4.

[54] Anderson BJ, Holford NH. Understanding dosing: children are small adults, neonates are immature children. Arch Dis Child. 2013;98(9):737–44.

[55] Oeser C, Lutsar I, Metsvaht T, Turner MA, Heath PT, Sharland M. Clinical trials in neonatal sepsis. J Antimicrob Chemother. 2013;68(12):2733–45.

[56] Stephenson T. How children's responses to drugs differ from adults. Br J Clin Pharmacol. 2005;59(6):670–3.

[57] Briggs SW, Galanopoulou AS. Altered GABA signaling in early life epilepsies. Neural Plast. 2011;2011.

[58] Montenegro MA, Guerreiro MM, Caldas JPS, Moura-Ribeiro MVL, Guerreiro CAM. Epileptic manifestations induced by midazolam in the neonatal period. Arq Neuropsiquiatr. 2001;59(2A):242–3.

[59] Bains I, Thiebaut R, Yates AJ, Callard R. Quantifying thymic export: combining models of naive T cell proliferation and TCR excision circle dynamics gives an explicit measure of thymic output. J Immunol. 2009;183(7):4329–36.

[60] Cuenca AG, Wynn JL, Moldawer LL, Levy O. Role of innate immunity in neonatal infection. Am J Perinatol. 2013;30(2):105–12.

[61] Levy O. Innate immunity of the newborn: basic mechanisms and clinical correlates. Nat Rev Immunol. 2007;7(5):379–90.

[62] Basha S, Surendran N, Pichichero M. Immune responses in neonates. Expert Rev Clin Immunol. 2014;10(9):1171–84.

[63] Turnidge JD. The Pharmacodynamics of β-Lactams. Clin Infect Dis. 1998;27(1):10–22.

[64] Lutsar I, Metsvaht T. Understanding pharmacokinetics/pharmacodynamics in managing neonatal sepsis. Curr Opin Infect Dis. 2010;23(3):201–7.

[65] Moore RD, Lietman PS, Smith CR. Clinical response to aminoglycoside therapy: importance of the ratio of peak concentration to minimal inhibitory concentration. J Infect Dis. 1987;155(1):93–9.

[66] Levison ME. Pharmacodynamics of antimicrobial drugs. Infect Dis Clin North Am. 2004;18(3):451–65, vii.

[67] Freeman CD, Nicolau DP, Belliveau PP, Nightingale CH. Once-daily dosing of aminoglycosides: review and recommendations for clinical practice. J Antimicrob Chemother. 1997;39(6):677–86.

[68] Mouton JW, Touw DJ, Horrevorts AM, Vinks AA. Comparative pharmacokinetics of the carbapenems. Clin Pharmacokinet. 2000;39(3):185–201.

[69] Holford N, Heo YA, Anderson B. A pharmacokinetic standard for babies and adults. J Pharm Sci. 2013;102(9):2941–52.

[70] Espié P, Tytgat D, Sargentini-Maier ML, Poggesi I, Watelet JB. Physiologically based pharmacokinetics (PBPK). Drug Metab Rev. 2009;41(3):391–407.

[71] Johnson TN, Rostami-Hodjegan A, Tucker GT. Prediction of the clearance of eleven drugs and associated variability in neonates, infants and children. Clin Pharmacokinet. 2006;45(9):931–956.

[72] Edginton AN, Willmann S. Physiology-based versus allometric scaling of clearance in children; an eliminating process based comparison. Paediatr Perinat Drug Ther. 2006;7(3):146–53.

[73] Mahmood I. Dosing in children: a critical review of the pharmacokinetic allometric scaling and modelling approaches in paediatric drug development and clinical settings. Clin Pharmacokinet. 2014;53(4):327–46.

[74] Langdon G, Gueorguieva I, Aarons L, Karlsson M. Linking preclinical and clinical whole-body physiologically based pharmacokinetic models with prior distributions in NONMEM. Eur J Clin Pharmacol. 2007;63(5):485–98.

[75] Sadiq MW, Nielsen EI, Karlsson MO, Friberg LE. A whole-body physiologically based pharmacokinetic (WBPBPK) model of ciprofloxacin for prediction of bacterial killing at the site of infection; 2015. PAGE 24 (2015) Abstr 3563 www.page-meeting.org/?abstract=3563.

[76] Crawford JD, Terry ME, Rourke GM. Simplification of drug dosage calculation by application of the surface area principle. Pediatrics. 1950;5(5):783–90.

[77] Holford NH. A size standard for pharmacokinetics. Clin Pharmacokinet. 1996;30(5):329–32.

[78] Anderson BJ, Holford NH. Mechanistic basis of using body size and maturation to predict clearance in humans. Drug Metab Pharmacokinet. 2009;24(1):25–36.

[79] Benedict FG. Vital Energetics: A Study in Comparative Basal Metabolism. Carnegie Institution of Washington. Publication no. 503. Carnegie Institution of Washington; 1938. Available from: https://books.google.co.uk/books?id=6IQcAAAAMAAJ.

[80] Kleiber M. Body size and metabolism. Hilgardia. 1932;4(11):315–53.

[81] Kleiber M. Body size and metabolic rate. Physiol Rev. 1947;27(4):511–41.

[82] Fadrowski JJ, Neu AM, Schwartz GJ, Furth SL. Pediatric GFR estimating equations applied to adolescents in the general population. Clin J Am Soc Nephrol. 2011;6(6):1427–35.

[83] Schwartz GJ, Schneider MF, Maier PS, Moxey-Mims M, Dharnidharka VR, Warady BA, et al. Improved equations estimating GFR in children with

chronic kidney disease using an immunonephelometric determination of cystatin C. Kidney Int. 2012;82(4):445–53.

[84] Noda T, Todani T, Watanabe Y, Yamamoto S. Liver volume in children measured by computed tomography. Pediatr Radiol. 1997;27(3):250–2.

[85] Johnson TN, Tucker GT, Tanner MS, Rostami-Hodjegan A. Changes in liver volume from birth to adulthood: A meta-analysis. Liver Transpl. 2005;11(12):1481–93.

[86] McLeay SC, Morrish GA, Kirkpatrick CMJ, Green B. The Relationship between Drug Clearance and Body Size. Clin Pharmacokinet. 2012;51(5):319–30.

[87] Box GEP, Tiao GC. The collected works of George E.P. Box. Wadsworth Advancesd Books & Software; 1985.

[88] Wang C, Sadhavisvam S, Krekels EH, Dahan A, Tibboel D, Danhof M, et al. Developmental changes in morphine clearance across the entire paediatric age range are best described by a bodyweight-dependent exponent model. Clin Drug Investig. 2013;33(7):523–34.

[89] Anderson BJ, Allegaert K, Van den Anker JN, Cossey V, Holford NH. Vancomycin pharmacokinetics in preterm neonates and the prediction of adult clearance. Br J Clin Pharmacol. 2007;63(1):75–84.

[90] Anderson BJ, Larsson P. A maturation model for midazolam clearance. Paediatr Anaesth. 2011;21(3):302–8.

[91] Mahmood I. Mechanistic versus allometric models for the prediction of drug clearance in neonates (< 3 months of age). J Clin Pharmacol. 2015;55(6):718–20.

[92] NMUsers; 2015. `http://www.cognigencorp.com/index.php/resources_nonmem`, last accessed 09/04/2015.

[93] Uijtendaal EV, Rademaker CM, Schobben AF, Fleer A, Kramer WL, van Vught AJ, et al. Once-daily versus multiple-daily gentamicin in infants and children. Ther Drug Monit. 2001;23(5):506–13.

[94] Rosario M, Thomson A, Sharp C, Elliott H, et al. Population pharmacokinetics of gentamicin in patients with cancer. Br J Clin Pharmacol. 1998;46(3):229–236.

[95] Xuan D, Nicolau DP, Nightingale CH. Population pharmacokinetics of gentamicin in hospitalized patients receiving once-daily dosing. Int J Antimicrob Agents. 2004;23(3):291–4.

[96] Kirkpatrick C, Duffull S, Begg E. Phamacokinetics of gentamicin in 957 patients with varying renal function dosed once daily. Br J Clin Pharmacol. 1999;47:637–44.

[97] Bianco TM, Dwyer PN, Bertino J. Gentamicin pharmacokinetics, nephrotoxicity, and prediction of mortality in febrile neutropenic patients. Antimicrob Agents Chemother. 1989;33(11):1890–5.

[98] Bertino J, Booker L, Franck P, Rybicki B. Gentamicin pharmacokinetics in patients with malignancies. Antimicrob Agents Chemother. 1991;35(7):1501–3.

[99] Lewis D, Longman R, Wisheart J, Spencer R, Brown N. The pharmacokinetics of a single dose of gentamicin (4 mg/kg) as prophylaxis in cardiac surgery requiring cardiopulmonary bypass. Cardiovasc Surg. 1999;7(4):398–401.

[100] Goncalves-Pereira J, Martins A, Povoa P. Pharmacokinetics of gentamicin in critically ill patients: pilot study evaluating the first dose. Clin Microbiol Infect. 2010;16(8):1258–63.

[101] Zaske D, Cipolle R, Rotschafer J, Solem L, Mosier N, Strate R. Gentamicin pharmacokinetics in 1,640 patients: method for control of serum concentrations. Antimicrob Agents Chemother. 1982;21(3):407–411.

[102] Hilmer SN, Tran K, Rubie P, Wright J, Gnjidic D, Mitchell SJ, et al. Gentamicin pharmacokinetics in old age and frailty. Br J Clin Pharmacol. 2011;71(2):224–31.

[103] Johnston C, Hilmer SN, McLachlan AJ, Matthews ST, Carroll PR, Kirkpatrick CM. The impact of frailty on pharmacokinetics in older people: using gentamicin population pharmacokinetic modeling to investigate changes in renal drug clearance by glomerular filtration. Eur J Clin Pharmacol. 2014;70(5):549–55.

[104] Bass KD, Larkin SE, Paap C, Haase GM. Pharmacokinetics of once-daily gentamicin dosing in pediatric patients. J Pediatr Surg. 1998;33(7):1104–7.

[105] Cohen P, Collart L, Prober CG, Fisher AF, Blaschke TF. Gentamicin pharmacokinetics in neonates undergoing extracorporal membrane oxygenation. Pediatr Infect Dis J. 1990;9(8):562–5.

[106] Sumpter AL, Holford NH. Predicting weight using postmenstrual age–neonates to adults. Paediatr Anaesth. 2011;21(3):309–15.

[107] Bhatt-Mehta V, Donn SM. Gentamicin pharmacokinetics in term newborn infants receiving high-frequency oscillatory ventilation or conventional mechanical ventilation: a case-controlled study. J Perinatol. 2003;23(7):559–62.

[108] Vervelde ML, Rademaker CMA, Krediet TG, Fleer A, van Asten P, van Dijk A. Population Pharmacokinetics of Gentamicin in Preterm Neonates: Evaluation of a Once-Daily Dosage Regimen. Ther Drug Monit. 1999;21(5):514.

[109] Thomson AH, Way S, Bryson SM, McGovern EM, Kelman AW, Whiting

B. Population pharmacokinetics of gentamicin in neonates. Dev Pharmacol Ther. 1988;11(3):173–9.

[110] Mark LF, Solomon A, Northington FJ, Lee CK. Gentamicin pharmacokinetics in neonates undergoing therapeutic hypothermia. Ther Drug Monit. 2013;35(2):217.

[111] Botha JH, du Preez MJ, Adhikari M. Population pharmacokinetics of gentamicin in South African newborns. Eur J Clin Pharmacol. 2003;59(10):755–9.

[112] Izquierdo M, Lanao JM, Cervero L, Jimenez NV, Dominguez-Gil A. Population Pharmacokinetics of Gentamicin in Premature Infants. Ther Drug Monit. 1992;14(3):177–83.

[113] Garcia B, Barcia E, Perez F, Molina IT. Population pharmacokinetics of gentamicin in premature newborns. J Antimicrob Chemother. 2006;58(2):372–9.

[114] Lingvall M, Reith D, Broadbent R. The effect of sepsis upon gentamicin pharmacokinetics in neonates. Br J Clin Pharmacol. 2005;59(1):54–61.

[115] Lanao JM, Calvo MV, Mesa JA, Martin-Suarez A, Carbajosa MT, Miguelez F, et al. Pharmacokinetic basis for the use of extended interval dosage regimens of gentamicin in neonates. J Antimicrob Chemother. 2004;54(1):193–8.

[116] Knight JA, Davis EM, Manouilov K, Hoie EB. The effect of postnatal age on gentamicin pharmacokinetics in neonates. Pharmacotherapy. 2003;23(8):992–996.

[117] Nakae S, Yamada M, Ito T, Chiba Y, Sasaki E, Sakamoto M, et al. Gentamicin dosing and pharmacokinetics in low birth weight infants. Tohoku J Exp Med. 1988;155(3):213–223.

[118] Haughey DB, Hilligoss DM, Grassi A, Schentag JJ. Two-compartment gentamicin pharmacokinetics in premature neonates: a comparison to adults with decreased glomerular filtration rates. J Pediatr. 1980;96(2):325–330.

[119] Nielsen EI, Sandstrom M, Honore PH, Ewald U, Friberg LE. Developmental pharmacokinetics of gentamicin in preterm and term neonates: population modelling of a prospective study. Clin Pharmacokinet. 2009;48(4):253–63.

[120] DiCenzo R, Forrest A, Slish JC, Cole C, Guillet R. A Gentamicin Pharmacokinetic Population Model and Once-Daily Dosing Algorithm for Neonates. Pharmacotherapy. 2003;23(5):585–91.

[121] Medellín-Garibay SE, Rueda-Naharro A, Peña-Cabia S, García B, Romano-Moreno S, Barcia E. Population pharmacokinetics of gentamicin and dosing optimization for infants. Antimicrob Agents Chemother. 2015;59(1):482–9.

[122] Ho KK, Bryson SM, Thiessen JJ, Greenberg ML, Einarson TR, Leson CL. The effects of age and chemotherapy on gentamicin pharmacokinetics and dosing in pediatric oncology patients. Pharmacotherapy. 1995;15(6):754–64.

[123] Postovsky S, Arush MWB, Kassis E, Elhasid R, Krivoy N. Pharmacokinetic analysis of gentamicin thrice and single daily dosage in pediatric cancer patients. Pediatr Hematol Oncol. 1997;14(6):547–54.

[124] Lopez SA, Mulla H, Durward A, Tibby SM. Extended-interval gentamicin: population pharmacokinetics in pediatric critical illness. Pediatr Crit Care Med. 2010;11(2):267–74.

[125] Simon V, Mösinger E, Malerczy V. Pharmacokinetic studies of tobramycin and gentamicin. Antimicrob Agents Chemother. 1973;3(4):445–50.

[126] Walker J, Wise R, Mitchard M. The pharmacokinetics of amikacin and gentamicin in volunteers: a comparison of individual differences. J Antimicrob Chemother. 1979;5(1):95–9.

[127] Demczar DJ, Nafziger AN, Bertino J. Pharmacokinetics of gentamicin at traditional versus high doses: implications for once-daily aminoglycoside dosing. Antimicrob Agents Chemother. 1997;41(5):1115–9.

[128] Gilman T, Brunnemann S, Segal J. Comparison of population pharmacokinetic models for gentamicin in spinal cord-injured and able-bodied patients. Antimicrob Agents Chemother. 1993;37(1):93–9.

[129] Wang C, Peeters MY, Allegaert K, van Oud-Alblas HJB, Krekels EH, Tibboel D, et al. A bodyweight-dependent allometric exponent for scaling clearance across the human life-span. Pharm Res. 2012;29(6):1570–81.

[130] De Cock RF, Allegaert K, Schreuder MF, Sherwin CM, de Hoog M, van den Anker JN, et al. Maturation of the glomerular filtration rate in neonates, as reflected by amikacin clearance. Clin Pharmacokinet. 2012;51(2):105–17.

[131] Ince I, de Wildt SN, Wang C, Peeters MY, Burggraaf J, Jacqz-Aigrain E, et al. A novel maturation function for clearance of the cytochrome P450 3A substrate midazolam from preterm neonates to adults. Clin Pharmacokinet. 2013;52(7):555–65.

[132] Ding J, Wang Y, Lin W, Wang C, Zhao L, Li X, et al. A Population Pharmacokinetic Model of Valproic Acid in Pediatric Patients with Epilepsy: A Non-Linear Pharmacokinetic Model Based on Protein-Binding Saturation. Clin Pharmacokinet. 2015;54(3):305–17.

[133] Kimura T, Sunakawa K, Matsuura N, Kubo H, Shimada S, Yago K. Population pharmacokinetics of arbekacin, vancomycin, and panipenem in neonates. Antimicrob Agents Chemother. 2004;48(4):1159–67.

[134] Foissac F, Bouazza N, Valade E, De Sousa Mendes M, Fauchet F, Benaboud S, et al. Prediction of drug clearance in children. J Clin Pharmacol. 2015;.

[135] Robbie GJ, Zhao L, Mondick J, Losonsky G, Roskos LK. Population pharmacokinetics of palivizumab, a humanized anti-respiratory syncytial virus monoclonal antibody, in adults and children. Antimicrob Agents Chemother. 2012;56(9):4927–36.

[136] Savic RM, Cowan MJ, Dvorak CC, Pai SY, Pereira L, Bartelink IH, et al. Effect of weight and maturation on busulfan clearance in infants and small children undergoing hematopoietic cell transplantation. Biol Blood Marrow Transplant. 2013;19(11):1608–14.

[137] R Core Team. R: A Language and Environment for Statistical Computing. Vienna, Austria; 2014. Available from: `http://www.R-project.org/`.

[138] Wickham H. ggplot2: elegant graphics for data analysis. Springer Science & Business Media; 2009.

[139] International conference on harmonisation of technical requirements for registration of pharmaceuticals for human use (ICH). Clinical Investigation of Medicinal Products in the Pediatric Population; 2000. `http://www.ich.org/products/guidelines/efficacy/efficacy-single/article/clinical-investigation-of-medicinal-products-in-the-\pediatric-population.html`, last accessed 05/09/2015.

[140] Mahmood I, Staschen CM, Goteti K. Prediction of drug clearance in children: an evaluation of the predictive performance of several models. AAPS J. 2014;16(6):1334–43.

[141] Mahmood I. Evaluation of sigmoidal maturation and allometric models: prediction of propofol clearance in neonates and infants. Am J Ther. 2013;20(1):21–8.

[142] Lopez SA, Mulla H, Durward A, Tibby SM. Extended-interval gentamicin:

population pharmacokinetics in pediatric critical illness. Pediatr Crit Care Med. 2010;11(2):267–74.

[143] Ahsman MJ, Hanekamp M, Wildschut ED, Tibboel D, Mathot RA. Population pharmacokinetics of midazolam and its metabolites during venoarterial extracorporeal membrane oxygenation in neonates. Clin Pharmacokinet. 2010;49(6):407–19.

[144] Ramirez MS, Tolmasky ME. Aminoglycoside modifying enzymes. Drug Resist Updat. 2010;13(6):151–71.

[145] Craig WA. The pharmacology of meropenem, a new carbapenem antibiotic. Clin Infect Dis. 1997;24(Supplement 2):S266–S275.

[146] Weinstein MJ, Luedemann GM, Oden EM, Wagman GH, Rosselet JP, Marquez JA, et al. Gentamicin, a new antibiotic complex from micromonospora. J Med Chem. 1963;6(4):463–4.

[147] Gyselynck AM, Forrey A, Cutler R. Pharmacokinetics of gentamicin: distribution and plasma and renal clearance. J Infect Dis. 1971;124(Supplement 1):S70–6.

[148] McCracken GH. Gentamicin in the neonatal period. Am J Dis Child. 1970;120(6):524–33.

[149] NPSA, National Patient Safety Agency. Safer use of intravenous gentamicin for neonates; 2010. Available from `http://www.nrls.npsa.nhs.uk/alerts/?entryid45=66271`, last accessed 25/10/2014.

[150] Valitalo PA, van den Anker JN, Allegaert K, de Cock RF, de Hoog M, Simons SH, et al. Novel model-based dosing guidelines for gentamicin and tobramycin in preterm and term neonates. J Antimicrob Chemother. 2015;p. dkv052.

[151] Forge A, Schacht J. Aminoglycoside antibiotics. Audiol Neurootol. 2000;5(1):3–22.

[152] Martinez-Salgado C, Lopez-Hernandez FJ, Lopez-Novoa JM. Glomerular nephrotoxicity of aminoglycosides. Toxicol Appl Pharmacol. 2007;223(1):86–98.

[153] Touw DJ, Westerman EM, Sprij AJ. Therapeutic drug monitoring of aminoglycosides in neonates. Clin Pharmacokinet. 2009;48(2):71–88.

[154] Rho JP. Principles of Antimicrobial Therapy. In: Norman D, Yoshikawa T, editors. Infectious Disease in the Aging: A Clinical Handbook. Humana Press; 2009. p. 43–59.

[155] Gabrielsson J, Weiner D. Aminoglycosides. In: Root RK, Waldvogel F, Corey L, Stamm WE, editors. Clinical Infectious Diseases: A Practical Approach. Oxford University Press, Inc.; 1999. p. 273–84.

[156] Rudin A, Healey A, Phillips CA, Gump DW, Forsyth BR. Antibacterial activity of gentamicin sulfate in tissue culture. Appl Microbiol. 1970;20(6):989–90.

[157] Pacifici GM. Clinical pharmacokinetics of aminoglycosides in the neonate: a review. Eur J Clin Pharmacol. 2009;65(4):419–27.

[158] Stoll BJ, Hansen N, Fanaroff AA, Wright LL, Carlo WA, Ehrenkranz RA, et al. Changes in pathogens causing early-onset sepsis in very-low-birthweight infants. N Engl J Med. 2002;347(4):240–7.

[159] Stoll BJ, Hansen NI, Sanchez PJ, Faix RG, Poindexter BB, Van Meurs KP, et al. Early onset neonatal sepsis: the burden of group B Streptococcal and E. coli disease continues. Pediatrics. 2011;127(5):817–26.

[160] Turner MA, Lewis S, Hawcutt DB, Field D. Prioritising neonatal medicines research: UK Medicines for Children Research Network scoping survey. BMC Pediatr. 2009;9(1):50.

[161] Cantey JB, Wozniak PS, Sánchez PJ. Prospective surveillance of antibiotic use in the neonatal intensive care unit: results from the SCOUT study. Pediatr Infect Dis J. 2015;34(3):267–72.

[162] Begg EJ, Barclay ML, Kirkpatrick CM. The therapeutic monitoring of antimicrobial agents. Br J Clin Pharmacol. 2001;52 Suppl 1:35S–43S.

[163] Quiros Y, Vicente-Vicente L, Morales AI, Lopez-Novoa JM, Lopez-Hernandez FJ. An integrative overview on the mechanisms underlying the renal tubular cytotoxicity of gentamicin. Toxicol Sci. 2011;119(2):245–56.

[164] Ali BH. Gentamicin nephrotoxicity in humans and animals: some recent research. Gen Pharmacol. 1995;26(71):1477–87.

[165] de Hoog M, van den Anker JN. Therapeutic drug monitoring of aminoglycosides in neonates. Clin Pharmacokinet. 2009;48(5):343–4; author reply 344–5.

[166] Prayle A, Watson A, Fortnum H, Smyth A. Side effects of aminoglycosides on the kidney, ear and balance in cystic fibrosis. Thorax. 2010;65(7):654–8.

[167] Selimoglu E. Aminoglycoside-Induced Ototoxicity. Curr Pharm Des. 2007;13(1):119–26.

[168] Shahid M, Cooke R. Is a once daily dose of gentamicin safe and effective in the treatment of uti in infants and children? Arch Dis Child. 2007;92(9):823–4.

[169] Huth ME, Ricci AJ, Cheng AG. Mechanisms of aminoglycoside ototoxicity and targets of hair cell protection. Int J Otolaryngol. 2011;31(6):937861, 19 pages.

[170] Zimmerman E, Lahav A. Ototoxicity in preterm infants: effects of genetics, aminoglycosides, and loud environmental noise. J Perinatol. 2013;33(1):3–8.

[171] Bitner-Glindzicz M, Rahman S. Ototoxicity caused by aminoglycosides. BMJ. 2007 10;335(7624):784–5.

[172] Johnson RF, Cohen AP, Guo Y, Schibler K, Greinwald JH. Genetic mutations and aminoglycoside-induced ototoxicity in neonates. Otolaryngol Head Neck Surg. 2010;142(5):704–7.

[173] Ealy M, Lynch KA, Meyer NC, Smith RJH. The prevalence of mitochondrial mutations associated with aminoglycoside-induced sensorineural hearing loss in an NICU population. Laryngoscope. 2011;121(6):1184–6.

[174] Pokorna P, Martinkova J, Zahora J, Selke-Krulichova I, Chladek J. Therapeutic Drug Monitoring of Gentamicin in Neonates Critically Ill at the 1st Week of Life; 2008.

[175] Siber GR, Echeverria P, Smith AL, Paisley JW, Smith DH. Pharmacokinetics of gentamicin in children and adults. J Infect Dis. 1975;132(6):637–51.

[176] Triggs E, Charles B. Pharmacokinetics and therapeutic drug monitoring of gentamicin in the elderly. Clin Pharmacokinet. 1999;37(4):331–41.

[177] Dersch-Mills D, Akierman A, Alshaikh B, Yusuf K. Validation of a Dosage Individualization Table for Extended-Interval Gentamicin in Neonates. Ann Pharmacother. 2012;46(7-8):935–42.

[178] Dersch-Mills D, Akierman A, Alshaikh B, Sundaram A, Yusuf K. Performance of a dosage individualization table for extended interval gentamicin in neonates beyond the first week of life. J Matern Fetal Neonatal Med. 2015;(ahead-of-print):1–6.

[179] Stickland MD, Kirkpatrick CM, Begg EJ, Duffull SB, Oddie SJ, Darlow BA. An extended interval dosing method for gentamicin in neonates. J Antimicrob Chemother. 2001;48(6):887–93.

[180] Laskin OL, Longstreth JA, Smith CR, Lietman PS. Netilmicin and gentamicin multidose kinetics in normal subjects. Clin Pharmacol Ther. 1983;34(5):644–50.

[181] Burton ME, Brater DC, Chen PS, Day RB, Huber PJ, Vasko MR. A Bayesian feedback method of aminoglycoside dosing. Clin Pharmacol Ther. 1985;37(3):349–57.

[182] Rao SC, Srinivasjois R, Hagan R, Ahmed M. One dose per day compared to multiple doses per day of gentamicin for treatment of suspected or proven sepsis in neonates. Cochrane Database Syst Rev. 2011;11:CD005091.

[183] Chirico G, Barbieri F, Chirico C. Antibiotics for the newborn. J Matern Fetal Neonatal Med. 2009;22 Suppl 3:46–9.

[184] Alsaedi SA. Once daily gentamicin dosing in full term neonates. Saudi Med J. 2003;24(9):978–81.

[185] Darmstadt GL, Miller-Bell M, Batra M, Law P, Law K. Extended-interval dosing of gentamicin for treatment of neonatal sepsis in developed and developing countries. J Health Popul Nutr. 2008;26(2):163–82.

[186] BNFC, British National Formulary for Children. Gentamicin; 2015. `http://www.evidence.nhs.uk/formulary/bnfc/current/5-infections/51-antibacterial-drugs/514-aminoglycosides/gentamicin`, last accessed on 06/09/2015.

[187] The European Committee on Antimicrobial Susceptibility Testing (EUCAST). MIC distributions for Escherichia coli when treated with gentam-

icin; 2015. http://mic.eucast.org/Eucast2/regShow.jsp?Id=908, last accessed on 06/09/2015.

[188] The European Committee on Antimicrobial Susceptibility Testing (EUCAST). Breakpoint tables for interpretation of MICs and zone diameters. Version 5.0; 2015. www.eucast.org/fileadmin/src/media/PDFs/EUCAST_files/Breakpoint_tables/v_5.0_Breakpoint_Table_01.pdf, last accessed on 29/12/2015.

[189] NICE, National Institute for Health and Care Excellence. NICE guidelines: Therapeutic drug monitoring for gentamicin; 2012. http://www.nice.org.uk/guidance/CG149/chapter/1-Guidance#therapeutic-drug-monitoring-for-gentamicin, last accessed 06/09/2015.

[190] Gordon RC, Regamey C, Kirby WM. Serum protein binding of the aminoglycoside antibiotics. Antimicrob Agents Chemother. 1972;2(3):214–216.

[191] Touw DJ, Proost JH, Stevens R, Lafeber HN, van Weissenbruch MM. Gentamicin pharmacokinetics in preterm infants with a patent and a closed ductus arteriosus. Pharm World Sci. 2001;23(5):200–4.

[192] Gal P, Gilman JT. Drug disposition in neonates with patent ductus arteriosus. Ann Pharmacother. 1993;27(11):1383–8.

[193] Williams BS, Ransom JL, Gal P, Carlos RQ, Smith M, Schall SA. Gentamicin pharmacokinetics in neonates with patent ductus arteriosus. Crit Care Med. 1997;25(2):273–5.

[194] Ariano RE, Sitar DS, Davi M, Zelenitsky SA. Bayesian Pharmacokinetic Analysis of a Gentamicin Nomogram in Neonates: A Retrospective Study. Current therapeutic research, clinical and experimental. 2003;64(3):178–88.

[195] Murphy JE, Austin ML, Frye RF. Evaluation of gentamicin pharmacokinetics and dosing protocols in 195 neonates. Am J Health Syst Pharm. 1998;55(21):2280–8.

[196] Kelman AW, Thomson AH, Whiting B, Bryson SM, Steedman DA, Mawer GE, et al. Estimation of gentamicin clearance and volume of distribution in neonates and young children. Br J Clin Pharmacol. 1984;18(5):685–92.

[197] Grasela T, Ott R, Faix R. Population pharmacokinetics of gentamicin in neonates using routine clinical data; 1985. Abstr, American Society for Clinical Pharmacology and Therapeutics, 86th Annual Meeting.

[198] Jensen PD, Edgren BE, Brundage RC. Population Pharmacokinetics of Gentamicin in Neonates Using a Nonlinear, Mixed-Effects Model. Pharmacotherapy. 1992;12(3):178–82.

[199] Weber W, Kewitz G, Rost K, Looby M, Nitz M, Harnisch L. Population kinetics of gentamicin in neonates. Eur J Clin Pharmacol. 1993;44(1):S23–5.

[200] Fuchs A, Guidi M, Giannoni E, Werner D, Buclin T, Widmer N, et al. Population pharmacokinetic study of gentamicin in a large cohort of premature and term neonates. Br J Clin Pharmacol. 2014;78(5):1090–101.

[201] Heimann G. Renal toxicity of aminoglycosides in the neonatal period. Pediatr Pharmacol (New York). 1982;3(3-4):251–257.

[202] Price CP, Finney H. Developments in the assessment of glomerular filtration rate. Clin Chim Acta. 2000;297(1-2):55–66.

[203] Marshall SK William J Bangert. The kidneys. In: Marshall WJ, Bangert SK, editors. Clinical Chemistry. 6th ed. Elsevier; 2008. p. 71.

[204] Stevens LA, Stoycheff N. Standardization of serum creatinine and estimated GFR in the Kidney Early Evaluation Program (KEEP). Am J Kidney Dis. 2008;51(4 Suppl 2):S77–82.

[205] Hartmann AE. Nitrogen Metabolites and Renal Function. In: McClatchey KD, editor. Clinical Laboratory Medicine. 2nd ed. Lippicott Williams and Wilkins; 2002. p. 378–391.

[206] Earley A, Miskulin D, Lamb EJ, Levey AS, Uhlig K. Estimating equations for glomerular filtration rate in the era of creatinine standardization: a systematic review. Ann Intern Med. 2012;156(11):785–95, W–270–8.

[207] Swan SK. The search continues–an ideal marker of GFR. Clin Chem. 1997;43(6 Pt 1):913–4.

[208] Risch L, Huber AR. Assessing glomerular filtration rate in renal transplant recipients by estimates derived from serum measurements of creatinine and cystatin C. Clin Chim Acta. 2005;356(1-2):204–11.

[209] Andersen TB, Eskild-Jensen A, Frokiaer J, Brochner-Mortensen J. Measuring glomerular filtration rate in children; can cystatin C replace established methods? A review. Pediatr Nephrol. 2009;24(5):929–41.

[210] Peake M, Whiting M. Measurement of serum creatinine–current status and future goals. Clin Biochem Rev. 2006;27(4):173–84.

[211] Allegaert K, Kuppens M, Mekahli D, Levtchenko E, Vanstapel F, Vanhole C, et al. Creatinine reference values in ELBW infants: impact of quantification by Jaffe or enzymatic method. J Matern Fetal Neonatal Med. 2012;25(9):1678–81.

[212] Hosten AO. BUN and Creatinine. In: Walker HK, Hall WD, Hurst JW, editors. Clinical Methods: The History, Physical, and Laboratory Examinations. 3rd ed.; 1990. p. 874–8.

[213] Herget-Rosenthal S, Bokenkamp A, Hofmann W. How to estimate GFR-serum creatinine, serum cystatin C or equations? Clin Biochem. 2007;40(3-4):153–61.

[214] Boer DP, de Rijke YB, Hop WC, Cransberg K, Dorresteijn EM. Reference values for serum creatinine in children younger than 1 year of age. Pediatr Nephrol. 2010;25(10):2107–13.

[215] Bariciak E, Yasin A, Harrold J, Walker M, Lepage N, Filler G. Preliminary reference intervals for cystatin C and beta-trace protein in preterm and term neonates. Clin Biochem. 2011;44(13):1156–9.

[216] Schwartz GJ, Work DF. Measurement and estimation of GFR in children and adolescents. Clin J Am Soc Nephrol. 2009;4(11):1832–43.

[217] Narvaez-Sanchez R, Gonzalez L, Salamanca A, Silva M, Rios D, Arevalo S, et al. Cystatin C could be a replacement to serum creatinine for diagnosing and monitoring kidney function in children. Clin Biochem. 2008;41(7-8):498–503.

[218] Cockcroft DW, Gault MH. Prediction of creatinine clearance from serum creatinine. Nephron. 1976;16(1):31–41.

[219] Levey AS, Coresh J, Greene T, Stevens LA, Zhang YL, Hendriksen S, et al. Using standardized serum creatinine values in the modification of diet in renal disease study equation for estimating glomerular filtration rate. Ann Intern Med. 2006;145(4):247–54.

[220] Florkowski CM, Chew-Harris JS. Methods of Estimating GFR - Different Equations Including CKD-EPI. Clin Biochem Rev. 2011;32(2):75–9.

[221] Schwartz GJ, Brion LP, Spitzer A. The use of plasma creatinine concentration for estimating glomerular filtration rate in infants, children, and adolescents. Pediatr Clin North Am. 1987;34(3):571–90.

[222] Aperia A, Broberger O, Elinder G, Herin P, Zetterstrom R. Postnatal development of renal function in pre-term and full-term infants. Acta Paediatr Scand. 1981;70(2):183–7.

[223] Miall LS, Henderson MJ, Turner AJ, Brownlee KG, Brocklebank JT, Newell SJ, et al. Plasma creatinine rises dramatically in the first 48 hours of life in preterm infants. Pediatrics. 1999;104(6):e76.

[224] Pottel H, Vrydags N, Mahieu B, Vandewynckele E, Croes K, Martens F. Establishing age/sex related serum creatinine reference intervals from hospital laboratory data based on different statistical methods. Clin Chim Acta. 2008;396(1-2):49–55.

[225] Finney H, Newman DJ, Thakkar H, Fell JM, Price CP. Reference ranges for plasma cystatin C and creatinine measurements in premature infants, neonates, and older children. Arch Dis Child. 2000;82(1):71–5.

[226] Cuzzolin L, Fanos V, Pinna B, di Marzio M, Perin M, Tramontozzi P, et al. Postnatal renal function in preterm newborns: a role of diseases, drugs and therapeutic interventions. Pediatr Nephrol. 2006;21(7):931–8.

[227] Rudd PT, Hughes EA, Placzek MM, Hodes DT. Reference ranges for plasma creatinine during the first month of life. Arch Dis Child. 1983;58(3):212–5.

[228] Bueva A, Guignard JP. Renal function in preterm neonates. Pediatr Res. 1994;36(5):572–7.

[229] Guignard JP, Drukker A. Why do newborn infants have a high plasma creatinine? Pediatrics. 1999;103(4):e49.

[230] Manzar S, Al-Umran K, Al-Awary BH, Al-Faraidy A. Changes in plasma creatinine in first 72 hours of life. Arch Dis Child Fetal Neonatal Ed. 2001;85(2):F146–7.

[231] Feldman H, Guignard JP. Plasma creatinine in the first month of life. Arch Dis Child. 1982;57(2):123–6.

[232] Giapros V, Papadimitriou P, Challa A, Andronikou S. The effect of intrauterine growth retardation on renal function in the first two months of life. Nephrol Dial Transplant. 2007;22(1):96–103.

[233] Schlebusch H, Liappis N, Kalina E, Klein C. High Sensitive CRP and Creatinine: Reference Intervals from Infancy to Childhood. J Lab Med. 2002;26(5-6):341–6.

[234] Kim SM, Ko JH, Shim EJ, Lee DH, J CD, Kim DH, et al. Serum creatinine, blood urea nitrogen change in low birth weight infants during their first days of life. Korean J Perinatol. 2008;19(2):181–9.

[235] Ali AS, Farouq MF, Al-Faify KA. Pharmacokinetic approach for optimizing gentamicin use in neonates during the first week of life. Indian J Pharmacol. 2012;44(1):36.

[236] Lannigan R, Thomson A. Evaluation of 22 Neonatal Gentamicin Dosage Protocols Using a Bayesian Approach. Paediatr Perinat Drug Ther. 2001;4(3):92–100.

[237] Rastogi A, Agarwal G, Pyati S, Pildes RS. Comparison of two gentamicin dosing schedules in very low birth weight infants. Pediatr Infect Dis J. 2002;21(3):234–240.

[238] Lindbom L, Ribbing J, Jonsson EN. Perl-speaks-NONMEM (PsN)–a Perl module for NONMEM related programming. Comput Methods Programs Biomed. 2004;75(2):85–94.

[239] Jonsson EN, Karlsson MO. Xpose–an S-PLUS based population pharmacokinetic/pharmacodynamic model building aid for NONMEM. Comput Methods Programs Biomed. 1999;58(1):51–64.

[240] Sheiner LB, Beal SL. Some suggestions for measuring predictive performance. J Pharmacokinet Biopharm. 1981;9(4):503–512.

[241] Savic RM, Karlsson MO. Importance of shrinkage in empirical bayes estimates for diagnostics: problems and solutions. AAPS J. 2009;11(3):558–69.

[242] Schentag J, Jusko W. Renal clearance and tissue accumulation of gentamicin. Clin Pharmacol Ther. 1977;22(3):364–70.

[243] Barker CI, Germovsek E, Hoare RL, Lestner JM, Lewis J, Standing JF. Pharmacokinetic/pharmacodynamic modelling approaches in paediatric infectious diseases and immunology. Adv Drug Deliv Rev. 2014;73:127–39.

[244] Dong Y, Speer CP. Late-onset neonatal sepsis: recent developments. Arch Dis Child Fetal Neonatal Ed. 2015;100(3):F257–63.

[245] Kim KS. Acute bacterial meningitis in infants and children. Lancet Infect Dis. 2010;10(1):32–42.

[246] BNFC, British National Formulary for Children. Meropenem; 2015. `https://www.evidence.nhs.uk/formulary/bnfc/current/5-infections/51-antibacterial-drugs/512-cephalosporins-carbapenems-and-other-beta-lactams/5122-carbapenems/meropenem`, last accessed on 09/10/2015.

[247] Blumer JL. Meropenem: evaluation of a new generation carbapenem. Int J Antimicrob Agents. 1997;8(2):73–92.

[248] Zhanel GG, Johanson C, Embil JM, Noreddin A, Gin A, Vercaigne L, et al. Ertapenem: review of a new carbapenem. Expert Rev Anti Infect Ther. 2005;3(1):23–39.

[249] Nicolau DP. Pharmacokinetic and pharmacodynamic properties of meropenem. Clin Infect Dis. 2008;47(Supplement 1):S32–S40.

[250] Mattoes HM, Kuti JL, Drusano GL, Nicolau DP. Optimizing antimicrobial pharmacodynamics: dosage strategies for meropenem. Clin Ther. 2004;26(8):1187–98.

[251] Shah P. Parenteral carbapenems. Clin Microbiol Infect. 2008;14(s1):175–80.

[252] Dagan R, Velghe L, Rodda J, Klugman K. Penetration of meropenem into the cerebrospinal fluid of patients with inflamed meninges. J Antimicrob Chemother. 1994;34(1):175–9.

[253] The European Committee on Antimicrobial Susceptibility Testing (EUCAST). Data from the EUCAST MIC distribution website; Streptococcus agalactiae; 2015. `http://mic.eucast.org/Eucast2/regShow.jsp?Id=4081`, last accessed on 30/12/2015.

[254] The European Committee on Antimicrobial Susceptibility Testing (EUCAST). Data from the EUCAST MIC distribution website; Escherichia coli; 2015. `http://mic.eucast.org/Eucast2/regShow.jsp?Id=5402`, last accessed on 30/12/2015.

[255] The European Committee on Antimicrobial Susceptibility Testing (EUCAST). Data from the EUCAST MIC distribution website; Listeria monocytogenes; 2015. `http://mic.eucast.org/Eucast2/regShow.jsp?Id=16502`, last accessed on 28/09/2015.

[256] The European Committee on Antimicrobial Susceptibility Testing (EUCAST). Data from the EUCAST MIC distribution website; Haemophilus influenzae; 2015. `http://mic.eucast.org/Eucast2/regShow.jsp?Id=13679`, last accessed on 28/09/2015.

[257] The European Committee on Antimicrobial Susceptibility Testing (EUCAST). Data from the EUCAST MIC distribution website; Streptococcus pneumoniae; 2015. `http://mic.eucast.org/Eucast2/regShow.jsp?Id=6945`, last accessed on 28/09/2015.

[258] The European Committee on Antimicrobial Susceptibility Testing (EUCAST). Data from the EUCAST MIC distribution website; Neisseria menin-

gitidis; 2015. `http://mic.eucast.org/Eucast2/regShow.jsp?Id=22856`, last accessed on 28/09/2015.

[259] Topham J, Murgatroyd L, Jones D, Goonetilleke U, Wright J. Safety evaluation of meropenem in animals: studies on the kidney. J Antimicrob Chemother. 1989;24(suppl A):287–306.

[260] Schmutzhard E, Williams K, Vukmirovits G, Chmelik V, Pfausler B, Featherstone A, et al. A randomised comparison of meropenem with cefotaxime or ceftriaxone for the treatment of bacterial meningitis in adults. J Antimicrob Chemother. 1995;36(suppl A):85–97.

[261] Wong G, Briscoe S, Adnan S, McWhinney B, Ungerer J, Lipman J, et al. Protein binding of β-lactam antibiotics in critically ill patients: can we successfully predict unbound concentrations? Antimicrob Agents Chemother. 2013;57(12):6165–70.

[262] van Enk JG, Touw DJ, Lafeber HN. Pharmacokinetics of meropenem in preterm neonates. Ther Drug Monit. 2001;23(3):198–201.

[263] Bradley JS, Sauberan JB, Ambrose PG, Bhavnani SM, Rasmussen MR, Capparelli EV. Meropenem pharmacokinetics, pharmacodynamics, and Monte Carlo simulation in the neonate. Pediatr Infect Dis J. 2008;27(9):794–9.

[264] Padari H, Metsvaht T, Kõrgvee LT, Germovsek E, Ilmoja ML, Kipper K, et al. Short versus long infusion of meropenem in very-low-birth-weight neonates. Antimicrob Agents Chemother. 2012;56(9):4760–4.

[265] Smith PB, Cohen-Wolkowiez M, Castro LM, Poindexter B, Bidegain M, Weitkamp JH, et al. Population pharmacokinetics of meropenem in plasma and cerebrospinal fluid of infants with suspected or complicated intra-abdominal infections. Pediatr Infect Dis J. 2011;30(10):844–9.

[266] van den Anker JN, Pokorna P, Kinzig-Schippers M, Martinkova J, de Groot R, Drusano G, et al. Meropenem pharmacokinetics in the newborn. Antimicrob Agents Chemother. 2009;53(9):3871–9.

[267] Johanson CE, Duncan 3rd J, Klinge PM, Brinker T, Stopa EG, Silverberg GD. Multiplicity of cerebrospinal fluid functions: new challenges in health and disease. Cerebrospinal Fluid Res. 2008;5(10):441–50.

[268] Segal M. Extracellular and cerebrospinal fluids. J Inherit Metab Dis. 1993;16(4):617–38.

[269] Shen DD, Artru AA, Adkison KK. Principles and applicability of CSF sampling for the assessment of CNS drug delivery and pharmacodynamics. Adv Drug Deliv Rev. 2004;56(12):1825–57.

[270] Raza MW, Shad A, Pedler SJ, Karamat KA. Penetration and activity of antibiotics in brain abscess. J Coll Physicians Surg Pak. 2005;15(3):165–7.

[271] Lutsar I, McCracken Jr GH, Friedland IR. Antibiotic pharmacodynamics in cerebrospinal fluid. Clin Infect Dis. 1998;p. 1117–27.

[272] Barling R, Selkont J. The penetration of antibiotics into cerebrospinal fluid and brain tissue. J Antimicrob Chemother. 1978;4(3):203–27.

[273] Giulieri S, Chapuis-Taillard C, Jaton K, Cometta A, Chuard C, Hugli O, et al. CSF lactate for accurate diagnosis of community-acquired bacterial meningitis. Eur J Clin Microbiol Infect Dis. 2015;34(10):2049–2055.

[274] Guerra-Romero L, Täauber MG, Fournier MA, Tureen JH. Lactate and glucose concentrations in brain interstitial fluid, cerebrospinal fluid, and serum during experimental pneumococcal meningitis. J Infect Dis. 1992;166(3):546–50.

[275] Goldstein B, Giroir B, Randolph A, et al. International pediatric sepsis consensus conference: Definitions for sepsis and organ dysfunction in pediatrics. Pediatr Crit Care Med. 2005;6(1):2–8.

[276] European Medicines Agency (EMA). Report on the Expert Meeting on Neonatal and Paediatric Sepsis; 2010. `http://www.ema.europa.eu/docs/en_GB/document_library/Report/2010/12/WC500100199.pdf`.

[277] Välitalo P, Kumpulainen E, Manner M, Kokki M, Lehtonen M, Hooker AC, et al. Plasma and cerebrospinal fluid pharmacokinetics of naproxen in children. J Clin Pharmacol. 2012;52(10):1516–26.

[278] Kumpulainen E, Välitalo P, Kokki M, Lehtonen M, Hooker A, Ranta VP, et al. Plasma and cerebrospinal fluid pharmacokinetics of flurbiprofen in children. Br J Clin Pharmacol. 2010;70(4):557–66.

[279] Anderson B, Holford N, Woollard G, Chan P. Paracetamol plasma and cerebrospinal fluid pharmacokinetics in children. Br J Clin Pharmacol. 1998;46(3):237–43.

[280] Nalda-Molina R, Dokoumetzidis A, Charkoftaki G, Dimaraki E, Margetis K, Archontaki H, et al. Pharmacokinetics of doripenem in CSF of patients with non-inflamed meninges. J Antimicrob Chemother. 2012;67(7):1722–9.

[281] Nix DE, Goodwin SD, Peloquin CA, Rotella DL, Schentag JJ. Antibiotic tissue penetration and its relevance: impact of tissue penetration on infection response. Antimicrob Agents Chemother. 1991;35(10):1953.

[282] Shin SH, Kim KS. Treatment of bacterial meningitis: an update. Expert Opin Pharmacother. 2012;13(15):2189–06.

[283] Berthoin K, Le Duff CS, Marchand-Brynaert J, Carryn S, Tulkens PM.

Stability of meropenem and doripenem solutions for administration by continuous infusion. J Antimicrob Chemother. 2010;65(5):1073–5.

[284] Craig WA. Pharmacokinetic/pharmacodynamic parameters: rationale for antibacterial dosing of mice and men. Clin Infect Dis. 1998;p. 1–10.

[285] Nau R, Zysk G, Thiel A, Prange H. Pharmacokinetic quantification of the exchange of drugs between blood and cerebrospinal fluid in man. Eur J Clin Pharmacol. 1993;45(5):469–75.

[286] Cutler R, Page L, Galicich J, Watters G. Formation and absorption of cerebrospinal fluid in man. Brain. 1968;91(4):707–20.

[287] Silverberg G, Heit G, Huhn S, Jaffe R, Chang S, Bronte-Stewart H, et al. The cerebrospinal fluid production rate is reduced in dementia of the Alzheimers type. Neurology. 2001;57(10):1763–6.

[288] Modi N, Doré CJ, Saraswatula A, Richards M, Bamford KB, Coello R, et al. A case definition for national and international neonatal bloodstream infection surveillance. Arch Dis Child Fetal Neonatal Ed. 2009;94(1):F8–F12.

[289] Wynn JL, Wong HR, Shanley TP, Bizzarro MJ, Saiman L, Polin RA. Time for a neonatal-specific consensus definition for sepsis. Pediatr Crit Care Med. 2014;15(6):523–8.

[290] Bock RD. A brief history of item theory response. Educational Measurement: Issues and Practice. 1997;16(4):21–33.

[291] Thurstone LL. A method of scaling psychological and educational tests. Journal of educational psychology. 1925;16(7):433.

[292] Johansson AM, de Greef I, Muller B, van der Graaf PH. Application of an Item Response Theory model to describe Amyotrophic Lateral Sclerosis

Functional Rating Scale data; 2015. PAGE 24 (2015) Abstr 3585 www.page-meeting.org/?abstract=3585.

[293] DeMars C. Item Response Theory. Series in Understanding Statistics. Oxford University Press, USA; 2010. Available from: https://books.google.co.uk/books?id=KOADeYBt7sIC.

[294] Reeve BB. Item response theory modeling in health outcomes measurement. Expert Rev Pharmacoecon Outcomes Res. 2003;3(2):131–45.

[295] Reise SP, Waller NG. Item response theory and clinical measurement. Annu Rev Clin Psychol. 2009;5:27–48.

[296] Chang CH, Reeve BB. Item response theory and its applications to patient-reported outcomes measurement. Eval Health Prof. 2005;28(3):264–82.

[297] Reise SP, Haviland MG. Item response theory and the measurement of clinical change. J Pers Assess. 2005;84(3):228–38.

[298] Tzialla C, Borghesi A, Serra G, Stronati M, Corsello G. Antimicrobial therapy in neonatal intensive care unit. Ital J Pediatr. 2015;41(1):27.

[299] Polin RA, Papile LA, Baley JE, Bhutani VK, Carlo WA, Cummings J, et al. Management of neonates with suspected or proven early-onset bacterial sepsis. Pediatrics. 2012;129(5):1006–15.

[300] Blackburn RM, Muller-Pebody B, Planche T, Johnson A, Hopkins S, Sharland M, et al. Neonatal sepsis–many blood samples, few positive cultures: implications for improving antibiotic prescribing. Arch Dis Child Fetal Neonatal Ed. 2012;97(6):487–8.

[301] Simonsen KA, Anderson-Berry AL, Delair SF, Davies HD. Early-onset neonatal sepsis. Clin Microbiol Rev. 2014;27(1):21–47.

[302] Bergstrand M, Hooker AC, Karlsson MO. Visual Predictive Checks for Censored and Categorical data; 2009. PAGE 18 (2009) Abstr 1604 www.page-meeting.org/?abstract=1604.

[303] Fitzgerald MJ, Goto M, Myers TF, Zeller WP. Early metabolic effects of sepsis in the preterm infant: lactic acidosis and increased glucose requirement. J Pediatr. 1992;121(6):951–5.